T.59

"REALISATION OF ONE ELLIPTIC FUNCTION BASED FILTER USING STEPPED DIGITAL LEVELS"

A

THESIS

SUBMITTED TO THE DEPARTMENT OF ELECTRICAL ENGINEERING, BANGLADESH UNIVERSITY OF ENGINEERING & TECHNOLOGY, DHAKA, IN PARTIAL FULFILLMENT OF THE REQUIREMENTS FOR THE DEGREE OF MASTER OF SCIENCE IN ELECTRONICS (ELECTRICAL).

BY

SAMIUL ISLAM
DEPARTMENT OF ELECTRICAL ENGINEERING
BANGLADESH UNIVERSITY OF ENGINEERING
& TECHNOLOGY, DHAKA.

CERTIFICATE

THIS IS TO CERTIFY THAT THIS WORK HAS BEEN DONE BY ME AND THIS HAS NOT BEEN SUBMITTED ELSEWHERE FOR THE AWARD OF ANY DEGREE OR DIPLOMA OR FOR PUBLICATION.

Countersigned:

Saiful Islam

(Supervisor)

Signature of the Candidate

ACCEPTED AS SATISFACTORY FOR PARTIAL FULFILMENT OF THE REQUIREMENTS FOR THE DEGREE OF MASTER OF SCIENCE IN ENGINEERING (ELECTRICAL).

BOARD OF EXAMINERS:

I) _____ 20/8/77
Dr.Solaimanul Mahdi
Professor, Electrical Engg., BUET., Dacca — Chairman

II) _____ 20/8/77
Mr.Kazi Abdur Rauf,
Member, T & T Board,
Govt.of Bangladesh, Dacca — External Member

III) _____
Dr.A.M.Zahoorul Huq,
Professor & Head,
Electrical Engg.Deptt. BUET., Dacca — Member

IV) _____ 20.8.77
Dr.A.M.Patwari,
Professor, Electrical Engg.Deptt.
BUET., Dacca — Member

V) _____ 20/8/77
Dr.Shamsuddin Ahmed
Professor, Electrical Engg.Deptt.
BUET., Dacca. — Member

A C K N O W L E D G E M E N T

With deep sincerity, the author acknowledges his profound gratitude to Dr. Solaimanul Mahdi, Professor of Electrical Engineering Department with whose meticulous guidance, and constant cooperation this work has been done.

The author also wishes to acknowledge his indebtedness to Dr.A.M.Zahoorul Huq, Professor and Head and Dr.A.M.Patwari, Professor of Electrical Engineering for their all-out encouragement and inspiration at all stages of the work.

Thanks are due to Mr.Md.E.A.Bhuiya, Foreman Instructor of Sheet-Metal shop and Mr.Molla Ahmed Ali of Machine shop for their sincere assistance in casting brass plates and in machining the brass plates respectively. Also thanks are due to Mr. M.Rashid of Machine shop for his active help.

Last of all the author takes this opportunity to thank Dr.Mahfuzur Rahman, Assistant Professor of Electrical Engineering for his encouragement and for helping the author with his electronic calculator.

"REALIZATION OF UHF ELLIPTIC FUNCTION BANDPASS FILTER USING STEPPED DIGITAL LINES"

SYNOPSIS

Details of a realization procedure have been presented with the help of which UHF elliptic function bandpass filters may be designed and constructed in the digital form. Distributed equivalent of lumped bandpass elliptic function filter has been derived. It has been shown that the equivalent UHF network consists of parallel coupled array of rectangular bars between parallel ground planes. The static capacitance matrix of this array has been expressed in terms of the element values of lumped bandpass elliptic function filter which are dependent on its S-plane low-pass equivalent. The physical dimension of the elements of the filter has been found from the static capacitance values. The physical realization is in the form of a n-wire line, one quarter of a wavelength long at the center frequency. The coupled lines are stepped along the center of the array. Using this realization procedure two bandpass elliptic function filters were designed and constructed. The measured performances of these two filters were satisfactory.

TABLE OF CONTENTS

LIST OF ILLUSTRATIONS

Figure Numbers		Between Pages
8.4b	.....	77 and 78
8.5	.....	78 and 79
8.6	.....	On Page 79
8.7a	.....	84 and 85
8.7b	.....	85 and 86
9.1	.....	86 and 87
9.2, 9.3, 9.4, 9.5	.....	92 and 93
9.6, 9.7	.....	93 and 94
9.8	.....	95 and 96
10.1	.....	98 and 99

CHAPTER - 1

INTRODUCTION

Filters are used to separate or combine different frequencies as in frequency converters or multipliers or in multiplex communications. The electromagnetic spectrum is limited and has to be shared. Filters are used to confine the radiation from high-power transmitters within assigned spectral limits; conversely, other filters are used to protect receivers from interference outside their operating bands. There is need for filters at all frequencies, from very low through microwave to optical frequencies and beyond.

The importance of Microwave filters in communication systems is increasing as these communication systems are becoming more and more complex and as the electromagnetic spectrum is becoming more densely filled with signals. According to the application, demands for different characteristics of these filters vary, such as if the application is in satellites, spacecrafts or in missiles reliability in performance as well as compactness is very much needed. Again some operations may require sharp cutoff narrow band band-pass filters.

This study is concerned with bandpass filters in the UHF range. Various design procedures are available for the design and construction of this type of filters. These are constructed in parallel coupled strip line resonators[1], in two-part quarter wavelength transmission lines[2] and also in capacitive-gap-coupled transmission lines[2]. These filters exhibit either Chebyshev or maximally flat responses.

An approximate design procedure for UHF bandpass filters using

parallel coupled arrays of resonator line elements between ground planes was given by Matthaei[3] . An exact theory of networks using such arrays, also known as interdigital lines, was presented by R.J.Wenzel[4]. Rhodes[5] gave an outline of a design procedure for UHF elliptic function bandpass filters. Filters of this last type differs from others in that they can realize points of infinite attenuation at real frequencies and are therefore capable of achieving sharp cutoff response. These filters are constructed in interdigital lines and are very compact.

The object of this work is to present a systematic and an exact realization procedure for narrow-band bandpass elliptic function filters. The details of a method have been given whereby compact narrow-band bandpass elliptic function filters can be designed and constructed by using stepped digital lines. The physical realization is in the form of an n-wire parallel coupled lines between grounded plates. Each line is one quarter of a wavelength long at the center frequency of the passband, and the impedance levels are stepped along the center of the coupled lines.

CHAPTER- 2

REVIEW OF LITERATURE

This chapter is a review of literatures available in the field of Microwave band pass filters. There are a large number of publications in this field. This review is limited to only those works which deal with filters having physical structure similar to the one employed in this study i.e. multidire parallel coupled lines between parallel plates.

Matthaei and Belljahn [6] have shown that interdigital line structures have very interesting band-pass filter properties. Before this interdigital structures had been regarded as of interest mainly for use as slow-wave structures. Matthaei [3] gave an approximate design procedure of bandpass filters using interdigital arrays of resonator line elements between parallel ground planes. He presented two approximate design procedures both of which permit design directly from lumped element, low-pass, prototype filters for Chebychev response. Both design procedure could work either for narrow or wide-band filters, but one of his procedures gave more practical dimensions for filters having wide bandwidths (such as an octave), while the other could give more practical dimensions for filters having narrow or moderate bandwidth. In his language "The resulting filters are very compact, have relatively noncritical manufacturing tolerances, and strong stop bands with the second pass band centered at three times the center frequency of the first pass-band". Figure 2.1a and Fig. 2.1b show general structures of interdigital filter and Figures 2.3a and 2.3b show the filters he constructed using his design procedure. Matthaei used the results of Getsinger [7] for finding out the

physical dimensions from static capacitance values.

Matthaei[18] also completed a work on comb line band pass filter in strip line form. The resonators in this type of filter consist of TEM mode transmission line elements that are short-circuited at one end and other end of each line are grounded through capacitances. In fig. 2.2 lines 1 to n and their associated capacitances, C_1^s to C^s_n, constitute resonators, while lines 0 and n+1 are not resonators but simply part of impedance-transforming sections at the ends of the filter. Coupling between resonators is achieved in this type of filter by way of fringing fields between resonator lines. With the capacitors C_k^s present, the resonator lines will be less than $\lambda_0/4$ long at resonance and the coupling between resonators is predominantly magnetic.

In Fig.2.4 the drawing of the trial four resonator, comb-line filter which Matthaei constructed and tested is shown. According to Mathaei his combline filters have the following attractive features:-

i) They are compact.

ii) They have strong stop bands and the stop-band above the primary pass-band can be made to be very broad.

iii) If desired, they can be designed to have an unusually steep rate of cutoff on the high side of the pass-band.

iv) Adequate coupling can be maintained between resonator elements with sizeable spacings between resonator lines.

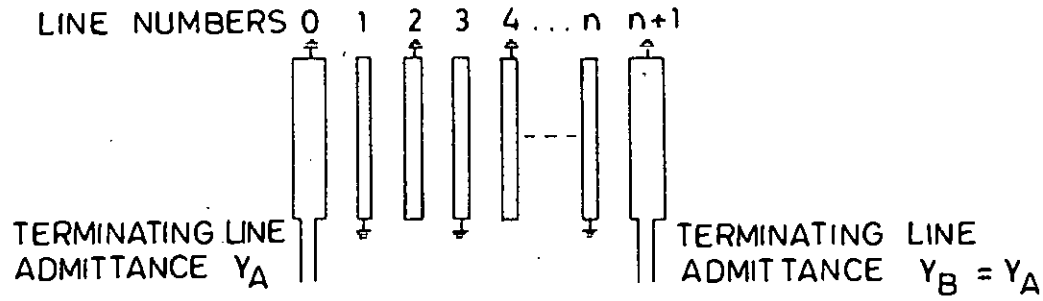

Fig. 2.1a. Interdigital filter with short circuited lines at the ends.

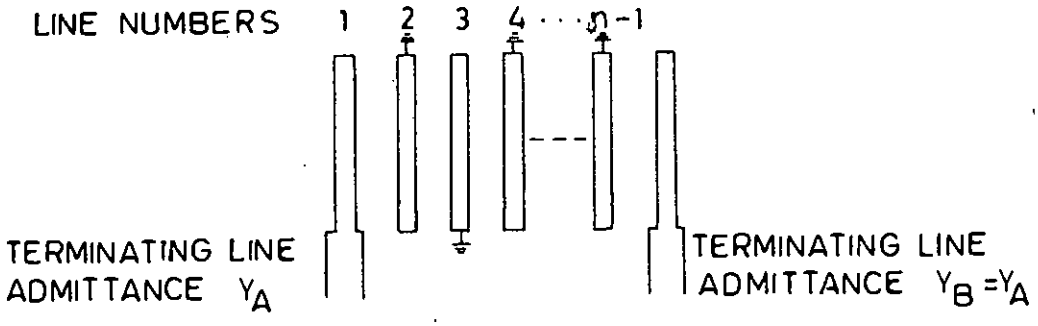

Fig. 2.1b. Interdigital filter with open circuited lines at the ends

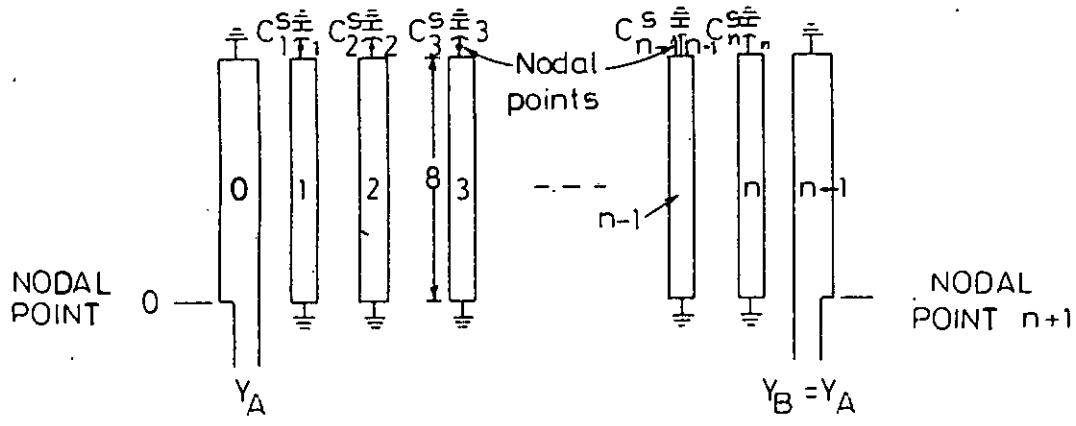

Fig. 2.2. A comb line band pass filter.

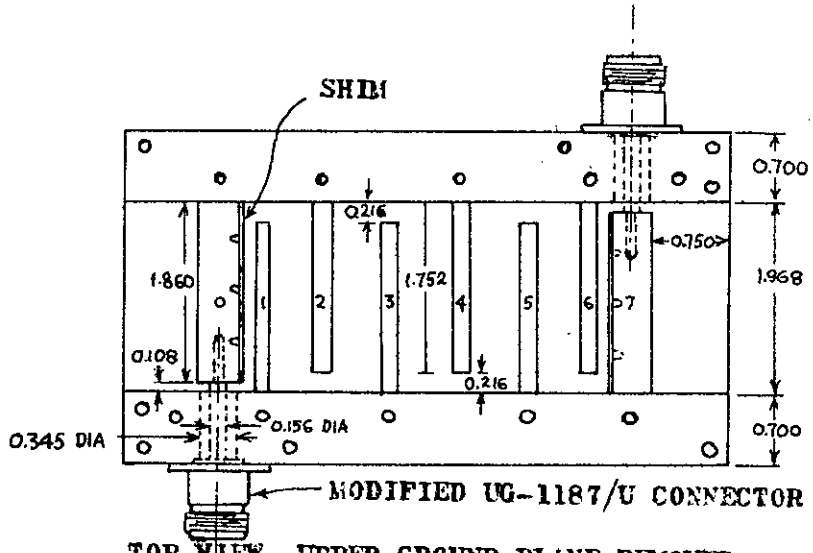

Fig. 2·3a. A 10% bandwith interdigital filter. (Matthaei[12])

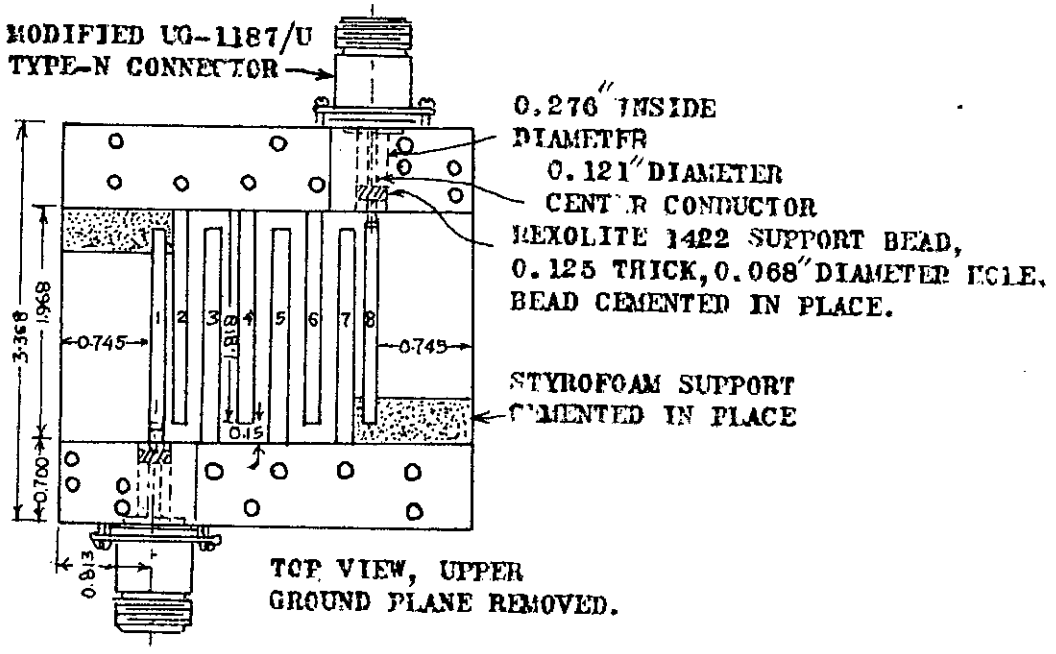

Fig. 2·3b. A experimental interdigital filter (Matthaei[12])

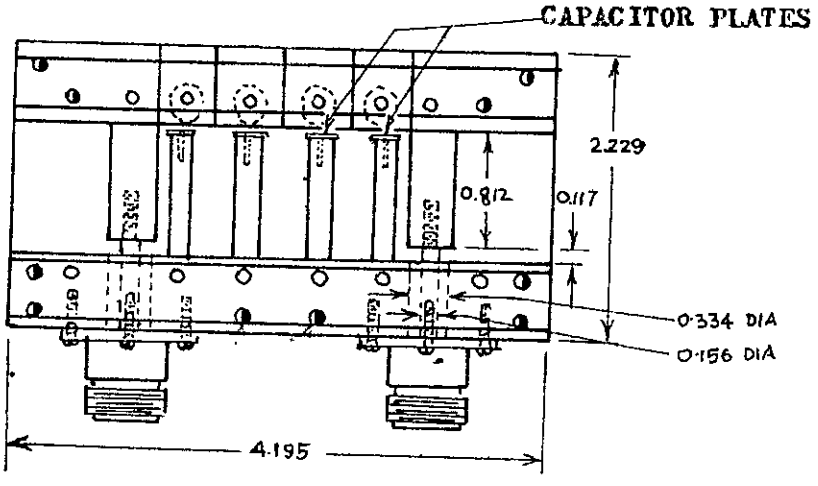

Fig. 2.4. An experimental comb line filter (Matthaei[13])

v) Filters of this type can usually be fabricated without the use of dielectric support materials so that if desired, dielectric losses can be eliminated.

According to Matthaei[3] the interdigital filters have some of these advantages, but comb-line filters are somewhat smaller and are capable of a broader stop-band above the primary pass-band.

The design procedure which Matthaei employed for "Combline filters" involved several approximations. Because of these approximations the accuracy was best for non-narrow-band designs only. Matthaei however used tuning screws for improving the performances. He used a sweep generator and recording reflectometer setup for having the attenuation plot after each time of tuning and thus he got the best tunned plot of attenuation.

Wenzel[4] presented an exact theory of interdigital line networks and related coupled structures. He reviewed the theory of parallel coupled line arrays and discussed the derivation of exact equivalent circuits from the impedance matrix using modern network synthesis techniques. He also introduced the theory of equivalent coupled structures in order to avoid the lengthy analysis required when using the impedance matrix approach. He showed how to find the equivalent networks for the interdigital line simply by inspection. The techniques presented by him were simple to apply and allowed a given transmission response to be obtained in a variety of line configurations. The practical drawing of the design example which he presented is given in Fig. 2.5. He used a combination of coaxial interdigital realization in order

to get relatively wide line spacings. His paper is full of detail informations and discussions on both theoretical and practical side. Although he said that the design procedure is exact but he had to find out the length of the input and output lines by means of almost trial and error method. Moreover he arbitrarily shortened the interdigital line sections by .200 inch. He also used tuning screws in order to achieve the desired characteristics. However, by doing all these he ultimately succeeded in constructing one such filter which gave him good results. Dansal[4] also used the results of Getsinger[9] in order to obtain the physical dimensions from the static capacitance matrix. The center frequency of his filter was 1.0 Gc/s and it had 3:1 bandwidth .05 dB Chebyshev ripple.

Horton and Wenzel[23] gave a detailed design procedure for a practical digital elliptic function filter which can provide either bandpass or band-stop characteristics. Examples were given by them to illustrate typical design procedure for both bandpass and band-stop applications. However he presented experimental results only for an octave band-stop design. Fig. 2.6 shows the drawing of the example of wide band-pass design of Horton and Wenzel. Regarding its advantages they mentioned about its compactness as because the realization is in the form of a coaxial and interdigital form. According to them it is often four or five times smaller than an interdigital band-pass filter of comparable selectivity. About its major limitations they mentioned that the structure is inherently wide-band (> 30 percent) and is not suited to narrowband designs due to physical limitations. Moreover the structure requires series internal stubs and therefore more machined parts than some filter forms.

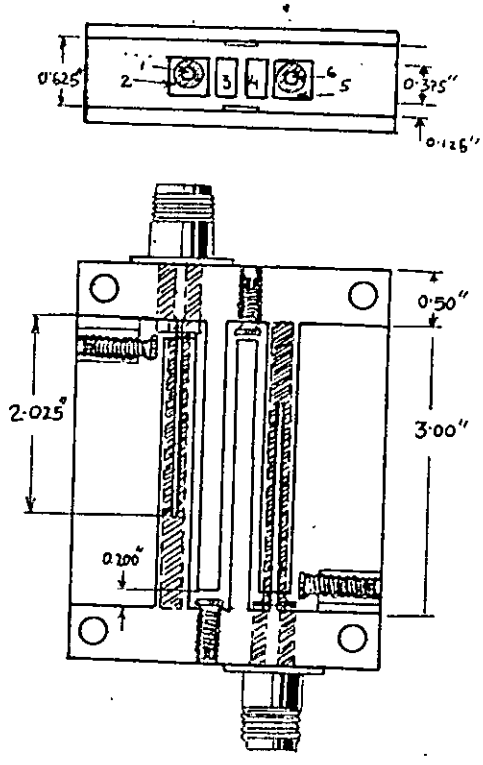

Fig. 2.5 A 3:1 band-width interdigital filter (Wenzel[5])

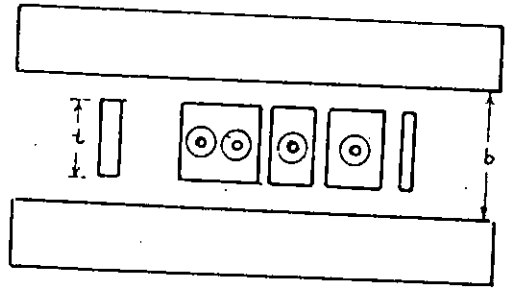

Fig. 2·6 A sample of wide bandpass filter (Cross section)

CHAPTER - 3

MATRIX REPRESENTATION OF AN ARRAY OF PARALLEL COUPLED TRANSMISSION LINES.

3.1 INTRODUCTION:

In this chapter the admittance matrix for two coupled transmission lines between parallel plates is presented. The admittance matrix for 2-N port, N-coupled transmission lines between parallel plates is given in an analogous manner. The capacitance matrix is introduced and the procedure for writing capacitance matrix from the admittance matrix for such a generalised N-coupled parallel transmission lines between grounded plates is also clearly shown. In addition important properties of capacitance matrices are also discussed.

3.2 ADMITTANCE MATRIX REPRESENTATION FOR TWO PARALLEL COUPLED CONDUCTORS BETWEEN GROUND PLANES:

Let us consider the two parallel coupled transmission lines between grounded parallel plates as shown in Fig. 3.1. The lengths are assumed to be same and it is also assumed that the central conductors are supported midway between the parallel plates.

It is necessary at this point to introduce the even and odd mode admittances. Referring to Fig. 3.2 the admittance to ground for a single conductor, when both conductors or transmission lines are at the same potential is Y_{oe}, the even mode admittance, the admittance to ground when the two conductors are oppositely charged with respect to ground is Y_{oo}, the odd mode admittance.

The relation between even mode admittance and normalized

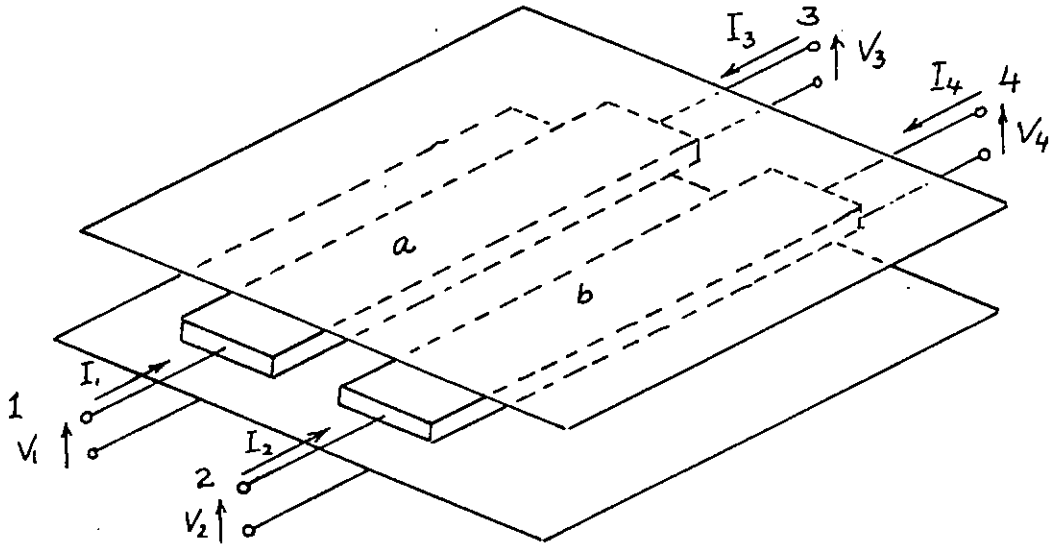

Fig. 3.1 Network consisting of two parallel plates between ground planes.

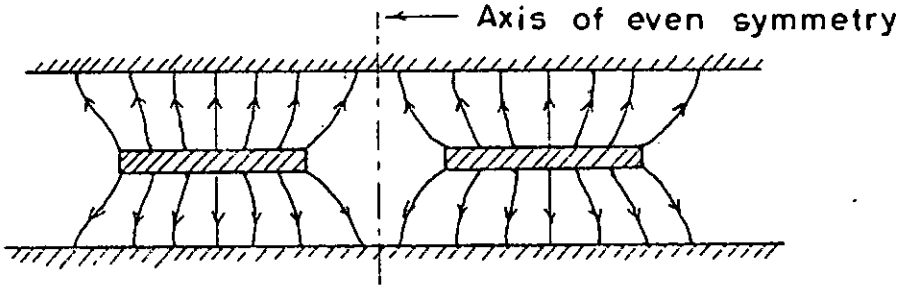

(a) Even mode electric field distribution

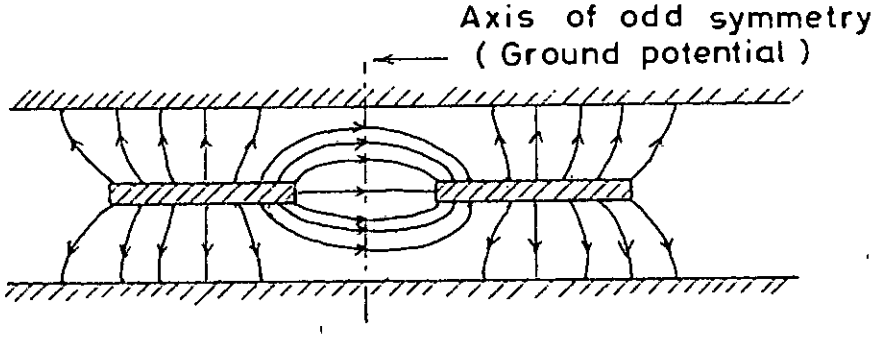

(b) Odd mode electric field distribution.

Fig. 3.2 Field distribution of the even and odd modes in parallel coupled trasmission lines between ground plates.

even mode capacitance is $Y_{oe} = \frac{\sqrt{\epsilon_r}}{\eta_o} C_{oe}$ ..... (3.1a)

Where, $C_{oe} = \frac{C'_{oe}}{\epsilon}$ = $\frac{\text{actual static even mode capacitance}}{\text{permittivity of the dielectric medium}}$

and the relation between odd mode admittance and normalized odd mode capacitance ($C_{oo} = C'_{oo}/\epsilon$), similary is $Y_{oo} = \frac{\sqrt{\epsilon_r}}{\eta_o} C_{oo}$ .. (3.1b)

where η_o = 376.6 ohms = the intrinsic impedance of free space.

For the diagram of Fig. 3.1 let ,

Y^a_{oe} = characteristic admittance of line 'a' with even excitation

Y^a_{oo} = characteristic admittance of line 'a' with odd excitation.

Y^b_{oe} and Y^b_{oo} are the even and odd mode characteristic admittances of line'b'.

Assuming four voltage sources at the four ports of Fig.3.1 and following the procedure of Ozaki and Ishii[10] the resulting admittance matrix is as follows:

$$\begin{bmatrix} Y_{11} & Y_{12} & Y_{13} & Y_{14} \\ Y_{21} & Y_{22} & Y_{23} & Y_{24} \\ Y_{31} & Y_{32} & Y_{33} & Y_{34} \\ Y_{41} & Y_{42} & Y_{43} & Y_{44} \end{bmatrix}$$

$$= \begin{bmatrix} \frac{Y_{oo}^a + Y_{oe}^a}{2} \cdot \frac{1}{S} & -\frac{Y_{oo}^a - Y_{oe}^a}{2} \cdot \frac{1}{S} & -\frac{Y_{oo}^a + Y_{oe}^a}{2} \frac{\sqrt{1-S^2}}{S} & -\frac{Y_{oo}^a - Y_{oe}^a}{2} \cdot \frac{\sqrt{1-S^2}}{S} \\ -\frac{Y_{oo}^b - Y_{oe}^b}{2} \cdot \frac{1}{S} & \frac{Y_{oo}^b + Y_{oe}^b}{2} \cdot \frac{1}{S} & -\frac{Y_{oo}^b - Y_{oe}^b}{2} \cdot \frac{\sqrt{1-S^2}}{S} & -\frac{Y_{oo}^b + Y_{oe}^b}{2} \frac{\sqrt{1-S^2}}{S} \\ -\frac{Y_{oo}^a + Y_{oe}^a}{2} \frac{\sqrt{1-S^2}}{S} & -\frac{Y_{oo}^a - Y_{oe}^a}{2} \cdot \frac{\sqrt{1-S^2}}{S} & \frac{Y_{oo}^a + Y_{oe}^a}{2} \cdot \frac{1}{S} & -\frac{Y_{oo}^a - Y_{oe}^a}{2} \cdot \frac{\sqrt{1-S^2}}{S} \\ -\frac{Y_{oo}^b - Y_{oe}^b}{2} \cdot \frac{\sqrt{1-S^2}}{S} & -\frac{Y_{oo}^b + Y_{oe}^b}{2} \cdot \frac{\sqrt{1-S^2}}{S} & -\frac{Y_{oo}^b - Y_{oe}^b}{2} \cdot \frac{1}{S} & \frac{Y_{oo}^b + Y_{oe}^b}{2} \cdot \frac{1}{S} \end{bmatrix} \quad \ldots\ldots\ldots(3.2)$$

where,

$$S = j \tan \beta l = j \tan \theta \quad \ldots\ldots\ldots(3.3)$$

$\theta = \frac{\pi\omega}{2\omega_o}$ = electrical length of the lines in radians, and

ω_o = the frequency at which the lines are a quarter wavelength.

Here, $Y_{oo}^a - Y_{oe}^a = Y_{oo}^b - Y_{oe}^b \quad \ldots\ldots\ldots(3.4)$

Now using equations (3.1a) and (3.1b), in terms of odd mode

and even mode capacitances we can write the admittance matrix of (3.2) as

$$\frac{\sqrt{\epsilon_r}}{\eta_0 S}\begin{bmatrix} \frac{C_{oo}^a+C_{oe}^a}{2}, & -\frac{C_{oo}^a-C_{oe}^a}{2}, & -\frac{C_{oo}^a+C_{oe}^a}{2}\sqrt{1-s^2}, & -\frac{C_{oo}^a-C_{oe}^a}{2}\sqrt{1-s^2} \\ -\frac{C_{oo}^b-C_{oe}^b}{2}, & \frac{C_{oo}^b+C_{oe}^b}{2}, & -\frac{C_{oo}^b-C_{oe}^b}{2}\sqrt{1-s^2}, & -\frac{C_{oo}^b+C_{oe}^b}{2}\sqrt{1-s^2} \\ -\frac{C_{oo}^a+C_{oe}^a}{2}\sqrt{1-s^2}, & -\frac{C_{oo}^a-C_{oe}^a}{2}\sqrt{1-s^2}, & \frac{C_{oo}^a+C_{oe}^a}{2}, & -\frac{C_{oo}^a-C_{oe}^a}{2} \\ -\frac{C_{oo}^b-C_{oe}^b}{2}\sqrt{1-s^2}, & -\frac{C_{oo}^b+C_{oe}^b}{2}\sqrt{1-s^2}, & -\frac{C_{oo}^b-C_{oe}^b}{2}, & \frac{C_{oo}^b+C_{oe}^b}{2} \end{bmatrix} \qquad (3.5)$$

Writing $\frac{1}{2}(c^a_{oo} - c^a_{oe}) = \frac{1}{2}(c^b_{oo} - c^b_{oo}) = c_{ab}$

and $\frac{c^a_{oo} + c^a_{oo}}{2} = c_a$, $\frac{c^b_{oo} + c^b_{oo}}{2} = c_b$ .....(3.6)

Matrix (3.5) now becomes as follows:

$$\frac{\sqrt{\epsilon_r}}{\eta_0 S}\begin{bmatrix} C_a & -C_{ab} & -C_a\sqrt{1-s^2} & -C_{ab}\sqrt{1-s^2} \\ -C_{ba} & C_b & -C_{ba}\sqrt{1-s^2} & -C_b\sqrt{1-s^2} \\ -C_a\sqrt{1-s^2} & -C_{ab}\sqrt{1-s^2} & C_a & -C_{ab} \\ -C_{ba}\sqrt{1-s^2} & -C_b\sqrt{1-s^2} & -C_{ba} & C_b \end{bmatrix} \qquad .....(3.7)$$

We can thus write that

$$\begin{bmatrix} I_1 \\ I_2 \\ I_3 \\ I_4 \end{bmatrix} = \frac{1}{\eta_0 S} \begin{bmatrix} C & \cdots & -C\sqrt{1-S^2} \\ \cdots & \cdots & \cdots \\ -C\sqrt{1-S^2} & \cdots & C \end{bmatrix} \begin{bmatrix} V_1 \\ V_2 \\ V_3 \\ V_4 \end{bmatrix} \qquad (3.8)$$

where $\epsilon_r = 1$ is assumed i.e. air is assumed as dielectric

In the equation (3.8)

$$C = \begin{bmatrix} C_a & \cdots & -C_{ab} \\ \cdots & \cdots & \cdots \\ -C_{ba} & \cdots & C_b \end{bmatrix} \qquad \ldots\ldots\ldots (3.9)$$

The static capacitance matrix C can be represented by the original network as shown in Fig. 3.3. Eq.(3.8) shows that the static capacitance matrix completely determines the behaviour of the networks at the ports.

3.3. THE STATIC CAPACITANCE MATRIX :

In section 3.2 the admittance matrix representation for the case of two coupled transmission lines (4-port) was shown. In a analogous manner it can be shown that for the case of the 2N-port array of N-parallel coupled lines between parallel plates of Fig.3.4 the relation between the currents and voltages is as follows :

$$\begin{bmatrix} I_A \\ \cdots \\ I_B \end{bmatrix} = \frac{1}{\eta_0 S} \begin{bmatrix} C & \cdots & -C\sqrt{1-S^2} \\ \cdots & \cdots & \cdots \\ -C\sqrt{1-S^2} & \cdots & C \end{bmatrix} \begin{bmatrix} V_A \\ \cdots \\ V_B \end{bmatrix} \qquad (3.10)$$

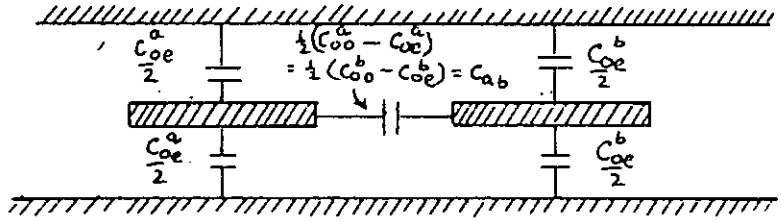

Fig. 3·3 The static capacitances of the network of Fig. 3·1

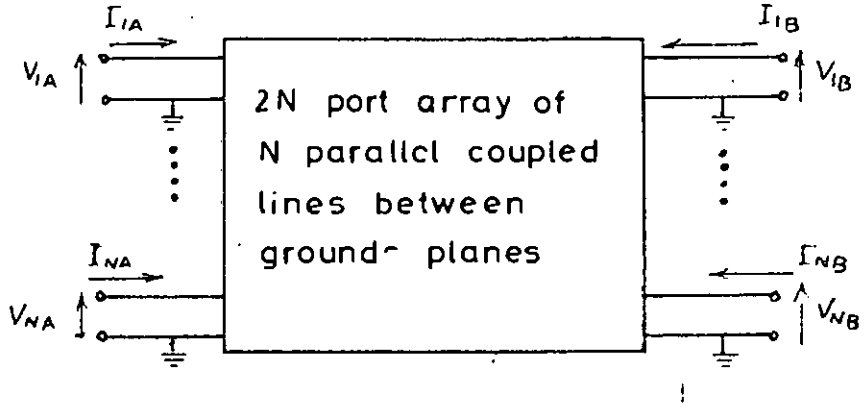

Fig. 3·4a Symbolic representation of 2N port network with parallel coupled transmission lines between ground planes.

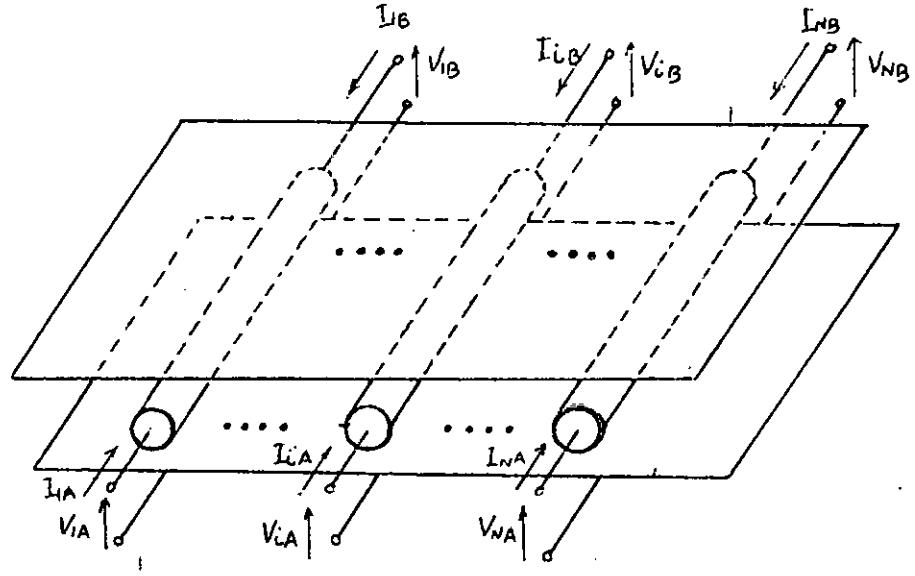

Fig. 3·4b Network representation of 2N port N-parallel coupled lines between ground planes.

where,

$$\begin{bmatrix} I_A \\ I_B \end{bmatrix} = \begin{bmatrix} I_{1A} \\ I_{2A} \\ \vdots \\ I_{NA} \\ I_{1B} \\ I_{2B} \\ \vdots \\ I_{NB} \end{bmatrix} \quad ; \quad \begin{bmatrix} V_A \\ V_B \end{bmatrix} = \begin{bmatrix} V_{1A} \\ V_{2A} \\ \vdots \\ V_{NA} \\ V_{1B} \\ V_{2B} \\ \vdots \\ V_{NB} \end{bmatrix} \tag{3.11a}$$

and

$$C = \begin{bmatrix} C_1+C_{12}+\cdots+C_{1N} & -C_{12} & -C_{13} & \cdots & -C_{1N} \\ -C_{21} & C_{21}+C_2+C_{23}+\cdots+C_{2N} & -C_{23} & \cdots & -C_{2N} \\ -C_{13} & -C_{32} & & & \\ \vdots & & & & \\ -C_{1N} & & & -C_{N-1,N} & \\ & & & C_{N1}+C_{N2}+\cdots+C_{N,N-1}+C_N & \end{bmatrix} \tag{3.11b}$$

where,

C = N x N normalized static capacitance matrix with elements c

c = c'/ϵ = ratio of static capacitance between conductors per unit length to the permittivity of the medium.

c_i = Capacitance of the ith conductor to ground

c_{ik} = mutual capacitance between ith and kth conductors

c_{ii} = sum of all capacitances connected to the ith conductor

= $C_{i,1}+C_{i,2}+\cdots+C_{i,i-1}+C_i+C_{i,i+1}+\cdots+C_{i,N}$

The elements of matrix (3.11b) satisfy the following relationships:

$$\text{a)} \quad \sum_{k=1}^{N} c_{ik} \geq 0 \qquad i = 1,2,3, \ldots\ldots\ldots N$$

$$\text{b)} \quad c_{ik} = c_{ki} \qquad i \neq k \qquad \ldots\ldots\ldots (3.12)$$

$$\text{c)} \quad c_{ii} \geq 0$$

$$\text{d)} \quad c_{ik} \geq 0 \qquad i \neq k.$$

Let us now consider an array of three parallel coupled conductors as shown in Fig. 3.5. The 3 by 3 capacitance matrix has the main diagonal terms given by the sum of all capacitors connected to each of the three ungrounded conductors and off diagonal terms given by the negative of the capacitors between conductors. Therefore,

$$C = \begin{bmatrix} C_1+C_2+C_{13} & -C_{12} & -C_{13} \\ -C_{12} & C_2+C_{12}+C_{23} & -C_{23} \\ -C_{13} & -C_{23} & C_3+C_{13}+C_{23} \end{bmatrix} \qquad \ldots\ldots\ldots (3.13)$$

To obtain a physical realization for a network of the type shown in Fig.3.5 starting from a given matrix C requires that physical dimensions be determined either experimentally or analytically by solution of Laplace's equation. Unfortunately, this is an extremely difficult problem for most geometric configurations, and solutions are known only for a few special cases. One case of particular interest is obtained by assuming that each conductor is coupled directly to its nearest neighbours only. This configuration is shown in Fig.3.6 for three conductors.

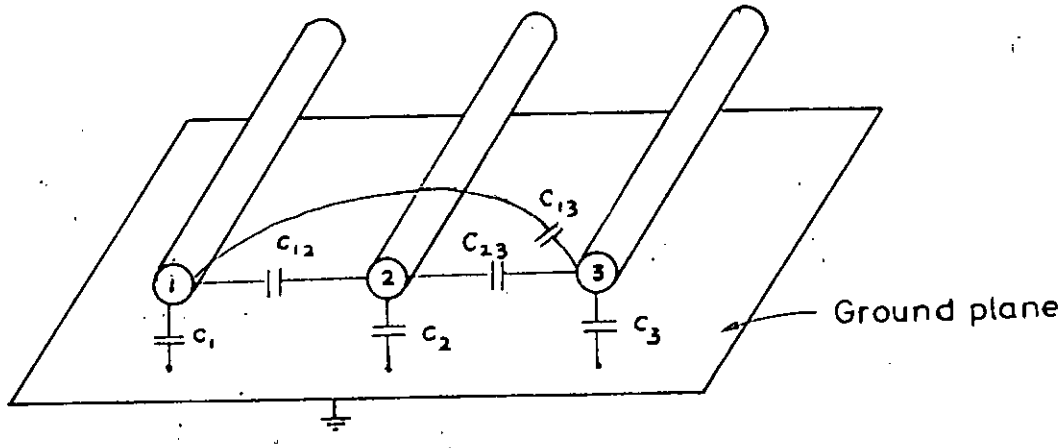

Fig. 3·5 3 line array of parallel coupled lines.

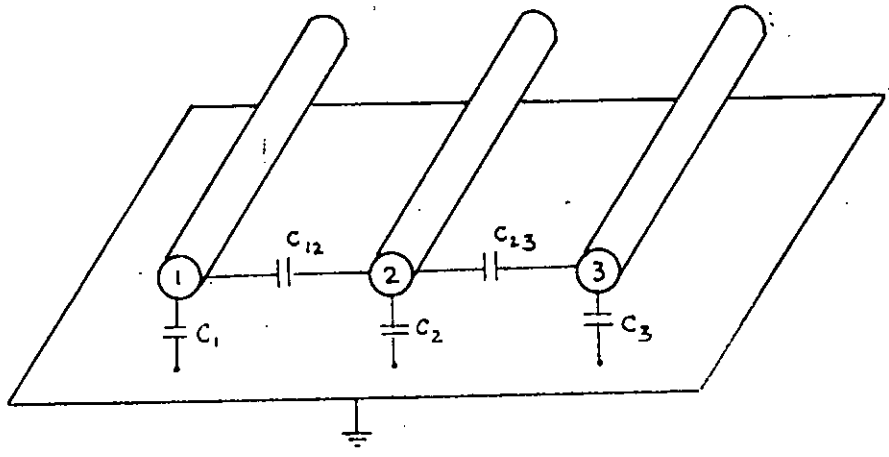

Fig 3·6 Parallel coupled array with coupling to nearest neighbours only.

The capacitance matrix for this network is given by

$$C = \left[\begin{array}{c|c|c} c_1+c_{12} & -c_{12} & 0 \\ \hline -c_{12} & c_{12}+c_2+c_{23} & -c_{23} \\ \hline 0 & -c_{23} & c_3+c_{23} \end{array}\right] \qquad (3.14)$$

The C matrix for a like array with any number of conductors is obtained in a similar manner. The assumption of coupling only to nearest neighbours results in a matrix with non zero elements on the main diagonal and adjacent to the main diagonal only. Given a C matrix of the above type, data exists from which physical dimensions can be determined from Getsinger's graph[7] or Cristal's paper[11].

3-4 THE CAPACITANCE MATRIX TRANSMISSION:

Different network configurations that leave some specified network response invariant are said to be "equivalent". A method of investigating possible equivalent circuits is to use a linear transformations of network variables (voltage and/or current, for example). Linear transformations of network variables can be performed in a manner such that network realizability is assured. However, any such transformation will be of practical utility only if it is easily interpreted and leads to a desirable physical structure.

Guillemin[29] has shown that a useful linear transformation is obtained by multiplying the rows and columns of a parameter matrix by suitable constants. In carrying out this transformation on a static capacitance matrix, symmetry requires that each operation be applied to both a row and its corresponding column.

Mathematically, the transformation is given by,

$$C' = n_N C n_N \rightarrow \begin{array}{c} \downarrow n_1 \quad \downarrow n_2 \qquad\qquad \downarrow n_N \\ \begin{matrix} n_1 \rightarrow \\ n_2 \rightarrow \\ \\ n_N \rightarrow \end{matrix} \begin{bmatrix} C_{11} & -C_{12} & 0 & \cdots \\ -C_{12} & C_{22} & \cdots & \\ \cdots & \cdots & \cdots & C_{NN} \end{bmatrix} \end{array} \qquad (3.15)$$

where, n_N is a diagonal matrix with elements n_1, n_2 ..... n_N. The transformed capacitance matrix C' is obtained by pre- and post-multiplication of a given matrix C by the diagonal matrix n_N. The right hand portion of (3.15) indicates notation for use in applying the transformation to practical problems and serves to illustrate how each ith row and its corresponding colum is multiplied by the same constant n_i .

To give a network interpretation to the capacitance matrix transformation of (3.15), let us consider the ideal transformers of turns ratio $n_i : 1$, connected to the 2N-ports of the N-line network shown in Fig.3.7a. The resultant network is shown in Fig.3.7b.

Physically, a new network has been formed with voltage and current variables related to these of the original network by

$$\begin{bmatrix} V_A' \\ \cdots \\ V_B' \end{bmatrix} = \begin{bmatrix} n_N^{-1} & \vdots & 0 \\ \cdots & \cdots & \cdots \\ 0 & \vdots & n_N^{-1} \end{bmatrix} \begin{bmatrix} V_A \\ \cdots \\ V_B \end{bmatrix} \text{ and } \begin{bmatrix} I_A' \\ \cdots \\ I_B' \end{bmatrix} = \begin{bmatrix} n_N & \vdots & 0 \\ \cdots & \cdots & \cdots \\ 0 & \vdots & n_N \end{bmatrix} \begin{bmatrix} I_A \\ \cdots \\ I_B \end{bmatrix} \qquad (3.16)$$

where n_N is a diagonal NxN matrix with elements n_1, n_2, ... n_N

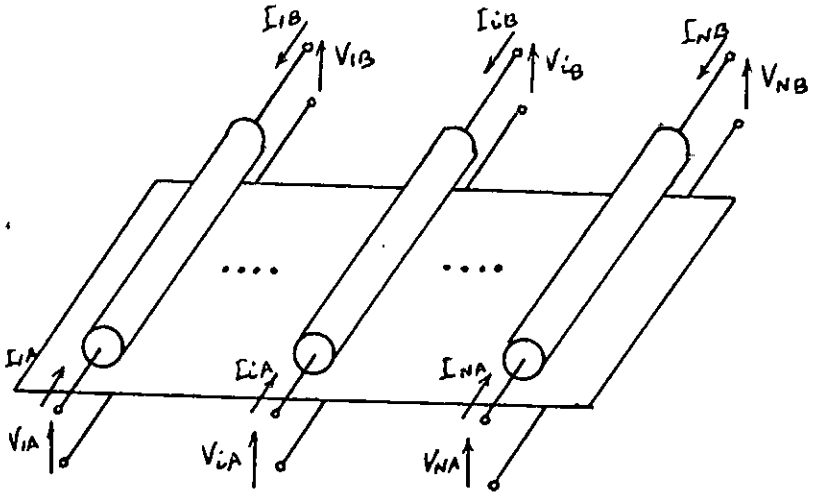

(a) Network with capacitance matrix C

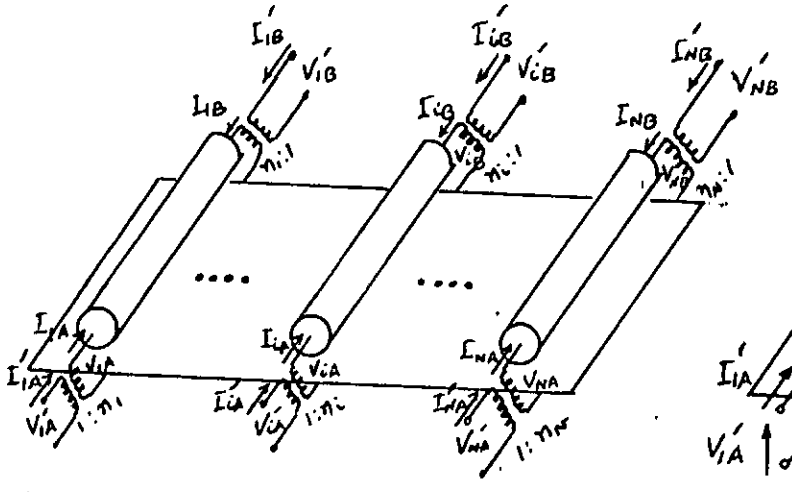

(b) Network with capacitance matrix C′ (at primed terminals)

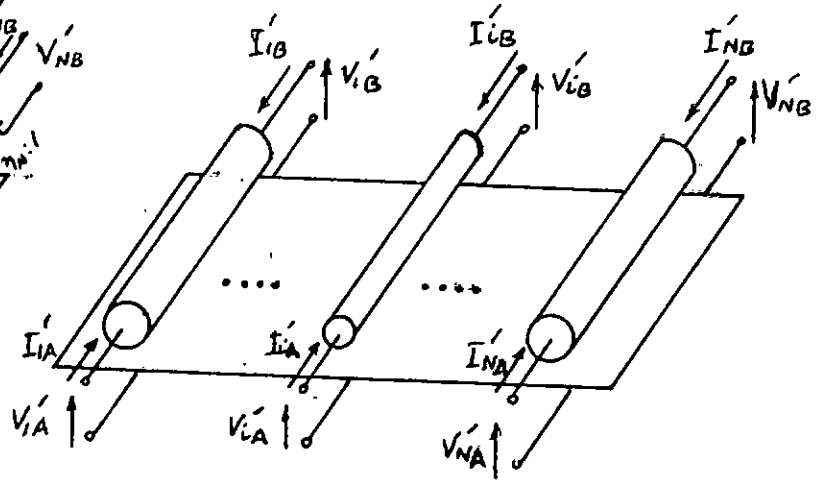

(c) Network with capacitance matrix C′ obtained by changing cross — sectional geometry.

Fig. 3·7 Network and physical interpretation of the capacitance matrix transformation.

$$\begin{bmatrix} I_A' \\ I_B' \end{bmatrix} = \frac{1}{\eta_0 S} \left[\begin{array}{c|c} \eta_N & 0 \\ \hline 0 & \eta_N \end{array}\right] \left[\begin{array}{c:c} C & -C\sqrt{1-S^2} \\ \hdashline -C\sqrt{1-S^2} & C \end{array}\right] \left[\begin{array}{c:c} \eta_N & 0 \\ \hdashline 0 & \eta_N \end{array}\right] \begin{bmatrix} V_A' \\ V_B' \end{bmatrix}$$

$$\left[\begin{array}{c:c} \eta_N^{-1} & 0 \\ \hdashline 0 & \eta_N^{-1} \end{array}\right]^{-1} = \left[\begin{array}{c:c} \eta_N & 0 \\ \hdashline 0 & \eta_N \end{array}\right]$$

$$\begin{bmatrix} I_A' \\ I_B' \end{bmatrix} = \frac{1}{\eta_0 S} \left[\begin{array}{c:c} \eta_N C \eta_N & -\eta_N C \eta_N \sqrt{1-S^2} \\ \hdashline -\eta_N C \eta_N \sqrt{1-S^2} & \eta_N C \eta_N \end{array}\right] \begin{bmatrix} V_A' \\ V_B' \end{bmatrix}$$

$$= \frac{1}{\eta_0 S} \left[\begin{array}{c:c} C' & -C'\sqrt{1-S^2} \\ \hdashline -C'\sqrt{1-S^2} & C' \end{array}\right] \begin{bmatrix} V_A' \\ V_B' \end{bmatrix}$$

The following statement summarises the network and physical implications of the capacitance matrix transformation.

Given a parallel line array, transformation of the corresponding matrix C results in a matrix C' that corresponds to a new network identical to the original with ideal transformers of turns ratio $n_i : 1$ added at both ends of each line. Physically, the new network can be realized by a change in cross-sectional geometry.

The factors n_i used in performing a capacitance matrix transformation can be chosen arbitrarily as long as they lead to a transformed capacitance matrix whose elements obey the restrictions given by (3.12). The conditions under which the cross sectional geometry be altered while a specified network response is held invariant are as follows: If each of the 2N-ports of the parallel line arrays of Fig.3.7a is terminated in a passive admittance $Y_i (i = 1, 2 \ldots\ldots 2N)$ then addition of ideal transformers (as in Fig.3.7b) will affect only the network admittance level at any driven port. However, each terminating admittance Y_i can be transformed through ideal transformers to yield primed terminating admittance $Y'_i = n_i^2 Y_i$. The original network and ideal transformers can then be replaced by a new network with a different cross sectional geometry as described. The above statements are summarized as follows: The transmission response of a parallel line network with capacitance matrix C and line terminations Y_i is identical to that of a parallel line network with capacitance matrix C' and terminations $Y'_i = n_i^2 Y_i$ where the n_i are the constants utilised in transforming C into C'.

Regarding the capacitance matrix transformation we must

remember the following facts: Multiplying the kth row and column of a capacitance matrix by any factor n' corresponds to multiplying the admittance level of the kth node by n'^2, and the transfer admittance between nodes adjacent to the kth node by n'. If this transformation is performed on any interior row and column, the two-port performance of the network is unchanged; if performed on an end row and column, the admittance level of the corresponding port is multiplied by n'^2 and the overall transfer admittance is multiplied by n'. Performing multiple transformations allows an infinite number of equivalent networks and port-admittance levels to be obtained. In performing these transformations, care must be taken to insure that the final circuit contains no negative elements. Physical realizeability requires that the sum of elements of any row or column be greater than (or e ual to)zero, and gives a limitation on the choice of n'.

C H A P T E R - 4

DERIVATION OF S-PLANE EQUIVALENT CIRCUIT OF DIGITAL LINES

4.1. INTRODUCTION:

This chapter mainly deals with the derivation of S-plane equivalent circuit of parallel coupled transmission lines between ground plates for only two special cases. Section 4.2 introduces Richard's transformation by which a distributed network can be treated as a lumped network. In section 4.3 different natures of couplings are discussed. By transforming an array of parallel coupled transmission lines to a structure in which the nature of coupling become easily recognizeable the S-plane equivalent circuit can be found by inspection only.

4.2. TRANSFORMATION OF DISTRIBUTED NETWORK TO LUMPED NETWORK:

In this section the S-plane capacitor and S-plane inductor are introduced. The application of modern network theory to the design of microwave distributed network is based upon a complex plane transformation demonstrated by Richards[13]. He showed that distributed networks, composed of commensurate lengths of transmission line and lumped resistor, could be treated in analysis or synthesis as lumped L-C-R networks by using the complex frequency variable.

$$S = j\Omega = j \tan\theta = j \tan\beta l = j \tan\frac{\pi\omega}{2\omega_0} \qquad \ldots\ldots(4.1)$$

where Ω is real and ω_0 is the radian frequency for which the transmission lines are a quarter wavelength.

The one port impedance Z of a short-circuited quarter wave transmission line of characteristic impedance Z_0.

$$Z = \left(j \tan \frac{\pi\omega}{2\omega_0} \right) Z_0 = j\Omega Z_0 \qquad \text{.....(4.2).}$$

corresponds in the transformed frequency variable S to the impedance of a lumped inductor $L = Z_0$.

Similarly, the admittance Y of an open circuit line of characteristic admittance Y_0

$$Y = \left(j \tan \frac{\pi\omega}{2\omega_0} \right) Y_0 = j\Omega Y_0 \qquad \text{.....(4.3)}$$

corresponds to the admittance of a lumped capacitor $C = Y_0 = 1/Z_0$.

The distributed characteristic values of Z_0 and Y_0 thus corresponds, respectively, to L and C for lumped elements. The symbol L (inductor) and C (capacitor) are S-plane inductors and capacitors respectively.

4.3. FORMS OF COUPLING:

In carrying out the capacitance matrix transformation as shown in chapter-3 the capacitances are treated as though they represent static capacitors in a planar geometry. From a microwave viewpoint they represent coupling between quarter-wave lines and if the form of the coupling could be determined the microwave equivalent circuit could be obtained by inspection.

Let us consider, for example, the single-line network of Fig.4.1a, and its capacitor representation in Fig.4.1b. The static

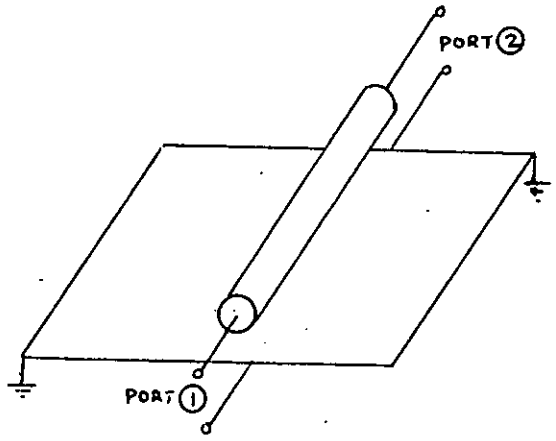

(a)

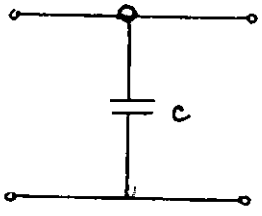

(b)

Fig. 4·1. A single line above ground and its static capacitance representation.

capacitor of Fig.4.1b can represent three distinct forms of coupling, depending on the terminal conditions and the terminals between which the electrical performance is observed:

i) An S-plane Capacitor: The electrical behaviour of the line at either port with the other port open circuited. The value of the S-plane capacitor is given by $C = 1/Z_0 = \sqrt{\epsilon_r}\, c/\eta_0$ where Z_0 is the characteristic impedance of the line. ~~e.g. defined~~

ii) An S-plane Inductor: The electrical behaviour of the lines at either port with the other port short circuited. The value of the inductor is given by $L = Z_0 = \eta_0 / \sqrt{\epsilon_r}\, c$.

iii) A unit element: The electrical behaviour of the line between the ports. The impedance of the unit element is equal to $Z_0 = \frac{\eta_0}{\sqrt{\epsilon_r}\, c}$

If the array of Fig.3.4b can be put into a form in which the previously mentioned types of coupling become easily recognizable, an equivalent S-plane network can be found by inspection. Transformation of the capacitance matrix preserve the performance of the network, with the possible exception of a change in impedance level, and offer the possibility of changing the network form into one in which the nature of each coupling is easily recognizable. Furthermore, the capacitance network also represents static capacitors and can be used to obtain dimensions for a physical realization.

4.4. DERIVATION OF S-PLANE EQUIVALENT CIRCUIT FOR PARALLEL COUPLED TRANSMISSION LINES BETWEEN PARALLEL PLANES:

While finding out the physical realisation of the elliptic function filter in chapter-6 it will be necessary to find out the equivalent digital representation of an S-plane network having all inductances or all capacitances.

In this section equivalence has been established between a digital line network with all the lines grounded at one end and an S-plane network having shunt and series S-plane inductors as shown in Fig. 4.2c. Also equivalence has been established between a digital line network with lines all open at both ends and an S-plane capacitance network having shunt and series S-plane capacitance as shown in Fig.4.3c.

a) Parallel coupled transmission lines between ground plates with one end grounded:

Let us consider the case of three parallel coupled transmission lines between grounded plates. It is assumed that the lines are of equal length and all the lines are grounded at one end. The three lines are shown in Fig. 4.2a.

The representation of this network by static capacitance will obviously be as shown in Fig.4.2b. After writing the capacitance matrix for the network of Fig.4.2b and carrying out transformation on node number 2 we can make the capacitance between node 2 and ground equal to zero. In order to show this let us assume that the value of each capacitance in network 4.2b is equal to 1. Then we can write the

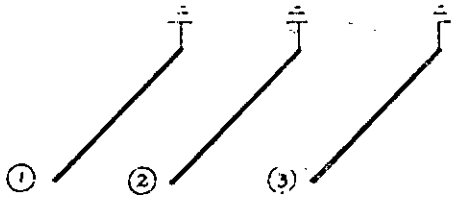

(a) 3-parallel coupled lines between ground plates all grounded at one side (Ground plates not shown).

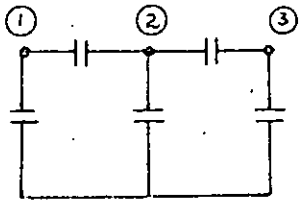

(b) Representation of the above network by static capacitances.

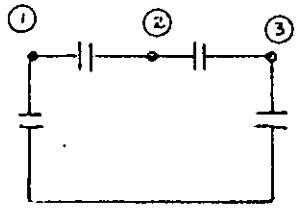

(c) Static capacitance network after transformation.

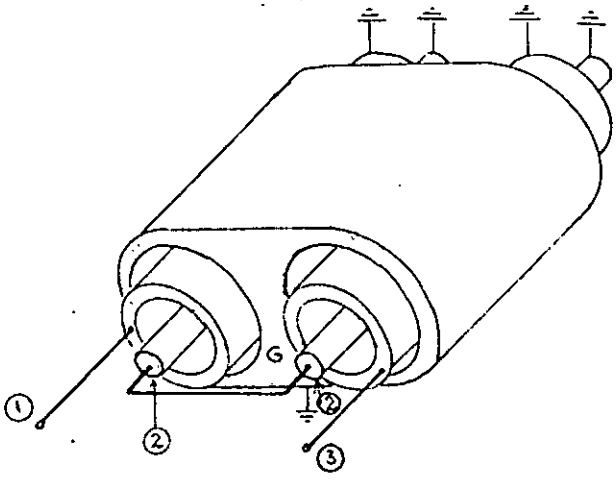

(d) Possible coaxial representation.

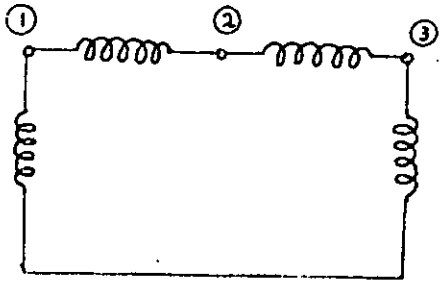

(e) Equivalent S-plane network

Fig. 4·2. Derivation of S-plane equivalent ckt. for 3-parallel coupled transmission lines between ground plates, all grounded at one end.

following capacitance matrix for this network

$$n' \rightarrow \begin{bmatrix} 2 & -1 & 0 \\ -1 & 3 & -1 \\ 0 & -1 & 2 \end{bmatrix} \qquad \text{.....(4.4)}$$

$\uparrow n'$

multiplying the 2nd row and column of the above matrix by n' leaves the two port properties invariant, but yields an equivalent network with a capacitance matrix given by

$$\begin{bmatrix} 2 & -n' & 0 \\ -n' & 3n'^2 & -n' \\ 0 & -n' & 2 \end{bmatrix} \qquad \text{.....(4.5)}$$

physical realizability requires that

$$3n'^2 \geq 2n' \quad \text{and} \quad 2 \geq n',$$

$$\therefore \quad 2/3 \leq n' \leq 2 \qquad \text{.....(4.6)}$$

If we now choose $n' = 2/3$, the resulting capacitance matrix is given by

$$\begin{bmatrix} 2 & -2/3 & 0 \\ -2/3 & 4/3 & -2/3 \\ 0 & -2/3 & 2 \end{bmatrix} \qquad \text{.....(4.7)}$$

The static capacitance network and a physical realization with the help of coaxial lines are shown in Figs.4.2c and 4.2d respectively. Line no. 2 is now not at all coupled to ground but only to line 1 and line 3 . From Fig.4.2d the form of each coupling

is readily determined and an exact S-plane equivalent circuit can be written by inspection. The coupling between outer line and line(1) is that of an S-plane inductance because the other end of line 1 is grounded. Between lines 1 and 2 the coupling is in the form of a S-plane inductance since other ends of both lines (1) and (2) are grounded. Based on a similar reasoning the coupling between line 2 and 3 is in the form of a S-plane inductance. Line 2 has however no coupling with the ground. We can easily find the coupling between line 3 and ground as a S-plane inductance. The complete S-plane equivalent circuit is shown in Fig.4.2c. We can now say that the network shown in Fig.4.2c is an equivalent S-plane representation of the network shown in Fig.4.2a, so that given a S-plane network of Fig.4.2(c) we can think immediately of the digital network of Fig.4.2a as an equivalent network.

(b) Parallel coupled transmission lines between ground plates both end open circuited:

Let us now consider the case of three parallel coupled transmission lines of equal lengths between ground planes as shown in Fig.4.3a. It is assumed that the lines are open circuited at both ends.

In this case also Fig.4.3b represents the static capacitance network of Fig.4.3a. Fig.4.3c shows the static capacitance network after making the value of the capacitance between node 2 and ground equal to zero. This has been shown in the case of all lines

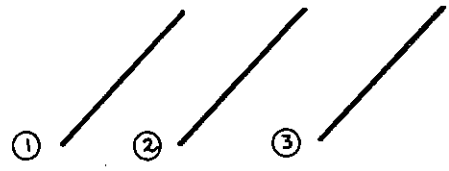

(a) 3-parallel coupled lines between ground planes, all open at both ends (Ground plate not shown).

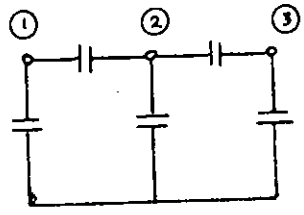

(b) Representation of the network by static capacitances.

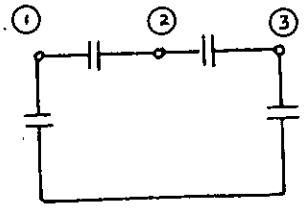

(c) Static capacitance network after transformation.

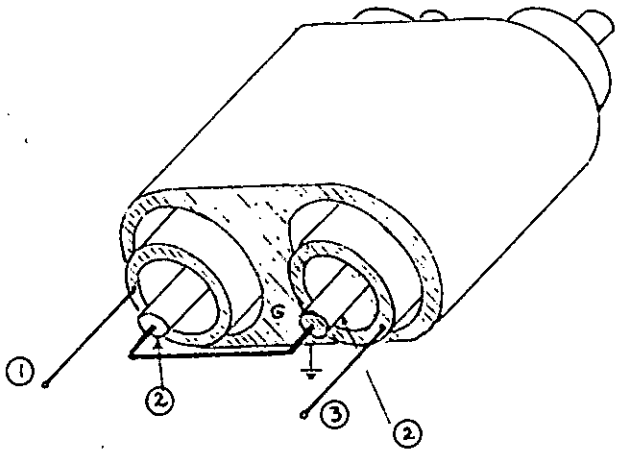

(d) Coaxial representation.

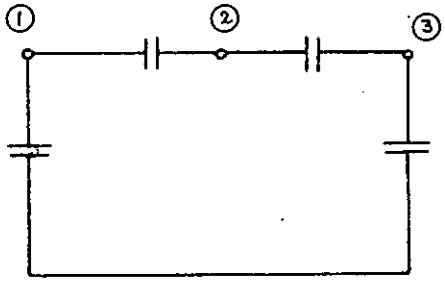

(e) Equivalant S-plane network.

Fig. 4.3 Derivation of S-plane equivalent ckt. for 3-parallel coupled transmission lines, all open at both ends.

grounded at one end. As mentioned earlier the network in Fig.4.3b and in Fig.4.3c are equivalent. An equivalent co-axial representation of the network of Fig.4.3c is shown in Fig.4.3d. As before the S-plane equivalent circuit can now be drawn by inspection. Line 1 couples to ground by a S-plane capacitor since line 1 is an open circuited line. The other ends of both line 1 and 2 are open circuited and thus the coupling between line 1 and 2 is in the form of a S-plane capacitor. In the same manner and based on the same reasoning the coupling between lines 2 and 3 is a S-plane capacitor. As in the case of line 1 , line 3 also couples to ground conductor by a S-plane capacitor.

It is thus clear that given a S-plane equivalent circuit as shown in Fig.4.3c one can realize the network physically by means of the network of Fig.4.3a, since they are equivalent.

CHAPTER - 5

INSERTION POWER CHARACTERISTIC OF LOW-PASS ELLIPTIC FUNCTION FILTER:

5.1. INTRODUCTION

In this chapter a definition of the insertion power function along-with its relationship with the reflection coefficiet is presented. In order to achieve a particular insertion power characteristic we can therefore find out the reflection coefficient function. From this reflection coefficient function we can form input impedance and hence we can synthesize the network to achieve the required insertion power-function. A brief discussion on insertion power characteristic of the elliptic function type is presented. The technique for designing a lowpass elliptic function filter for achieving a prescribed insertion loss characteristic is also given in this chapter.

5.2. THE RELATION BETWEEN INSERTION POWER FUNCTION AND REFLECTION COEFFICIENT FUNCTION:

The input impedance of the equivalent two terminal network in Fig.5.1b is

$$Z_i (j\Omega) = R_i (\Omega) + j X_i (\Omega) \qquad \ldots\ldots(5.1)$$

which has a resistive component $R (\Omega)$ and a reactive component $X_i(\Omega)$, where $\Omega = \frac{\Omega'}{\Omega_p'}$ is the normalized frequency with respect to Ω_p'.

The power delivered to the equivalent two terminal network in Fig.5.1b is

$$P_1 = |I_1|^2 R_i = \left| \frac{E_1}{R_1 + Z_i} \right|^2 R_i \qquad \ldots\ldots\ldots(5.2).$$

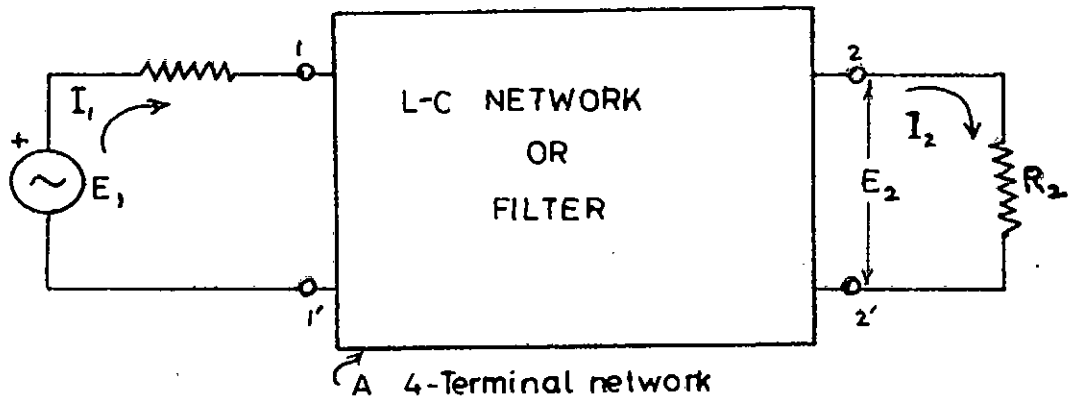

(a) Power supplied to the load through the filter.

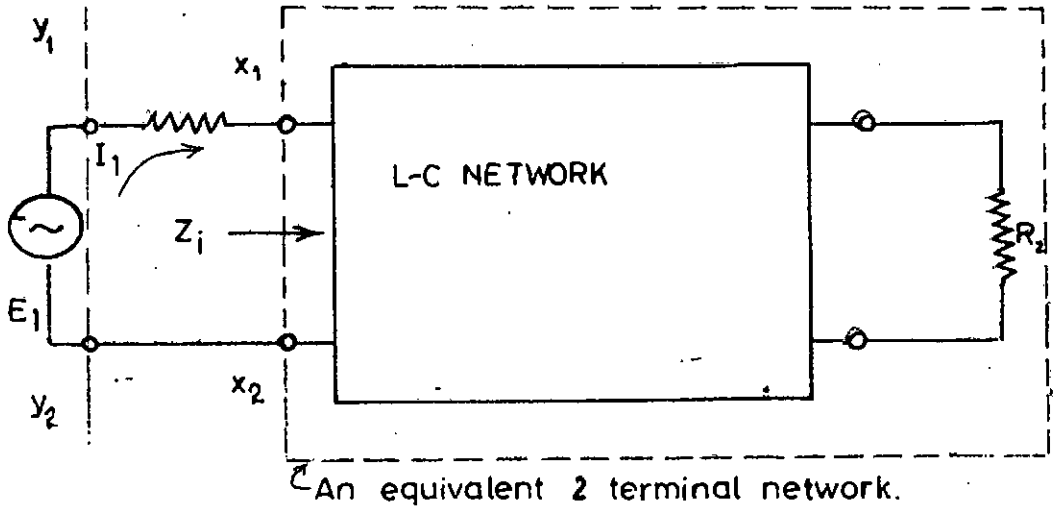

(b)

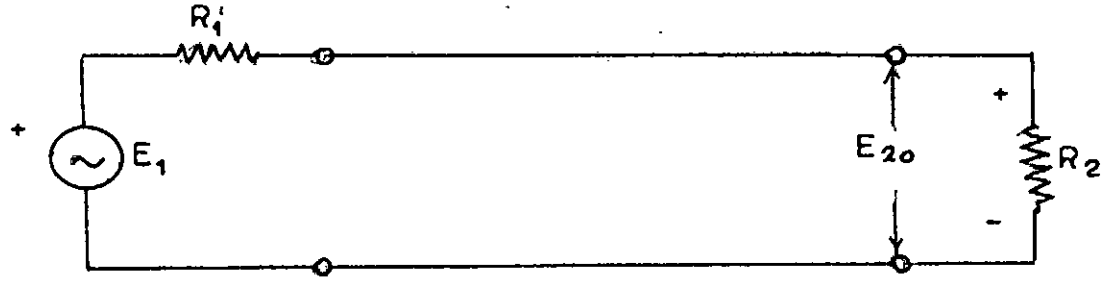

(c). Power supplied to the load directly.

Fig. 5·1 Determination of insertion voltage ratio and insertion power function of L–C filter.

$$e^{\theta(s)} = \frac{E_{20}}{E_2}$$

$$\theta(s)\Big|_{j\Omega} = \alpha(\Omega) + j\beta(\Omega) =$$

$\alpha(\Omega)$

$\beta(\Omega)$

$$e^{2\alpha(\Omega)} = \left[e^{\alpha}\right]^2 = \left|\frac{E_{20}}{E_2}\right|^2 = \frac{|E_{20}|^2/R_2}{|E_2|^2/R_2}$$

$$= \frac{P_{20}}{P_2}$$

$$e^{-2\alpha} = \frac{|E_1|^2 R_2}{(R_1+R_2)^2} e^{-2\alpha}$$

$$\left|\frac{E_1}{(R_1+Z_i)}\right|^2 R_i = \frac{|E_1|^2 R_2}{(R_1+R_2)^2} e^{-2\alpha}$$

or, $$e^{2\alpha} = \frac{|R_1+Z_i|^2 R_2}{(R_1+R_2)^2 R_i}$$

or, $$\frac{4R_1R_2}{(R_1+R_2)^2} e^{-2\alpha} = \frac{4R_1R_i}{|R_1+Z_i|^2}$$

$$\text{or,}\quad 1-\frac{4R_1R_2}{(R_1+R_2)^2}e^{-2\alpha}=\frac{|R_1+Z_i|^2-4R_1R_i}{|R_1+Z_i|^2}$$

$$=\frac{(R_i-R_1)^2+X_i^2}{|Z_i+R_1|^2}$$

$$\therefore\quad 1-\frac{4R_1R_2}{(R_1+R_2)^2}e^{-2\alpha}=\frac{|Z_i(j\Omega)-R_1|^2}{|Z_i(j\Omega)+R_1|^2} \qquad \text{.....(5.9)}$$

From the definition of reflection coefficient we get reflection coefficient. $\Gamma(s)=\dfrac{Z_i(s)-R_1}{Z_i(s)+R_1}$ $\qquad R_1\neq 0$

$$\therefore\quad \Gamma(j\Omega)=\frac{Z_i(j\Omega)-R_1}{Z_i(j\Omega)+R_1}$$

Eqn.(5.9) can be written as

$$1-\frac{4R_1R_2}{(R_1+R_2)^2}e^{2\alpha}=|\Gamma(j\Omega)|^2=\Gamma(j\Omega)\,\Gamma(-j\Omega) \qquad \text{.....(5.10)}$$

$$\therefore\quad \Gamma(s)\,\Gamma(-s)=1-\frac{4R_1R_2}{(R_1+R_2)^2}\cdot\frac{1}{P(s)} \qquad \text{.....(5.11)}$$

where $P(s)=e^{2\alpha}$ = insertion power function. This is the relation between the insertion power function and reflection coefficient.

It is therefore clear that if we can find the expression for the insertion power function of a L-C filter circuit we can immediately

find out the reflection coefficient from Eqn. (5.11). From this reflection coefficient it will thus be convenient to synthesize the network by the usual synthesis procedures after finding the input impedance.

5.3. THE RELATION BETWEEN ATTENUATION OF A FILTER AND THE REFLECTION COEFFICIENT:

The relation between attenuation in dB and reflection coefficient can easily be found from Eq.(5.11). From Eq.(5.11) we get at $s = j\Omega$

$$\Gamma(j\Omega)\,\Gamma(-j\Omega) = 1 - \frac{4R_1R_2}{(R_1+R_2)^2}e^{-2\alpha} = 1 - e^{-2\alpha}, \quad \text{putting } R_1 = R_2$$

$$\therefore\ e^{-2\alpha} = 1 - \Gamma(j\Omega)\Gamma(-j\Omega)$$

$$= 1 - \rho^2 \quad \text{where, } \rho = |\Gamma(j\Omega)|$$

$$\therefore\ \alpha = -\tfrac{1}{2}\ln(1-\rho^2) = -\ln\sqrt{1-\rho^2} \quad \text{nepers}$$

i.e.
$$A = -\frac{8.686}{2}\ln(1-\rho^2) \quad dB$$
$$= -10\log_{10}(1-\rho^2) \quad dB \qquad \text{.....(5.12).}$$

where A is the attenuation in decibels.

5.4. LOW-PASS INSERTION POWER CHARACTERISTIC OF THE ELLIPTIC FUNCTION TYPE:

A lowpass insertion power characteristic of the elliptic function type for the case of n-odd can be written as [23]

$$P = e^{2\alpha} = \bar{K}\left[1 + \epsilon_1 S_0(\Omega)\right] \qquad \text{.....(5.13)}$$

where,

$$S_0(\Omega) = S_n(\Omega) \qquad \text{for n=odd}$$

and

$$S_0(\Omega) = \frac{k^n}{k_1}\,\Omega^2\left[\frac{(\Omega^2-\Omega_1^2)(\Omega^2-\Omega_2^2)\cdots\cdots(\Omega^2-\Omega_\ell^2)}{(1-k^2\Omega_1^2\Omega_2^2)(1-k^2\Omega_2^2\Omega^2)\cdots(1-k^2\Omega_\ell^2\Omega^2)}\right] \qquad (5.14)$$

and $\Omega_m = sn\left(\frac{2mK}{n}, k\right)$, $m = 1, 2, \ldots, \ell$; $\ell = \frac{n-1}{2}$

here, K = complete elliptic integral of modulus k

K_1 = complete elliptic integral of modulus k_1

$\Omega = \frac{\Omega'}{\Omega_p'}$ = low pass normalized frequency with respect to Ω_p'

By plotting Eqn.(5.13) we obtain the insertion power characteristic of Fig.5.2a. This plot is particularly for n=7. The index n tells us how many horizontal tangents the characteristic has in the pass band.

In Fig.5.2a $0 \text{ --- } \Omega_p'$ represent the passband frequency range, $\Omega_p' - \Omega_s'$ represent the transitional frequency range, $\Omega_s' - \infty$ represent the stop-band frequency range, and $\Omega = \frac{\Omega'}{\Omega_p'}$ represents the normalized frequency with respect to Ω_p'

In Fig.5.2a we see that insertion power loss is infinite somewhere in the high frequency stopband of a lowpass network for this case. This is usually a desirable feature in a lowpass network.

A plot of $S_0(\Omega)$ (in Eq.5.14) is also given in Fig.5.2b. In the pass band at $\Omega=0$, $S_0(\Omega) = 0$ as is evident from the plot of $S_0(\Omega)$

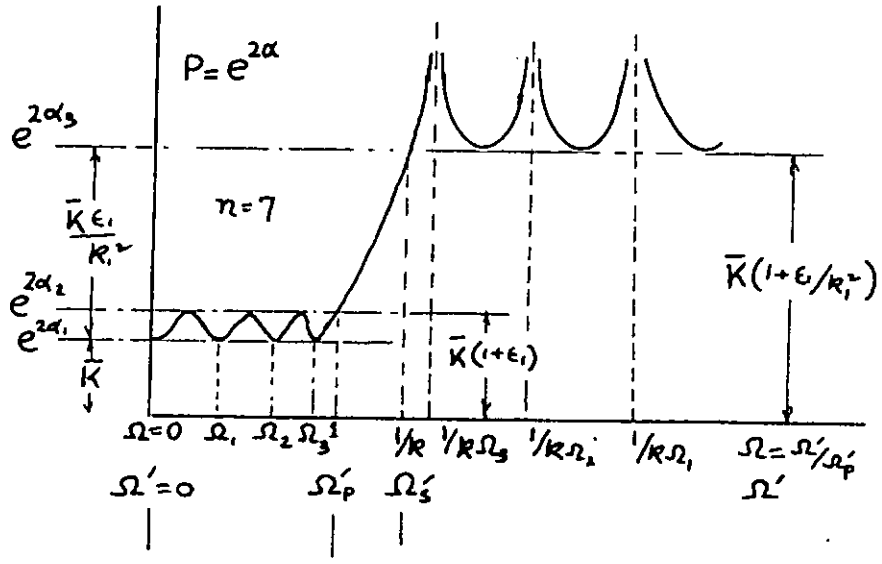

Fig. 5·2a. A plot of insertion power characteristic of the elliptic function type (n = odd).

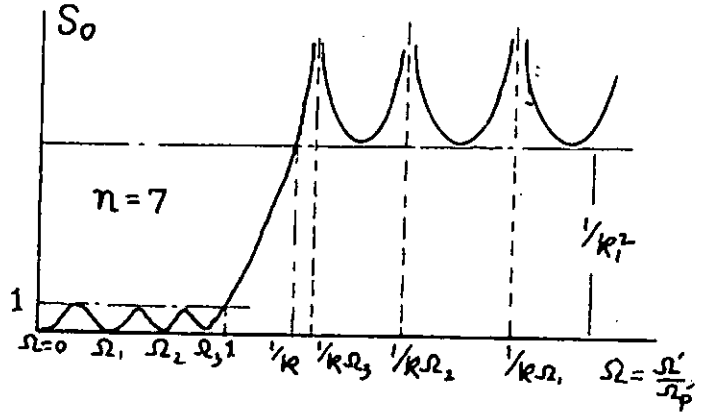

Fig. 5·2b. A plot of $S_0(\Omega)$ for n = odd.

Hence from Eq.(5.13) we get $P_1 = e^{2\alpha_1} = \bar{K}$. Again in the passband at $\Omega = 1$. So $(\Omega) = 1$, hence $\& P_2 = e^{2\alpha_2}$ becomes equal to $\bar{K}(1+\epsilon_1)$ At the edge of the transition region i.e. at $\Omega' = \Omega_s'$, $S_0(\Omega) = \frac{1}{K_1^2}$ and thus we get $P_3 = e^{2\alpha_3} = \bar{K}\,\frac{\epsilon_1 + K_1^2}{K_1^2}$. The transition frequency range is between the frequencies Ω_p' and Ω_s' . The parameter $K = \frac{\Omega_p'}{\Omega_s'}$ is obviously a measure of the steepness of the insertion power characteristic in the transition frequency range.

Passband distortion tolerance:

α_1 and α_2 are, respectively, the minimum loss and the maximum loss in the passband as depicted in Fig.5.2a. The tolerance in the passband distortion is

$$\alpha_p = \alpha_2 - \alpha_1 \quad \text{nepers} \qquad \ldots\ldots\ldots(5.15)$$

or, $$X_p = 8.686\,\alpha_p = 8.686(\alpha_2 - \alpha_1) \quad \text{db} \qquad \ldots\ldots\ldots(5.16)$$

where X_p is the passband distortion tolerance in db.

We also find that

$$e^{2\alpha_p} = \frac{e^{2\alpha_2}}{e^{2\alpha_1}} = \frac{\bar{K}(1+\epsilon_1)}{\bar{K}} = 1+\epsilon_1 \qquad \ldots\ldots\ldots(5.17)$$

and $$\alpha_p = \tfrac{1}{2}\ln(1+\epsilon_1) \quad \text{nepers} \qquad \ldots\ldots\ldots(5.18a)$$

$$X_p = \frac{8.686}{2}\ln(1+\epsilon_1) \quad \text{db} \qquad \ldots\ldots\ldots(5.18b)$$

Therefore ϵ_1 is a measure of the tolerance in the passband distortion.

Discrimination against high-frequency signals:

α_1 and α_3 are, respectively, the minimum loss in the passband and that in the stop-band as depicted in Fig.5.2a; the minimum

discrimination against high-frequency signals in the stop-band is

$$\alpha_s = \alpha_3 - \alpha_1 \quad \text{nepers} \qquad (5.19a)$$

$$\text{or,} \quad X_s = 8.686\,\alpha_s = 8.686\,(\alpha_3 - \alpha_1)\ \text{db} \qquad (5.19b)$$

We also find that

$$e^{2\alpha_s} = \frac{e^{2\alpha_3}}{e^{2\alpha_1}} = 1 + \frac{\epsilon_1}{k_1^2} \qquad (5.20a)$$

$$\text{or,} \quad e^{2\alpha_s} = 1 + \frac{e^{2\alpha_p} - 1}{k_1^2} \qquad (5.20b)$$

Evaluation of the insertion power characteristic at the edge of the passband:

At $\Omega = 1$ i.e. at $\omega' = \omega_p'$ we find that

$$sn^{-1}(\Omega, k) = sn^{-1}(1, k) = K$$

and Eqn.(5.14) becomes

$$\begin{aligned} \delta_0(1) &= sn^2\left(\frac{nK_1}{K} K, k_1\right) \\ &= sn^2(nK_1, k_1) \end{aligned} \qquad (5.21a)$$

for n odd.

This is indicated in Fig.5.2b. Equation (5.13) now have the form

$$\begin{aligned} P = e^{2\alpha} &= \bar{k}(1+\epsilon_1) \\ &= \bar{k}(1+e^{2\alpha_p} - 1) \quad \because \epsilon_1 = e^{2\alpha_p} - 1 \ \text{ from (5.17)} \\ &= \bar{k}\, e^{2\alpha_p} \end{aligned} \qquad (5.21b)$$

Also, we find that Eq.5.14 at $-\Omega$ el yields

$$k_1 = k^n \frac{(1-\Omega_1^2)(1-\Omega_2^2)\cdots(1-\Omega_\ell^2)}{(1-k^2\Omega_1^2)(1-k^2\Omega_2^2)\cdots(1-k^2\Omega_\ell^2)} \qquad (5.22)$$

where,

$$\Omega_m = sn\left(2m\frac{K}{n}, k\right), \qquad m = 1, 2, \ldots\ldots\ldots\ldots \frac{n-1}{2}$$

Equation (5.22) can be used to evaluate k_1 if k and n are known. K is a constant for a given k.

Evaluation of the insertion power characteristic at the edge of the stop-band.

By replacing Ω with $\frac{1}{k\Omega}$ in Eqn.(5.14) we find $S_0\left(\frac{1}{k\Omega}\right) = \frac{1}{k_1^2 S_0(\Omega)}$

Therefore with the aid of Eq.(5.21a), we find that at $\Omega = \frac{1}{k}$ i.e. at $\Omega' = \Omega_s' = \Omega_p'/k$

$$S_0\left(\frac{1}{k}\right) = \frac{1}{k_1^2} \qquad (5.24)$$

This is indicated in Fig.5.2b.

Significance of the index n

Depending upon the methods of synthesis and their associated network configurations, the index n is related to the number of circuit elements in different configurations and is, therefore, a measure of the complexity of a network having an elliptic-function characteristic. In general, the larger the n, the more circuit elements are required and steepness of the insertion power characteristic curve in the transition region also increases.

The maximum attenuation in the passband -A_{max} and the minimum attenuation in the stop band- A_{min}.

In the synthesis procedure, $\bar{K}$ of Eqn. (5.13) is assumed to be equal to unity. In that case the passband distortion tolerance α_p will give us the maximum attenuation in nepers in the passband, since $\alpha_1 = 0$ Therefore the passband distortion tolerance X_p in decibels would now become the maximum attenuation in the pass band in dB. We shall call this maximum attenuation in the pass band to be A_{max}(dB).

Similarly in the stopband α_s will be equal to α_3 nepers (since $\alpha_1 = 0$). The corresponding attenuation in dB is X_s. We shall say now that this X_s is equal to the minimum attenuation in the stopband in dB. We shall call this minimum attenuation in the stop band to be A_{min}(dB).

5.5. DETERMINATION OF FILTER COMPLEXITY n WITH NOMOGRAPH:

Fig.5.3 shows the nomograph published by Kawakami, which is very much useful in determining the required degree of transmission function in order to satisfy a given design condition. (Source Ref. 14). This nomograph avoids direct reference to any elliptic function parameter. The maximum value of ripples in the passband (A_{max}) is given at the left side of the nomograph. The minimum attenuation in the stopband (A_{min}) is also given in the left hand side of the nomograph. The horizontal axis of the nomograph represents the steepness $\Omega = \frac{\Omega_s}{\Omega_p}$ of the low pass insertion (dB) loss characteristic curve. If the value of A_{max},

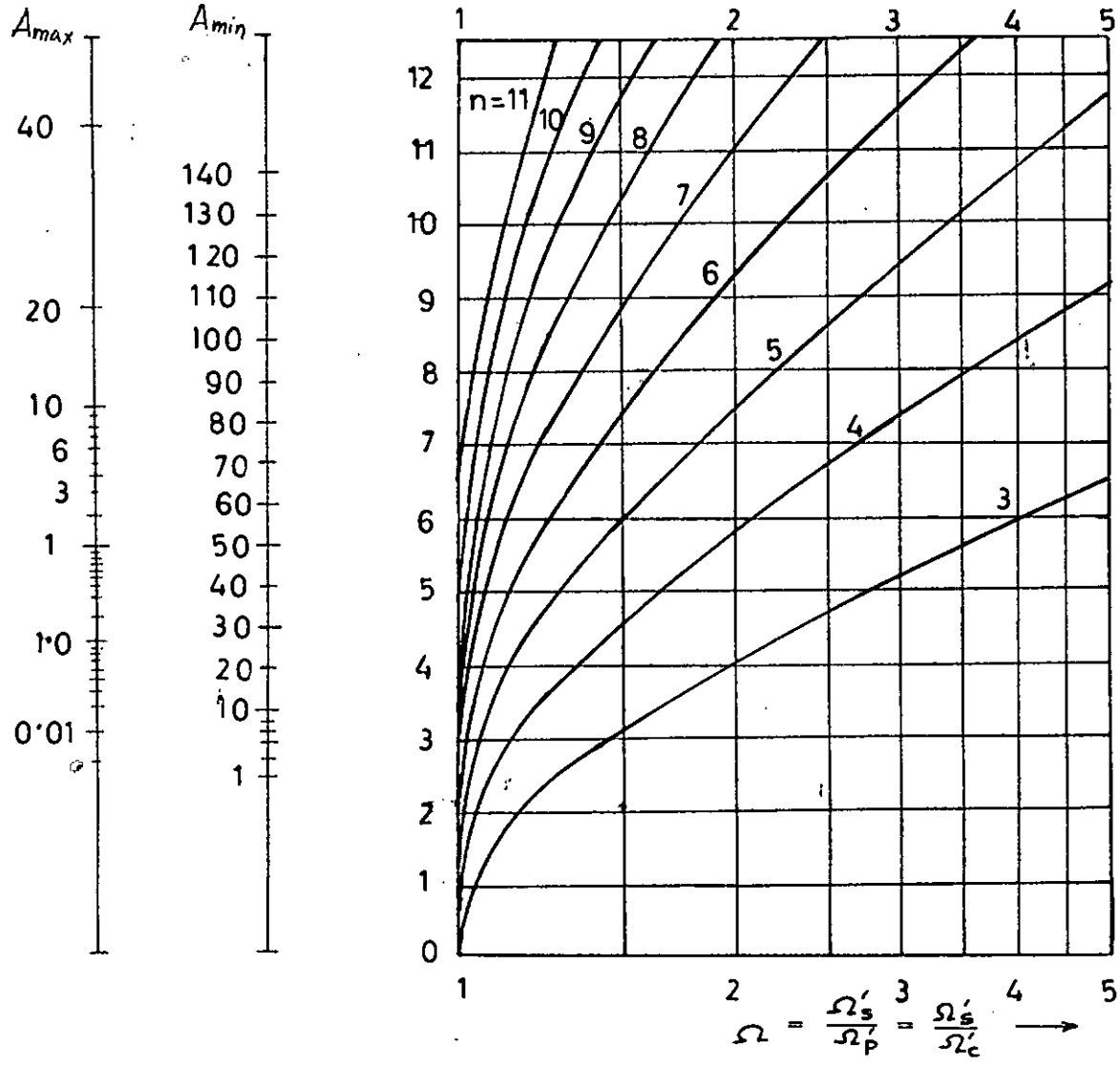

Fig. 5·3 Nomograph for determining n for elliptic function filters (Ref. 7).

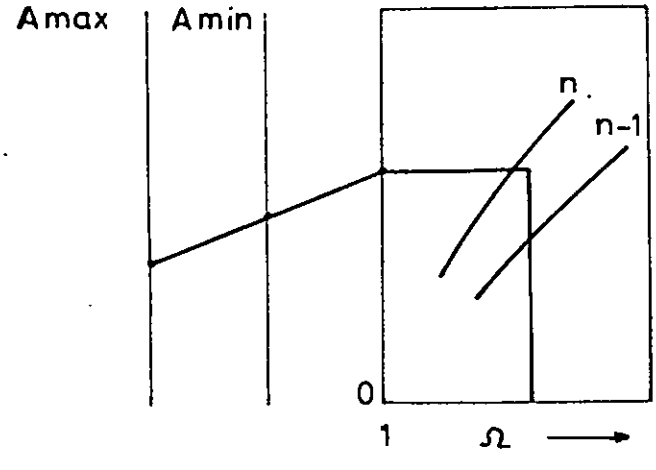

Fig. 5·4 Use of Nomograph.

A_{min} and the steepness $\Omega = \frac{\Omega_s'}{\Omega_p'}$ is prescribed for a particular lowpass filter we can immediately find out the value of the filter complexity n by the following procedure.

A straight line is drawn from the value of A_{max} permitted through the desired value of attenuation in the stopband (A_{min}). The line runs up to the third vertical line and is then rotated to run parallel to the Ω -scale. The desired amount of attenuation at a given frequency will be guaranteed if the filtering function is of the order found at the intersection of the vertical line erected from the Ω-scale value and the line which runs parallel to the Ω -scale. If the crossing appears between two curves as shown in Fig.5.4, the order that must be chosen is the largest integer, written above the curve.

C H A P T E R - 6

REALIZATION OF BANDPASS DIGITAL FILTERS FROM LOWPASS ELLIPTIC FUNCTION PROTOTYPE

6.1. INTRODUCTION:

In this chapter a method has been presented to transform odd-order low-pass prototype elliptic function filter into networks that can be realized by stepped digital coupled lines. In section 6.2 low-pass to bandpass frequency transformation is presented. A typical pi-section of the odd-order low-pass prototype elliptic function filter is transformed into bandpass form in section 6.4. The resonated pi-section bandpass network is then realized in the form of two networks of digital coupled lines. The method of achieving transformer coupling at the input and output ports of the digital bandpass filter is also shown in section 6.7. The characteristic admittance matrices for both networks are obtained . The necessity of admittance scaling is discussed in section 6.8.

6.2. THE LOWPASS PROTOTYPE ELLIPTIC FUNCTION FILTER:

Fig. 6.1 shows a cascade of pi-sections of the odd order lowpass prototype elliptic function filter of filter complexity n. First of all we shall consider the realization of a typical pi-section as shown in Fig.6.1 with shunt capacitance Cr-1 and C_{r+1} and with a transmission zero at $\Omega_r = 1/\sqrt{L_r C_r}$.

6.3. LOWPASS-BANDPASS FREQUENCY TRANSFORMATION:

For converting this lumped lowpass filter into a lumped

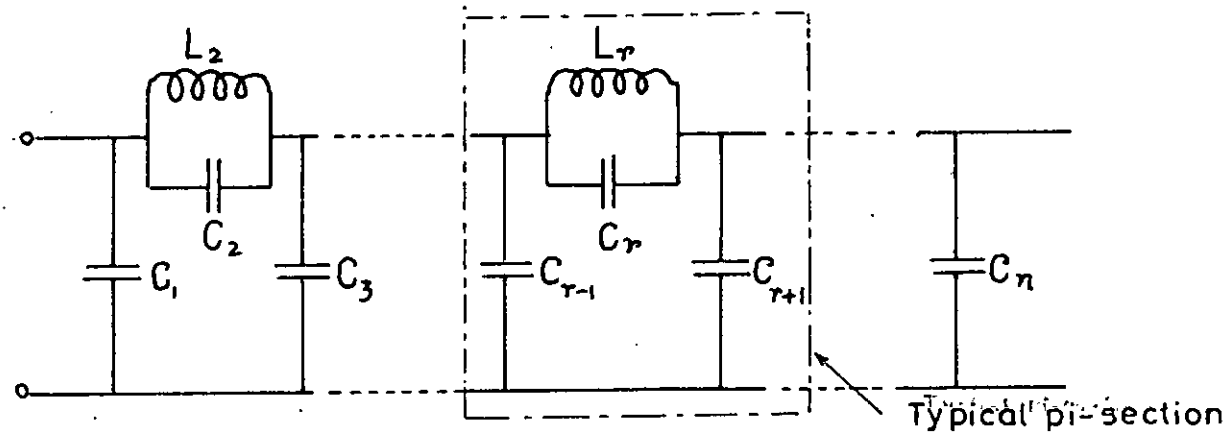

Fig. 6·1 The odd order low pass prototype elliptic function filter.

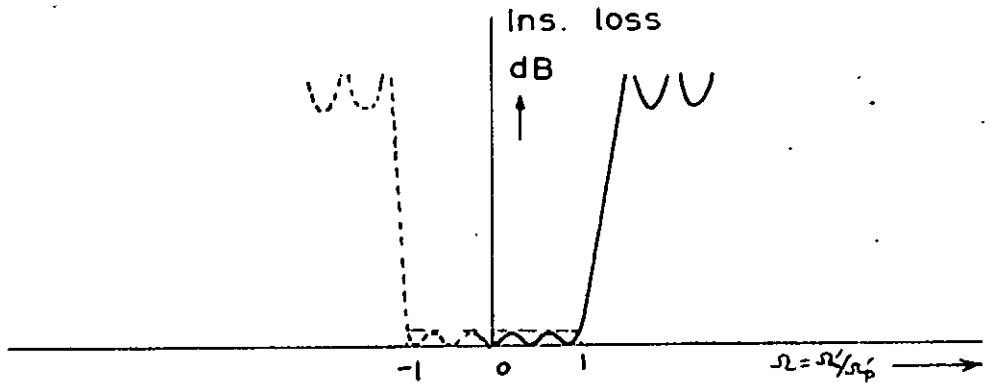

a. Low pass (lumped)

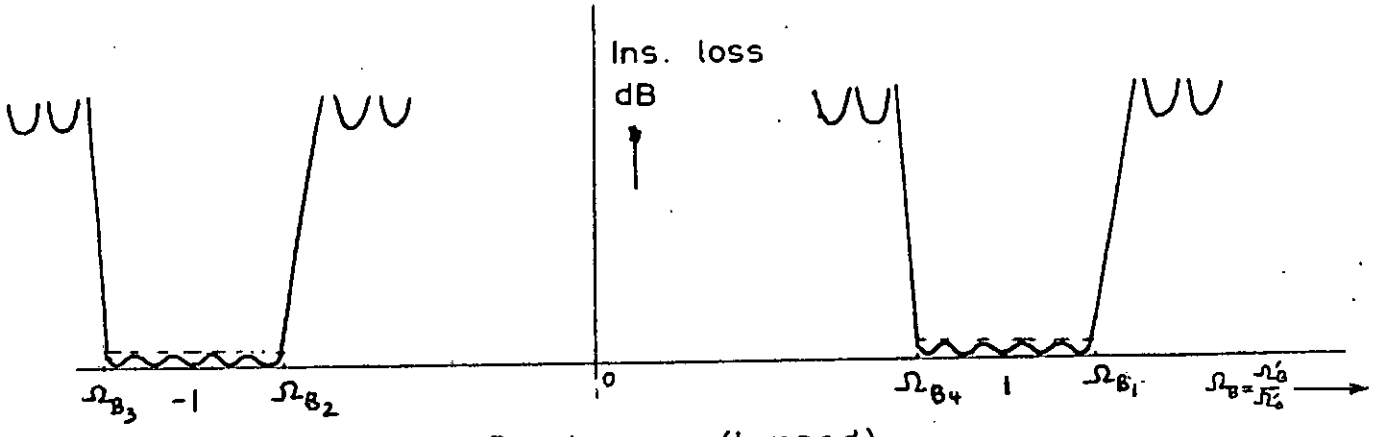

b. Band pass (lumped)

Fig. 6·2. Lumped low-pass and bandpass insertion loss characteristics.

bandpass filter we shall use the lowpass to bandpass transformation

$$\Omega = a\left(\Omega_B - \frac{1}{\Omega_B}\right) \qquad \text{.....(6.1a)}$$

where $\Omega = \frac{\Omega'}{\Omega_{p'}}$ = normalized lowpass frequency.

$\Omega_B = \frac{\Omega_B}{\Omega_{0'}}$ = normalized bandpass frequency, the primed values are actual frequencies. From (6.1a) we get

$$\Omega_B = \frac{\Omega}{2a} \pm \sqrt{\frac{\Omega^2}{4a^2}+1} \qquad \text{.....(6.1b)}$$

The low pass insertion loss (dB) characteristic is shown in Fig.6.2a.

From Eq.(6.1b) we get

for lowpass frequency $\Omega = 0$, $\Omega_B' = \pm\Omega_0$ i.e $\Omega_B = \pm 1$

for low pass frequency $\Omega = 1$, $\Omega_{B_1} = \frac{1}{2a} + \sqrt{\frac{1}{4a^2}+1}$ ..... (6.1c)

$$\Omega_{B_2} = \frac{1}{2a} - \sqrt{\frac{1}{4a^2}+1}$$

for low pass frequency $\Omega = -1$, $\Omega_{B_3} = -\frac{1}{2a} - \sqrt{\frac{1}{4a^2}+1}$

$$\Omega_{B4} = -\frac{1}{2a} + \sqrt{\frac{1}{4a^2}+1}$$

The bandpass insertion loss (dB) characteristic is shown in Fig.6.2b. Here we get $\Omega_{B_1} - \Omega_{B4} = \frac{1}{a}$

also $\Omega_{B_2} - \Omega_{B_3} = \frac{1}{a}$ ...(6.1d)

In order to convert this bandpass response of lumped network into that of distributed network we apply the transformation $\Omega_B = \tan\beta l$ where l is the length of the transmission lines of the distributed bandpass filter and $\beta = \frac{2\pi}{\lambda}$ is the propagation constant. To assume the length of the lines to be equal to one eighth wave length at the band center frequency i.e. $l = \lambda_0/8$

$$\therefore \beta l = \frac{2\pi}{\lambda} \cdot \frac{\lambda_0}{8} = \frac{\pi f'}{4 f_0'} = \frac{\pi \omega'}{4\omega_0}$$

where ω_0' is the ffequency at which the transmission lines of the filter are one eighth wave length.

If we now normalise the band center frequency ω_0' to $\pi/4$; βl becomes equal to ω where ω corresponds to the frequency scale in which the center frequency is $\frac{\pi}{4}$. Therefore the transformation now becomes $\Omega_B = \tan\omega$

i.e. $S = j\Omega_B = j\tan\omega$ .....(6.2)

where $\omega = \frac{\pi\omega'}{4\omega_0'}$ = the normalized bandpass frequency of the distributed network filter. A plot of Ω_B Vs. ω is given in Fig.6.3a. The repetetive characteristic of $\tan\omega$ with respect to Ω_B makes the band pass insertion loss characteristic of Fig.6.2b a repetitive one as shown in Fig.6.3b. The period is $\omega = \pi$.

Therefore the complete low-pass (lumped network) to the band-pass (distributed network) frequency transformation is actually

$$\Omega = a\left(\tan\omega - \frac{1}{\tan\omega}\right) \qquad \text{.....(6.3a)}$$

The band center frequency is thus normalized to $\omega = \pi/4$ and the band edge frequencies $\omega = \omega_c$ and $\omega = \frac{\pi}{2} - \omega_c$, $(\omega_c < \pi/4)$

In the above equation we can find the value of 'a' since we know that $\frac{1}{a} = \Omega_{B_1} - \Omega_{B4}$

Now $\frac{1}{a} = \tan\left(\frac{\pi}{2} - \omega_c\right) - \tan\omega_c$

$$= \cot\omega_c - \tan\omega_c = \frac{1-\tan^2\omega_c}{\tan\omega_c} = \frac{2}{\tan 2\omega_c}$$

$$\therefore a = \frac{\tan 2\omega_c}{2} \qquad \text{.....(6.3b)}$$

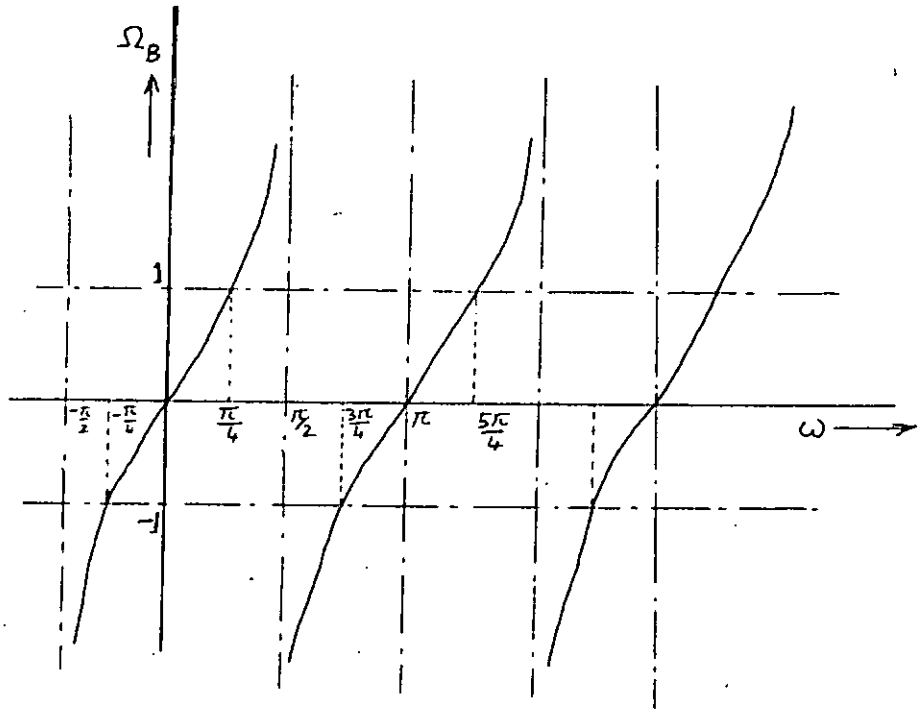

Fig. 6·3a. Plot of Ω_B vs. ω

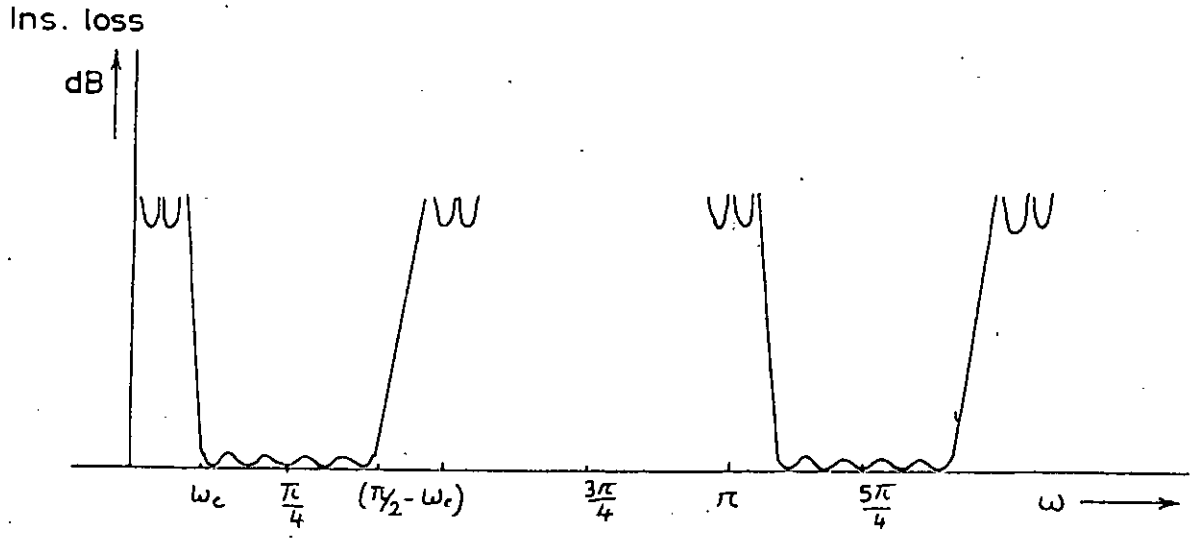

Fig. 6·3b. Repetative bandpass characteristic of the distributed bandpass filter.

Applying the low pass to bandpass transformation to one of the low-pass pi-section it will now be shown that this procedure has theoretically doubled the degree of the network. But ultimately it will be seen that by using the proposed stepped digital realisation the number of non-redundant coupled lines necessary to realize any given filter is equal to the degree of the low-pass prototype.

6.4. BANDPASS TRANSFORMATION OF A SINGLE PI-SECTION OF THE LOW-PASS PROTOTYPE

Let us consider the central pi-section of the lowpass prototype filter of Fig.6.1 which is again shown in Fig. 6.4.

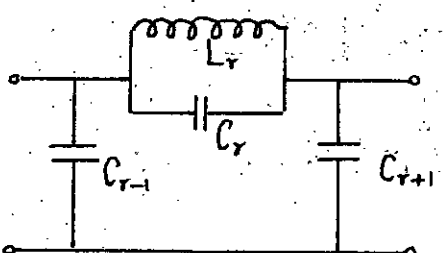

Fig.6.4. Typical pi-section of the odd order lowpass prototype elliptic function filter.

Let us rewrite equation (6.1)

$$\Omega = a\left(\Omega_B - \frac{1}{\Omega_B}\right) \qquad \ldots\ldots\ldots(6.4)$$

where $\Omega_B = \tan\omega$

We shall now apply this transformation to the single lowpass section of Fig.6.4.

Z_r = impedance of the branch containing L_r and C_r

$$= \frac{(j\Omega L_r)\left(\frac{1}{j\Omega C_r}\right)}{j\left(\Omega L_r - \frac{1}{\Omega C_r}\right)} = \frac{-j\Omega L_r}{\Omega^2 L_r C_r - 1} \qquad (6.5)$$

applying the lowpass-bandpass transformation of Eq.(6.4) we get.

$$Z_r = -j\,\frac{a\left(\Omega_B - \frac{1}{\Omega_B}\right)L_r}{a^2\left(\Omega_B - \frac{1}{\Omega_B}\right)^2 L_r C_r - 1}$$

$$= \frac{a\left(j\Omega_B - j\frac{1}{\Omega_B}\right)L_r}{a^2\left(j\Omega_B - j\frac{1}{\Omega_B}\right)^2 L_r C_r + 1}$$

$$= \frac{a\left(s + \frac{1}{s}\right)L_r}{a^2\left(s + \frac{1}{s}\right)^2 L_r C_r + 1} \qquad \text{where, } s = j\Omega_B$$

$$= \frac{a\left(\frac{s^2+1}{s}\right)L_r}{\frac{a^2\left(s^4+1+2s^2\right)L_r C_r + s^2}{s^2}}$$

$$= \frac{\frac{a}{C_r}\,s(s^2+1)}{a^2\left[s^4+2s^2+1+\frac{\Omega_r^2}{a^2}s^2\right]} \qquad \text{where, } \Omega_r = \frac{1}{\sqrt{L_r C_r}}$$

$$= \frac{\frac{1}{aC_r}\,s(s^2+1)}{s^4+\left(2+\frac{\Omega_r^2}{a^2}\right)s^2+1}$$

Equating the demominator to zero we get

$$s^2 = \frac{-\left(\frac{\Omega_r^2}{a^2}+2\right) \pm \sqrt{\left(2+\frac{\Omega_r^2}{a^2}\right)^2 - 4}}{2}$$

$$= -\left[\frac{\Omega_r^2}{2a^2}+1\right] \pm \sqrt{\frac{\Omega^4}{4a^4} + \frac{\Omega_r^2}{a^2}}$$

$$= \frac{\Omega_r^2}{a}\left[\left(-\frac{\Omega_r}{2a} + \frac{a}{\Omega_r}\right) \pm \sqrt{\frac{\Omega_r^2}{4a^2}+1}\right] \qquad \cdots \qquad (6.6)$$

$$\therefore \quad S_1^2 = \frac{\Omega_r}{a}\left[-\frac{\Omega_r}{2a} - \frac{a}{\Omega_r} + \sqrt{\left(\frac{\Omega_r}{2a}\right)^2 + 1}\right] \quad \ldots\ldots \quad (6.7a)$$

and $$S_2^2 = \frac{\Omega_r}{a}\left[-\frac{\Omega_r}{2a} - \frac{a}{\Omega_r} - \sqrt{\left(\frac{\Omega_r}{2a}\right)^2 + 1}\right] \quad \ldots\ldots \quad (6.7b)$$

We can rewrite the above equation, as follows

$$S_1^2 = \frac{\Omega_r}{a}\left[-\frac{a}{\Omega_r} + \lambda_{r-}\right] \quad \ldots\ldots \quad (6.8a)$$

$$S_2^2 = \frac{\Omega_r}{a}\left[-\frac{a}{\Omega_r} - \lambda_{r+}\right] \quad \ldots\ldots \quad (6.8b)$$

where, $$\lambda_{r+} = \sqrt{\left(\frac{\Omega_r}{2a}\right)^2 + 1} + \frac{\Omega_r}{2a} \quad \ldots\ldots \quad (6.9a)$$

$$\lambda_{r-} = \sqrt{\left(\frac{\Omega_r}{2a}\right)^2 + 1} - \frac{\Omega_r}{2a} \quad \ldots\ldots \quad (6.9b)$$

Now we can write

$$Z_r' = \frac{Z_r}{\frac{1}{aC_r}} = \frac{s(s^2+1)}{(s^2-s_1^2)(s^2-s_2^2)} = \frac{K_1' s}{s^2-s_1^2} + \frac{K_2' s}{s^2-s_2^2} = Z_{r_1}' + Z_{r_2}' \quad \ldots(6.10)$$

$$\therefore \quad K_1' = \left.\frac{s^2+1}{s^2-s_2^2}\right|_{s^2=s_1^2} = \frac{\frac{\Omega_r}{a}\left[\lambda_{r-} - \frac{a}{\Omega_r}\right] + 1}{\frac{\Omega_r^2}{a}\left[\lambda_{r-} - \frac{a}{\Omega_r}\right] - \frac{\Omega_r}{a}\left[\frac{-a}{\Omega_r} - \lambda_{r+}\right]}$$

$$= \frac{\frac{\Omega_r}{a}\lambda_{r-}}{\frac{\Omega_r}{a}\lambda_{r-} + \frac{\Omega_r}{a}\lambda_{r+}} = \frac{\lambda_{r-}}{\lambda_{r-} + \lambda_{r+}} = \frac{\lambda_{r-}\lambda_{r+}}{\lambda_{r+}^2 + \lambda_{r-}\lambda_{r+}}$$

$$= \frac{1}{1 + \lambda_{r+}^2} \quad \ldots\ldots \quad \ldots\ldots \quad (6.11)$$

since from Eq.(6.9) it follows that $\lambda_{r+}\lambda_{r-} = 1$

similarly

$$K_1' = \frac{S^2+1}{S^2-S_1^2}\Bigg|_{S^2=S_2^2} = \frac{\lambda_{r+}}{\lambda_{r+}+\lambda_{r-}} = \frac{1}{1+\lambda_{r-}^2} \quad \ldots\ldots (6\cdot12)$$

$$\therefore \quad Z_{r_1} = \frac{Z_{r_1}'}{aC_r} = \frac{1}{aC_r}\,\frac{K_1' S}{S^2-S_1^2}$$

putting the value of S_1^2 from (6.8a) and the value of K_1' from Eq.(6.11) we get

$$Z_{r_1} = \frac{1}{\frac{(1+\lambda_{r+}^2)S}{\frac{1}{aC_r}} - \frac{\Omega_r}{Sa}\left[\lambda_{r-} - \frac{a}{\Omega_r}\right]\frac{(1+\lambda_{r+}^2)}{\frac{1}{aC_r}}} \quad \ldots(6\cdot13)$$

It is thus clearly seen that Z_{r1} contains an inductance L_{r-} and a capacitance C_{r-} in parallel and their values are given by

$$C_{r-} = \frac{1+\lambda_{r+}^2}{\frac{1}{aC_r}} = aC_r(1+\lambda_{r+}^2) \quad \ldots\ldots (6\cdot14a)$$

$$L_{r-} = \frac{\frac{1}{aC_r}}{\frac{\Omega_r}{a}\left[\frac{a}{\Omega_r} - \lambda_{r-}\right]\left[1+\lambda_{r+}^2\right]}$$

$$= \frac{1}{C_r\Omega_r\left[\frac{a}{\Omega_r} + \frac{a}{\Omega_r}\lambda_{r+}^2 - \lambda_{r-} - \lambda_{r-}\lambda_{r+}^2\right]}$$

putting the values of λ_{r+} and λ_{r-} in λ_{r+}^2 and $\lambda_{r-}\lambda_{r+}^2$ in the above equation we get

$$L_{r-} = \frac{1}{aC_r\left[1+\lambda_{r-}^2\right]} \quad \ldots\ldots \quad \ldots\ldots \quad (6\cdot14b)$$

similarly from (6;10)

$$Z_{r_2} = \frac{1}{aC_r} \quad Z'_{r_2} = \frac{1}{aC_r} \frac{K'_2 S}{S^2 - S_2^2} \qquad \ldots \qquad \ldots \qquad (6{\cdot}15)$$

putting the value of S^2_2 and K'_2 we get

$$Z_{r_2} = \frac{1}{\dfrac{S \cdot aC_r}{(1+\lambda_{r-}^2)} - \dfrac{\dfrac{\Omega_r}{a}\left[-\dfrac{a}{\Omega_r} - \lambda_{r+}\right](1+\lambda_{r-}^2)}{\dfrac{S}{aC_r}}} \qquad \ldots (6{\cdot}16)$$

It is thus seen that Z_{r2} contains a capacitance C_{r+} and an inductance L_{r+} in parallel

$$\therefore C_{r+} = \frac{1+\lambda_{r-}^2}{\frac{1}{aC_r}} = aC_r(1+\lambda_{r-}^2) \qquad \ldots \qquad (6{\cdot}17a)$$

and

$$L_{r+} = \frac{\frac{1}{aC_r}}{\frac{\Omega_r}{a}\left[\frac{\Omega a}{\Omega_r} + \lambda_{r+}\right]\left[1+\lambda_{r-}^2\right]}$$

$$= \frac{1}{C_r \Omega_r \left[\frac{a}{\Omega_r} + \frac{a}{\Omega_r}\lambda_{r-}^2 + \lambda_{r+} + \lambda_{r+}\lambda_{r-}^2\right]}$$

$$= \frac{1}{aC_r\left[1+\lambda_{r+}^2\right]} \qquad \ldots \qquad \ldots (6{\cdot}17b)$$

Now applying this transformation to the shunt capacitance of the low-pass pisection

$$Z_{c_1} = \frac{1}{j\Omega C_{r-1}}$$

becomes

$$\frac{1}{ja(\Omega_B - \frac{1}{\Omega_B})C_{r-1}}$$

$$= \frac{1}{j\Omega_B a C_{r-1} + \frac{1}{j\frac{\Omega_B}{aC_{r-1}}}} \qquad (6.18)$$

Therefore this Z_{c1} contains an inductance L'_{r-1} and a capacitance C'_{r-1} in parallel. It follows from Eq. (6.18) that

$$L'_{r-1} = \frac{1}{aC_{r-1}} \qquad (6.19a)$$

and $$C'_{r-1} = aC_{r-1} \qquad (6.19b)$$

$$\therefore \quad L'_{r-1} = \frac{1}{C'_{r-1}} \qquad (6.19c)$$

Similarly we can also write for Z_{c2}

$$C'_{r+1} = aC_{r+1} \qquad (6.20a)$$

and

$$L'_{r+1} = \frac{1}{C'_{r+1}} \qquad (6.20b)$$

It is therefore clear that we get the circuit of Fig.6.6 after applying the lowpass to bandpass frequency transformation to the single pi-section of the low-pass prototype elliptic function filter. The circuit values are given by Equations (6.9a), (6.9b), (6.14a), (6.14b), (6.17a), (6.17b), (6.19b), (6.19c), (6.20a) and (6.20b).

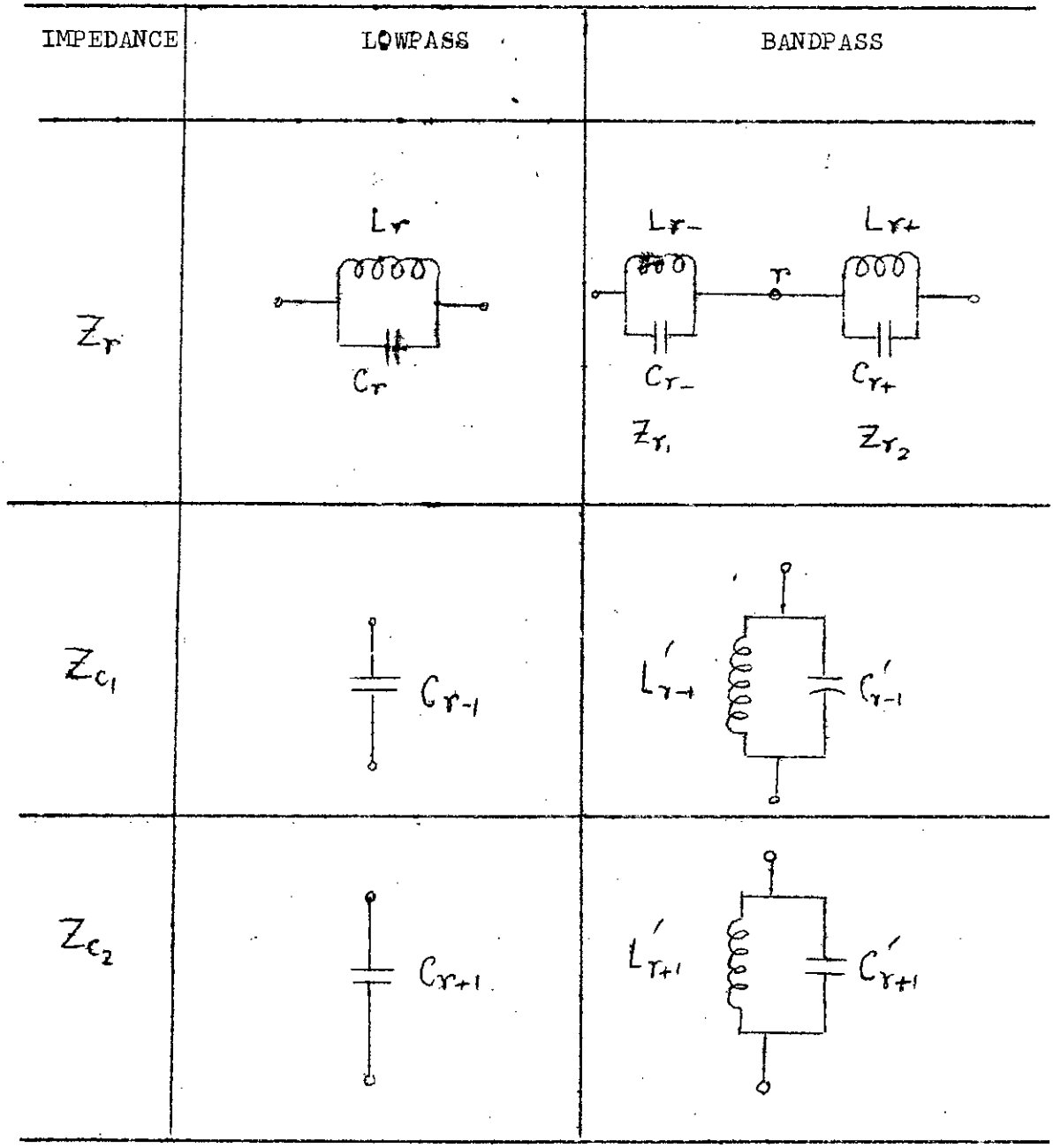

Fig.6.5 Lowpass to bandpass transformation.

The resonated pi-section shown in Fig.6.6 can now be considered as the result of the shunt connection of Network -1 and Network-2 of Fig.6.7 at nodes r-1, r and r+1. It is clear that the structure of these two networks are identical with those of the networks shown in Fig.4.2a and Fig.4.3a. We shall now realise physically both network-1 and network-2 in distributed network form with the digital lines. After realising the two networks we will connect the two networks in shunt.

6.5. REALIZATION OF NETWORK-1 AND NETWORK-2 BY DIGITAL LINES:

In chapter-4 we have seen the physical realization of S-plane networks like network-1 and network-2 of Fig.6.7. From the discussions in chapter-4 it is seen that the network-1 can be realised in the form of three digital lines, all of them grounded at one end and opencircuited at the other end as shown in Fig.4.2. Network-2 can be realized in the form of three digital lines all of them open circuited at both ends as shown in Fig.4.3. Fig.6.8 clearly shows both the networks after shunt connection.

The characteristic admittance matrices of network-1 and network-2 may therefore, be written in the $\Omega = j\Omega_R = j \tan\omega$ plane as follows:

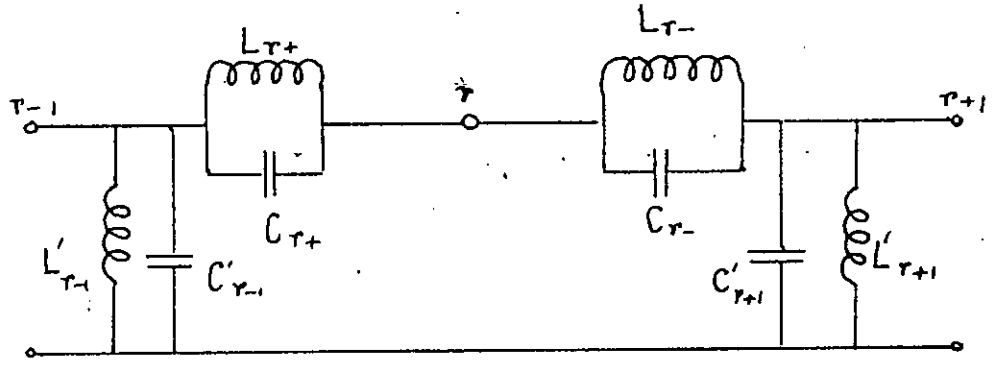

Fig. 6·6. A typical resonated pi - section

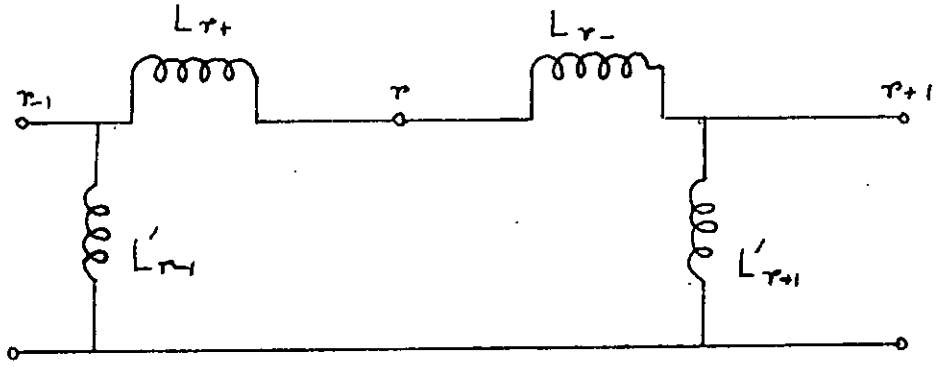

a. Network 1

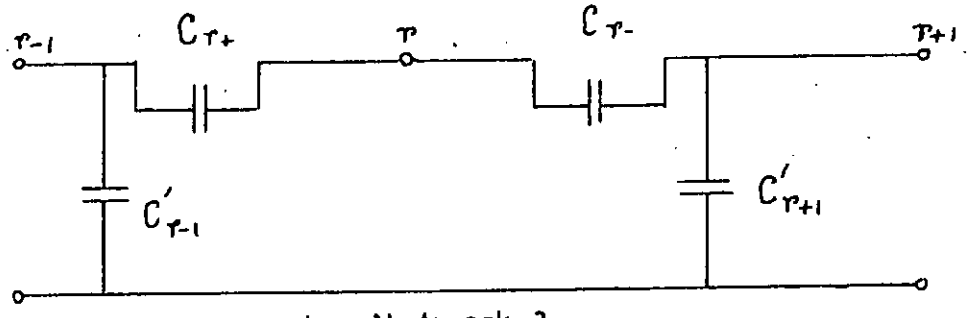

b. Network 2

Fig. 6·7 Splitting the resonated pi-section into Network 1 and Network 2.

Network 1 :

$$\begin{matrix} & (r-1) & (r) & (r+1) \\ \end{matrix}$$

$$\begin{bmatrix} \frac{1}{L_{r+}} + \frac{1}{L'_{r-1}} & -\frac{1}{L_{r+}} & 0 \\ \frac{1}{L_{r+}} & \frac{1}{L_{r+}} + \frac{1}{L_{r-}} & -\frac{1}{L_{r-}} \\ 0 & -\frac{1}{L_{r-}} & \frac{1}{L_{r-}} + \frac{1}{L'_{r+1}} \end{bmatrix} \qquad (6.21a)$$

Network 2 :

$$\begin{matrix} & (r-1) & (r) & (r+1) \end{matrix}$$

$$\begin{bmatrix} C_{r+} + C'_{r-1} & -C_{r+} & 0 \\ -C_{r+} & C_{r+} + C_{r-} & -C_{r-} \\ 0 & -C_{r-} & C_{r-} + C'_{r+1} \end{bmatrix} \qquad (6.22a)$$

Using Eqns. (6.14a),(6.14b),(6.17b),(6.19a),(6.19b),(6.20a), (6.20b);

from the above matrices we can write the following matrices.

Network 1 :

$$\begin{matrix} & (r-1) & (r) & (r+1) \end{matrix}$$

$$\begin{bmatrix} a\left[C_{r-1} + C_r\left(1+\lambda^2_{r+}\right)\right] & -aC_r\left(1+\lambda^2_{r+}\right) & 0 \\ -aC_r\left(1+\lambda^2_{r+}\right) & aC_r\left(2+\lambda^2_{r+}+\lambda^2_{r-}\right) & -aC_r\left(1+\lambda^2_{r-}\right) \\ 0 & -aC_r\left(1+\lambda^2_{r-}\right) & a\left[C_{r+1} + C_r\left(1+\lambda^2_{r-}\right)\right] \end{bmatrix} \qquad (6.21b)$$

Network 2 :

$$\begin{matrix} & (r-1) & (r) & (r+1) \end{matrix}$$

$$\begin{bmatrix} a\left[C_{r-1} + C_r\left(1+\lambda^2_{r-}\right)\right] & -aC_r\left(1+\lambda^2_{r-}\right) & 0 \\ -aC_r\left(1+\lambda^2_{r-}\right) & aC_r\left(2+\lambda^2_{r+}+\lambda^2_{r-}\right) & -aC_r\left(1+\lambda^2_{r+}\right) \\ 0 & -aC_r\left(1+\lambda^2_{r+}\right) & a\left[C_{r+1} + C_r\left(1+\lambda^2_{r+}\right)\right] \end{bmatrix} \qquad (6.22b)$$

The characteristic admittance of line r to ground is not finite at this moment. This can be made finite by scaling the admittance level of the center rows and columns in the above matrices by a factor greater than unity. In order to get the capacitance matrix from these characteristic admittance matrices, we need to multiply each element of matrices (6.21) and (6.22) by η_0. Hence it can now be said that this type of admittance scaling has been shown in chapter-3 and chapter-4. From previous discussions it follows that this operation does not alter the external performance of the section between nodes r-1 and r+1 if the same scaling factor is used on both networks. The distance between adjacent lines of one network must approximately be equal to the distance between corresponding lines on the other network, in order to obtain simple physical interconnections. This condition is necessary for physical realization other than the normal hyperdominancy condition as mentioned in chapter-3 in Equation(3.13).

It is therefore clear from matrices (6.21) and (6.22) that the admittance to ground of lines r on both networks 1 and 2 will be the same after necessary admittance scaling. Also since the sum of the coupling element values between lines r-1 and r, r and r+1 are almost same for both networks, the distance between lines r-1 and r+1 must inherently be approximately equal. In addition, since λ_{r+} and λ_{r-} are of the order of unity, the physical separation in a transverse direction of lines r on both networks must necessarily be small.

6.6. LINE CONDENSATION:

We have just seen how each of the basic resonated pi-sections

in the bandpass microwave elliptic function filter may be constructed utilizing a pair of 3-wire digital lines. Often it will be necessary to have interconnections of two or more than two basic resonated pi-section for filters having higher n.

If any pair of conductors in a uniform n-wire line are at the same potential at both ends, then at any intermediate point they are at the same potential and may consequently be replaced by a single line. For the overall filter, the interconnection of consecutive sections requires that the node at the junction of the outer pair of lines of one section be at the same potential as the node at the junction of the corresponding pair of lines of the adjacent section. Since the opposite ends of the lines in network-1 are short circuited to ground, and therefore at the same zero potential, the appropriate pair of lines from adjacent sections in network-1 may be condensed into a single line.

The opposite ends of the lines in network-2 are open circuited, and therefore not necessarily at the same potential. For this reason this simple principle may not be applied directly. However it may be shown that a sufficient condition for the condensation of open-circuited lines together at one end is that neither line couples directly nor indirectly to any other line which is not also open circuited. This property is of fundamental importance when consideration is given to the method of transformer coupling into the network at the input and output ports.

As an example of the line condensation procedure for a two s section (fifth degree) filter the overall network reduces to a pair of

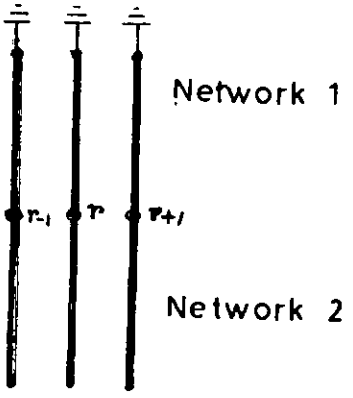

Fig. 6·8 The coupled line realization of the basic resonated section.

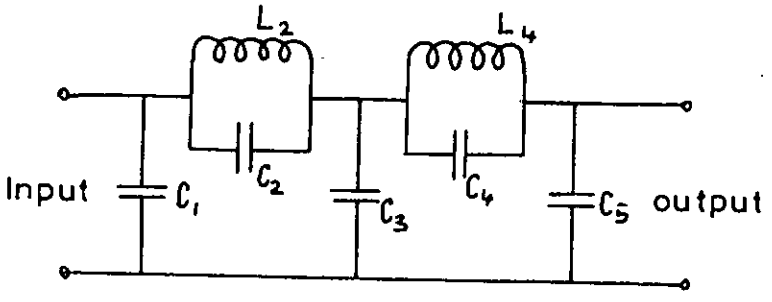

Fig. 6·9a. Lowpass prototype elliptic function filter for n = 5

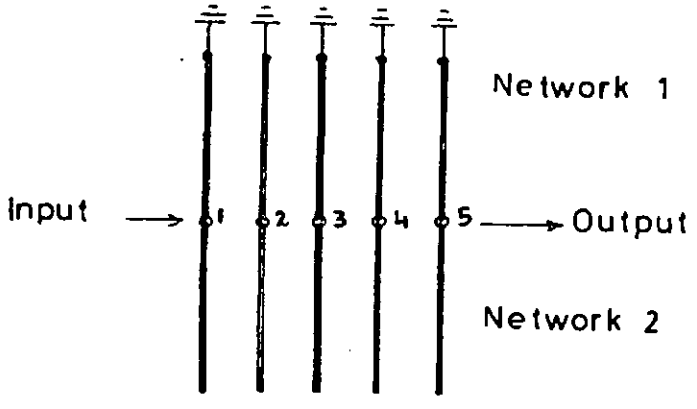

Fig. 6·9b. Realization of a two section filter (n = 5) in digital lines form.

five wire lines as shown in Fig.6.9b.

The lowpass prototype elliptic function filter for n=5 is shown in Fig.6.9a. Following the procedures whose details have been given in sections 6.2 to 6.5 andfollowing the procedure of line condensation the lowpass prototype of Fig.6.9a can be converted to the stepped digital network shown in Fig.6.9b.

The characteristic admittance matrices of thetwo networks(network-1 and network-2) for this case of n=5 are given below.The values of λ_{2+}, λ_{2-}, λ_{4+}, λ_{4-} and other necessary values can be found out from the relations given in section 6.4.

Network 1:

$$\begin{bmatrix} a[C_1+C_2(1+\tilde{\lambda}_{2+}^2)] & -aC_2(1+\tilde{\lambda}_{2+}^2) & 0 & 0 & 0 \\ -aC_2(1+\tilde{\lambda}_{2+}^2) & aC_2(2+\tilde{\lambda}_{2+}^2+\tilde{\lambda}_{2-}^2), & -aC_2(1+\tilde{\lambda}_{2-}^2) & 0 & 0 \\ 0 & -aC_2(1+\tilde{\lambda}_{2-}^2) & a[C_3+C_2(1+\tilde{\lambda}_{2-}^2)+C_4(1+\tilde{\lambda}_{4+}^2), & -aC_4(1+\tilde{\lambda}_{4+}^2), & 0 \\ 0 & 0 & -aC_4(1+\tilde{\lambda}_{4+}^2), & a(2+\tilde{\lambda}_{4+}^2+\tilde{\lambda}_{4-}^2), & -aC_4(1+\tilde{\lambda}_{4-}^2) \\ 0 & 0 & 0 & -aC_4(1+\tilde{\lambda}_{4-}^2), & a[C_5+C_4(1+\tilde{\lambda}_{4-}^2)] \end{bmatrix} \quad (6.23)$$

Network 2:

$$\begin{bmatrix} a[C_1+C_2(1+\tilde{\lambda}_{2-}^2), & -aC_2(1+\tilde{\lambda}_{2-}^2) & 0 & 0 & 0 \\ -aC_2(1+\tilde{\lambda}_{2-}^2), & aC_2(2+\tilde{\lambda}_{2+}^2+\tilde{\lambda}_{2-}^2), & -aC_2(1+\tilde{\lambda}_{2+}^2) & 0 & 0 \\ 0 & -aC_2(1+\tilde{\lambda}_{2+}^2), & a[C_3+C_2(1+\tilde{\lambda}_{2+}^2)+C_4(1+\tilde{\lambda}_{4-}^2)], & -aC_4(1+\tilde{\lambda}_{4-}^2) & 0 \\ 0 & 0 & -aC_4(1+\tilde{\lambda}_{4-}^2), & aC_4(2+\tilde{\lambda}_{4+}^2+\tilde{\lambda}_{4-}^2), & -aC_4(1+\tilde{\lambda}_{4+}^2) \\ 0 & 0 & 0 & -aC_4(1+\tilde{\lambda}_{4+}^2), & a[C_5+C_4(1+\tilde{\lambda}_{4+}^2)] \end{bmatrix} \quad (6.24)$$

We can now say that for an elliptic function filter of degree 5 in the low-pass prototype version the complete network in the bandpass form converts into a pair of uniform digital 5-wire line which are one eighth of a wavelength long at the band-center frequency. In general for an elliptic function filter of degree n, the complete network converts into a pair of uniform digital n-wire lines which are one eighth of a wavelength long at the band center frequency. This pair of digital network is shunt connected and the complete network may be viewed as consisting of a single stepped digital line which is one quarter of a wavelength long at the band center frequency.

6.7. COUPLING AT THE INPUT AND OUTPUT OF THE FILTER:

The input and output terminals are situated at the centers of the first and last lines as shown in Fig.6.9. The direct connection of these points to the external ports would yield a filter with the required electrical response, but the internal elements would be of low impedance. To overcome this problem coupling from ports to the centers of these lines must be made using transformer action. To accomplish this, unit elements are introduced into the network, one at each end, of unity characteristic impedance, and one eighth of a wavelength long at the band center frequency as shown in Fig.6.10. The S-plane equivalent circuit of Fig.6.11 of the interdigital line at the input clearly shows how transformer coupling is achieved[5].

It is to be noted here that the number of lines in network-1

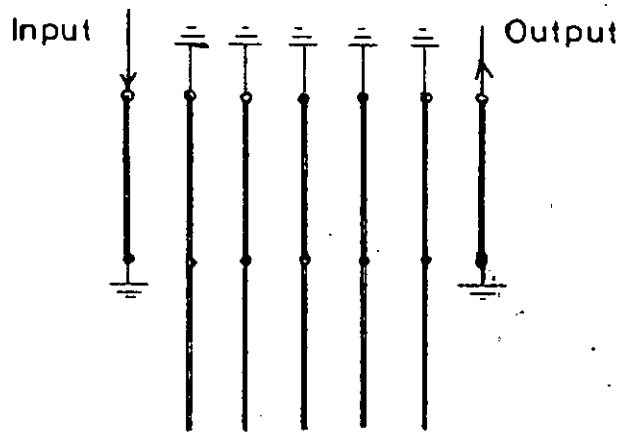

Fig. 6·10. Realization of fifth order filter with transformer coupling elements.

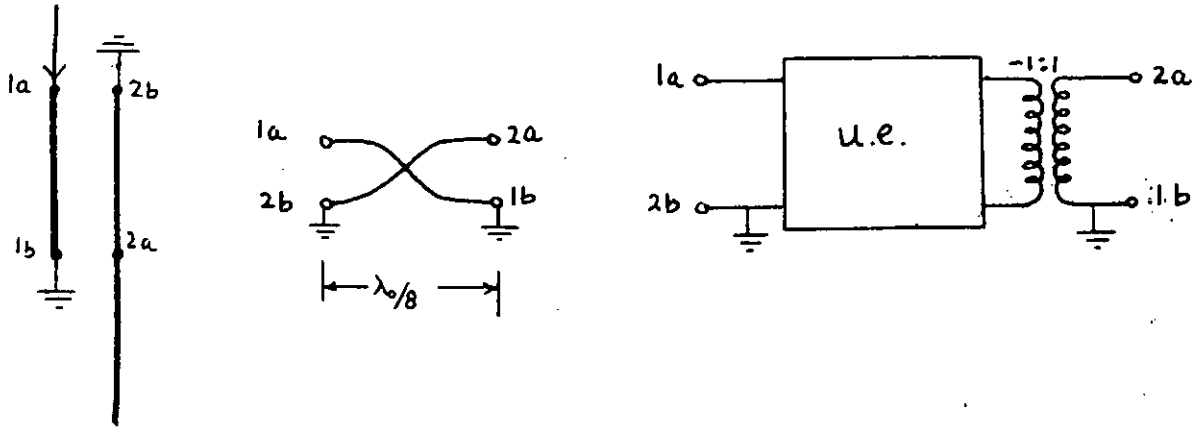

(a) (b) (c)

Fig. 6·11. S-plane equivalent circuit (right) shows how transformer coupling is achieved at the input or output ports.

has now increased to n+2 and its resulting characteristic admittance has now become :

$$\begin{bmatrix} 1 & -1 & 0 & \cdots\cdots \\ -1 & 1+a(C_1+C_2(1+\lambda_{1+}^{\sim})) & -a\,C_2(1+\lambda_{1+}^{\sim}) & \cdots\cdots\cdots \\ 0 & -a\,C_2(1+\lambda_{1+}^{\sim}) & a\,C_2(1+\lambda_{1+}^{\sim}+\lambda_{1-}^{\sim}) & \cdots\cdots\cdots \end{bmatrix} \quad (6.25)$$

But the characteristic admittance matrix of network-2 remains unchanged.

6.6. ADMITTANCE SCALING:

In conventional digital filters admittance scaling is necessary for physical realizability. The scaling factors are normally chosen such that the capacitances to ground of all the lines, except the input and output lines are almost equal. Physically, this results in bars of approximately the same width when a rectangular bar configuration is used . In the present case, however, additional points must be considered. In the case of a single section it is necessary for the complementary lines in networks-1 and 2 to be separated by approximately the same physical distance. The scaling factors should therefore be chosen such that there is a minimum amount of variation in the ground and coupling capacitances throughout both networks -1 and 2. Generally at the begining every line in the stepped digital filter, except the lines on which the input and output ports are situated may be scaled by the factor $1/\sqrt{a}$.

CHAPTER - 7

PHYSICAL DIMENSIONS OF COUPLED RECTANGULAR BARS BETWEEN PARALLEL PLATES:

7. 1. INTRODUCTION:

The characteristic admittance matrix obtained in chapter-6 differs from the static capacitance matrix by a constant factor of η_0. In this chapter the procedures are presented to determine the physical dimensions of the filter in the form of parallel coupled rectangular transmission lines between parallel plates from its static capacitance matrix. The graphs of Getsinger[7] are used for this purpose.

7.2. EVEN AND ODD MODE CAPACITANCES FOR TWO PARALLEL COUPLED TRANSMISSION LINES OF EQUAL WIDTHS:

Fig.7.1a and 7.1b show two parallel coupled rectangular transmission lines of equal width centered between ground plates. Fig.7.1a shows clearly the various capacitances involved in the even mode case and Fig.7.1b shows clearly the various capacitances involved in the odd-mode case. The terms odd mode and even mode capacitances were introduced in chapter-3. The total capacitance of a transmission line of Fig.7.1 is given by the parallel plane capacitances plus appropriate fringing capacitances (Fringing capacitances take into account of the distortion of the field lines in the vicinity of the edges of the rectangular bars).

Thus it can be seen that the total even-mode capacitance c_{oe}/ϵ from one bar to ground is

$$c_{oe}/\epsilon = 2 (c_p/\epsilon + c_{fo}'/\epsilon + c'_f/\epsilon) \quad .....(7.1)$$

and the total odd-mode capacitance c_{oo}/ϵ from one bar to ground is

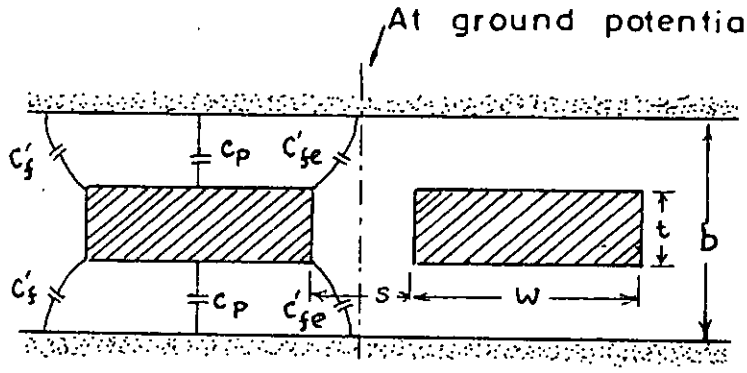

Fig. 7.1a Two parallel coupled rectangular bars between ground planes of equal width showing the capacitances for even mode case.

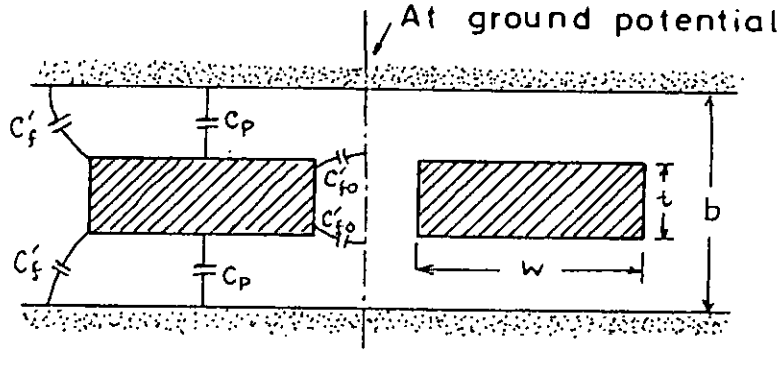

Fig. 7.1b. Two parallel coupled rectangular bars of equal width between ground planes showing the capacitances for odd mode case.

$$c_{oo}/\epsilon = 2\left(c_p/\epsilon + c'_{fo}/\epsilon + c'_f/\epsilon \right) \qquad \text{.....(7.2)}$$

In Eq.(7.1) and Eq.(7.2), c_p is the parallel-plate capacitance from the top or bottom side of one bar to the nearest ground plane; c'_{fe} is the capacitance to ground from one corner and half the associated vertical wall in the coupling region of a bar for even mode excitation; c'_{fo} is the capacitance to ground from one corner and half the associated vertical wall in the coupling region of a bar for odd-mode excitation; and c'_f is the capacitance to ground from one corner and half the associated vertical wall away from the coupling region of a bar for any excitation. From the definitions of even and odd-mode capacitances, we get for the two rectangular bars of Fig.7.1 that the capacitance, $\Delta c/\epsilon$, from one bar to the other is given by

$$\frac{\Delta c}{\epsilon} = \tfrac{1}{2}\left(c_{oo}/\epsilon - c_{oe}/\epsilon \right) \qquad \text{.....(7.3)}$$

Substraction of (7.1) from (7.2) shows that $\frac{\Delta c}{\epsilon}$ can be written entirely in terms of the fringing capacitances as

$$\frac{\Delta c}{\epsilon} = c'_{fo}/\epsilon - c'_{fe}/\epsilon \qquad \text{.....(7.4).}$$

Fig.7.2 is a plot of both even-mode fringing capacitance, c'_{fe}/ϵ, and the capacitance, $\Delta c/\epsilon$ between bars as functions of bar-thickness and spacing, while Fig.7.3 is a similar graph for the odd-mode fringing capacitance, c'_{fo}/ϵ. Fig.7.4 gives the fringing capacitance c'_f/ϵ from the outer edges of the bars as a function of thickness. The parallel plate capacitance c_p/ϵ is given by

$$c_p/\epsilon = 2\,\frac{w/b}{1-t/b} \qquad \text{.....(7.5)}$$

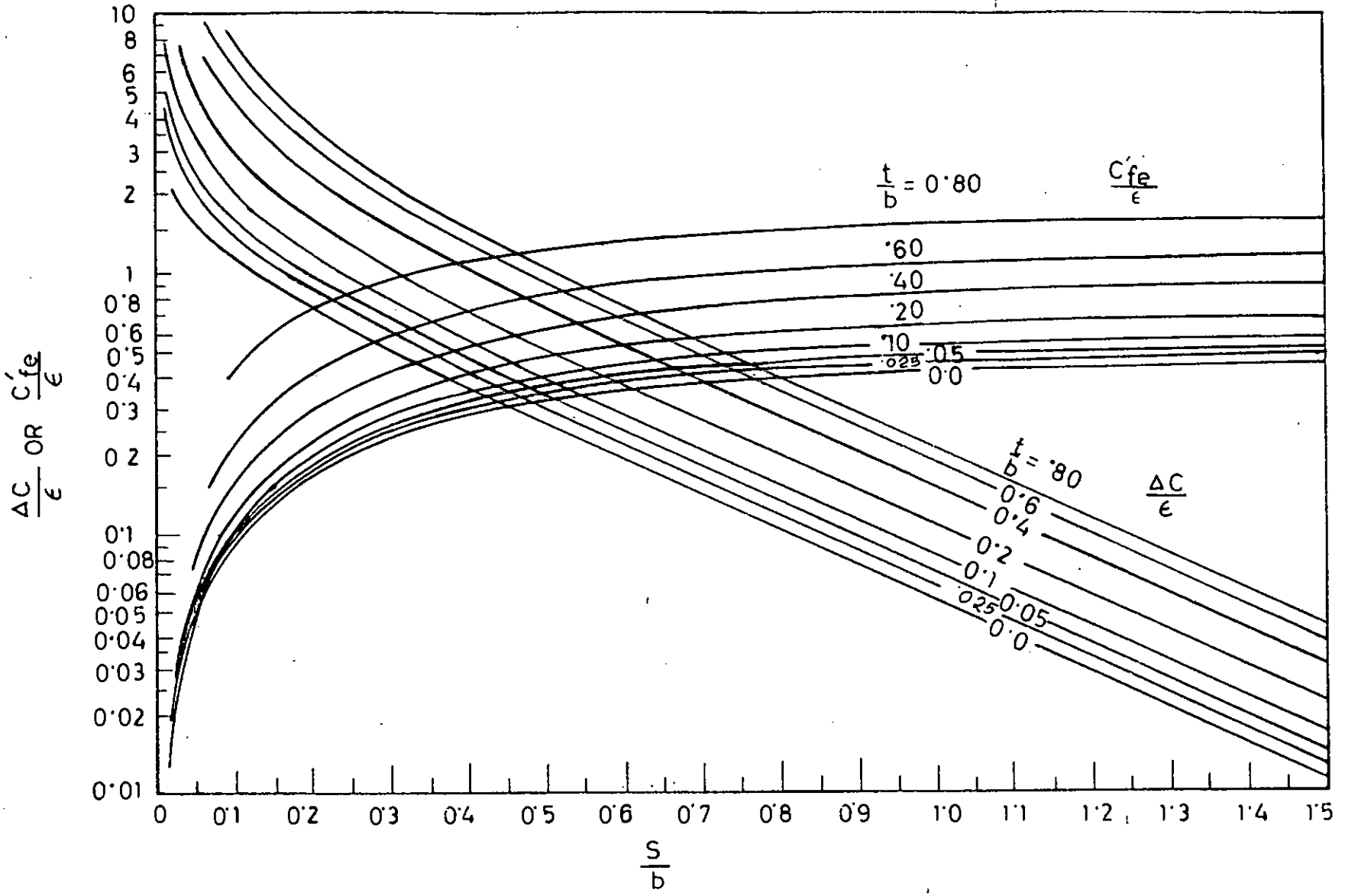

FIG. 7.2 NORMALIZED EVEN MODE FRINGING CAPACITANCE C'_{fe}/ϵ AND INTERBAR CAPACITANCE $\Delta C/\epsilon$ FOR COUPLED RECTANGULAR BARS.

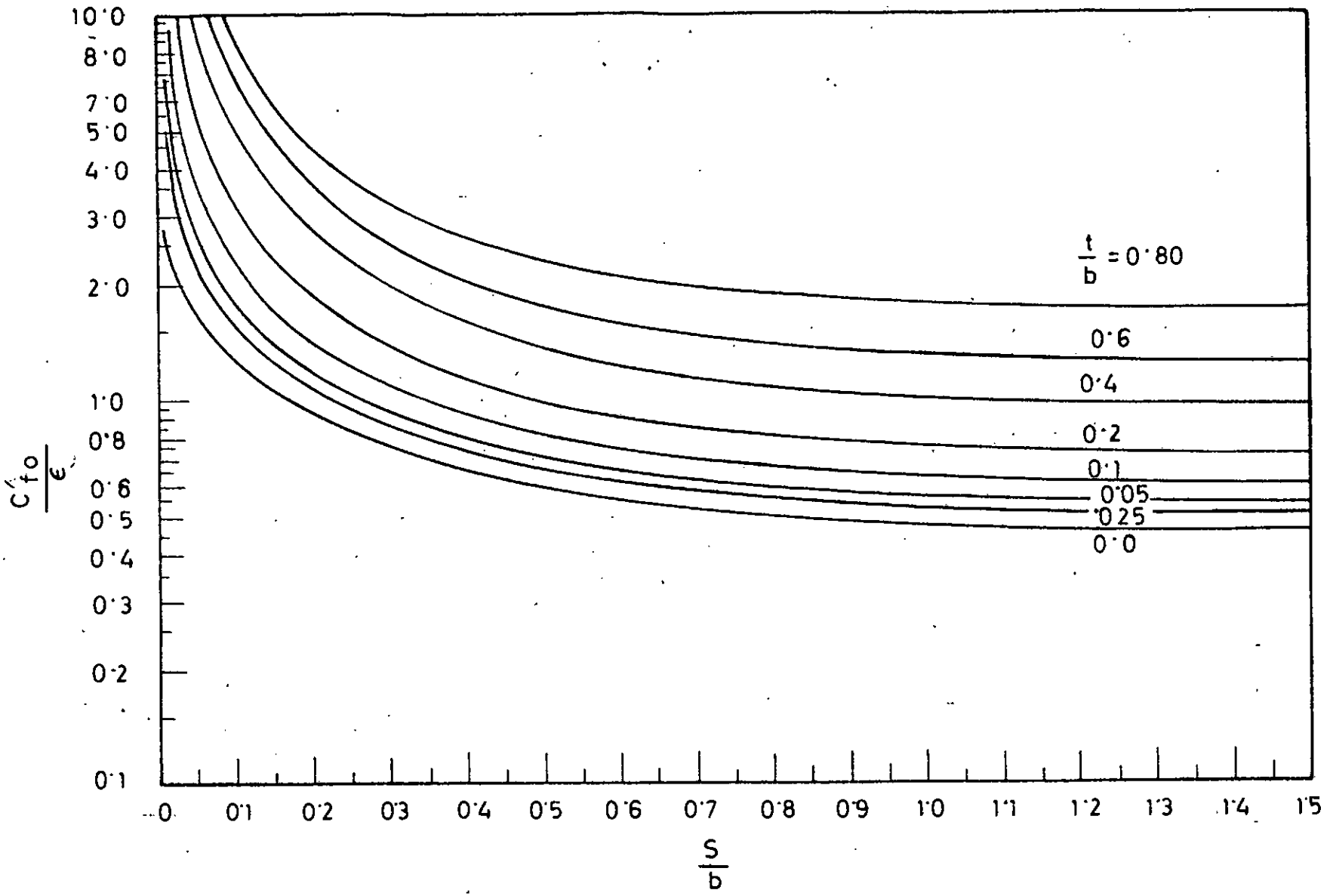

FIG. 7·3 NORMALIZED ODD–MODE FRINGING CAPACITANCE FOR RECTANGULAR BARS.

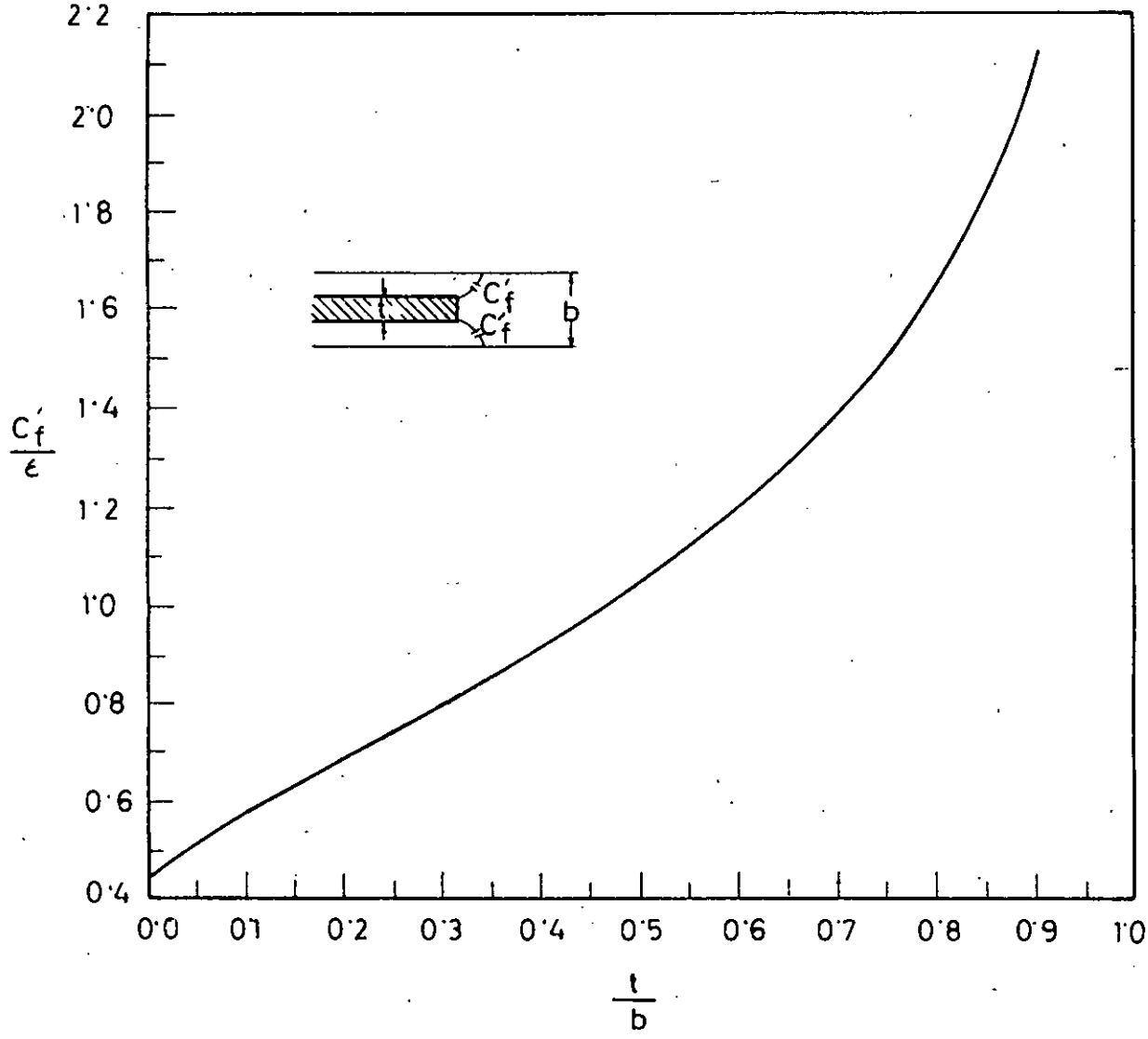

FIG. 7.4. NORMALIZED FRINGING CAPACITANCE FOR ISOLATED RECTANGULAR BAR.

where w and t are the width and thickness of the bar. Through the use of the above relations and figures, it is possible to relate physical dimensions of the given configuration to even-and odd-mode capacitances. Equation(7.5) may be written as follows

$$w/b = \tfrac{1}{2}\,(1-t/b)\left[c_p/\epsilon\right] \qquad \ldots\ldots\ldots\ldots\ldots(7.6)$$

7.3. CALCULATION OF WIDTHS OF THE RECTANGULAR BARS OF EQUAL WIDTHS BETWEEN PARALLEL PLANES

Let us again consider the parallel coupled rectangular bars of equal widths between parallel plates as shown in Fig.7.1.

Putting the value of c_p/ϵ from Equation (7.1) in (7.6) we get

$$w/b = \tfrac{1}{2}\,(1-t/b)\left[c_{\frac{oe}{2}}/\epsilon - c'_{fo}/\epsilon - c'_{f}/\epsilon\right] \qquad \ldots(7.7)$$

In fact we want to calculate the width of the rectangular bars from the capacitance matrix. For this simple case we shall get a 2 by 2 capacitance matrix. Adding a particular row or column of the capacitance matrix gives us the capacitance between the corresponding transmission line and ground. This capacitance is equal to c_{oe}/ϵ (It is assumed that the capacitances of the capacitance matrix are normalized with respect to ϵ). Hence if we write this capacitance equal to c/ϵ we can write the above equation as follows.

$$w/b = \tfrac{1}{2}\,(1-t/b)\left[(c/\epsilon)_{\frac{}{2}} - c'_{fo}/\epsilon - c'_{f}/\epsilon\right] \qquad \ldots(7.8)$$

where c is the capacitance between the transmission line and the ground.

Since both the bars are of equal widths, their capacitance c is also equal.

Hence the width can be calculated if we can find c'_{fo}/ϵ, c'_f/ϵ and also t and b.

7.4. WIDTH CALCULATION FOR TWO UNSYMMETRICAL PARALLEL COUPLED RECTANGULAR BARS BETWEEN GROUND PLANES:

Fig.7.5 shows two rectangular bars of different widths centered between ground planes. Both the bars have the same thickness. Let us call the bar on the left side as line 'a' and the other as line 'b'. The parallel plate capacitance of line 'a' is c_p^a and that of line 'b' is c_p^b. Let us assume that the total capacitance of line 'a' to ground is c_a and that of line 'b' is c_b. We shall call c_{ab} the capacitance between lines 'a' and 'b'. As mentioned before the value of c_a may be obtained by adding the first row or column of the static capacitance matrix for this case and similarly c_b may be obtained by adding the second row or column of the static capacitance matrix for this case. But since c_a and c_b are the summation of appropriate parallel plate capacitance and fringing capacitances from Eq.(7.1) we can write that

$$c_a = 2 (c_p^a + c'_f + c'_{fo})$$

$$c_b = 2 (c_p^b + c'_f + c'_{fo}) \qquad \ldots\ldots\ldots(7.9a)$$

and from Eq.(7.4) we can write

$$c_{ab} = \Delta c = 2 (c'_{fo} - c'_{fc}) \qquad \ldots\ldots\ldots(7.9b)$$

Using Eq. (7.6) we get two values of widths for the two values

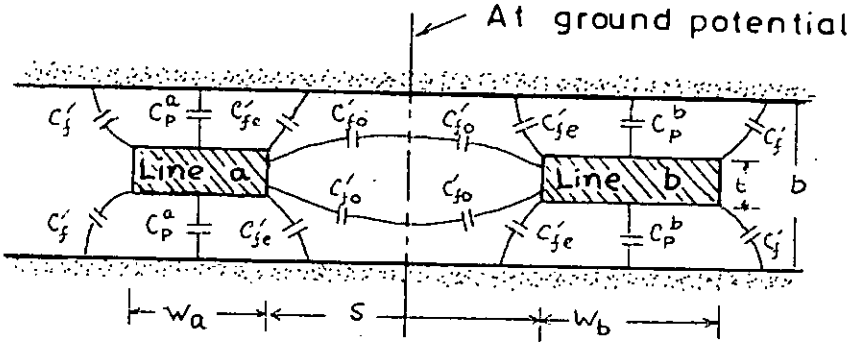

Fig. 7·5. Cross section of unsymmetrical rectangular bar parallel coupled lines showing different capacitances.

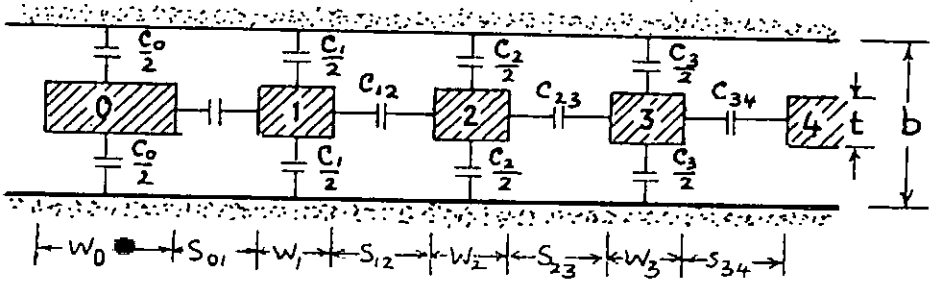

Fig. 7·6 Cross section of an array of parallel coupled lines between ground planes.

of parallel plate capacitances of the two lines.

The equations for the widths are thus

$$w_a/b = \tfrac{1}{2}(1 - t/b)\left[\left(\tfrac{1}{2}(c_a/\epsilon)\right) - c'_{fo}/\epsilon - c'_f/\epsilon\right] \quad \ldots\ldots\ldots(7.10)$$

$$w_b/b = \tfrac{1}{2}(1 - t/b)\left[\tfrac{1}{2}(c_b/\epsilon) - c'_{fo}/\epsilon - c'_f/\epsilon\right] \quad \ldots\ldots\ldots(7.11)$$

7.5. WIDTH CALCULATION FOR AN ARRAY OF PARALLEL COUPLED RECTANGULAR BARS BETWEEN GROUND PLANES:

Fig.7.6 shows an array of parallel coupled rectangular transmission lines between ground planes. The widths of different lines are assumed to be different but all of them are assumed to have the same thickness. The different lines are named as line no.0, 1, 2, 3, 4 etc. The capacitance of line no.0 to ground is assumed to be c_0. Similarly c_1, c_2, c_3, c_4 etc. represent the total capacitances to ground lines 1, 2, 3, and 4 respectively. In general c_k represents the total capacitance to ground of kth line. $c_{k,\,k+1}$ represents the capacitance between kth line and (k+1)th line and $c_{k-1,\,k}$ represents the capacitance of (k-1)th line and kth line.

Fig.7.6 clearly shows these capacitances. The capacitance values are all in per unit length. In the design of digital filters this type of arrays are found and it is necessary to write the generalised expression for width of kth line. Before that we shall write the expression for the capacitance of kth line to ground as we have seen in the case of two unsymmetrical parallel coupled transmission lines. The expressions are as follows:

the capacitance of 0th line to ground is

$$c_o = 2 \left[c^o_p + c'_f + (c'_{fe})_{0,1} \right] \qquad \ldots\ldots\ldots(7.12)$$

where c^o_p is the parallel plate capacitance of 0th line

c'_f is the fringing capacitance to the left of 0th line as defined in section 7.2

$(c'_{fe})_{0,1}$ is the fringing capacitance between 0th and 1st line as defined in section 7.2.

and the capacitance of kth line to ground is

$$c_k = 2 \left[c^k_p + (c'_{fe})_{k-1,k} + (c'_{fe})_{k-1,k} \right] \qquad (7.13)$$

where,

c^k_p is the parallel plate capacitance of kth line

$(c'_{fe})_{k-1,k}$ is the fringing capacitance existing between line nos. (k-1) and k as defined in section 7.2.

$(c'_{fe})_{k,k+1}$ is the fringing capacitance existing between line nos. k and (k+1)

Using Eq.(7.6) and using the values of c^o_p and c^k_p from Eqn. (7.12) and Eq.(7.13) we can write the expression for the width of 0th line and the width of kth line as follows:

$$\frac{W_o}{b} = \frac{1}{2}\left(1 - \frac{t}{b}\right)\left[\frac{1}{2}\left(\frac{C_o}{\epsilon}\right) - \frac{C'_f}{\epsilon} - \frac{(C'_{fe})_{o,1}}{\epsilon}\right] \qquad (7.14)$$

$$\frac{W_k}{b} = \frac{1}{2}\left(1 - \frac{t}{b}\right)\left[\frac{1}{2}\left(\frac{C_k}{\epsilon}\right] - \frac{(C'_{fe})_{k-1,k}}{\epsilon} - \frac{(C'_{fe})_{k,k+1}}{\epsilon}\right] \qquad (7.15)$$

line no.0 is the line which has no neighbour to the left of the line whereas kth line is any line except the end lines.

Since this type of array of parallel coupled rectangular conductors between ground plates will be used in the construction of our digital elliptic function filter, we shall need these formulae in order to find out the widths of our filter.

7.6. USE OF GRAPHS FOR THE CALCULATION OF WIDTHS OF THE LINES AND THE SPACING BETWEEN THE LINES

It has already been mentioned that the values of c/ϵ of section 7.3, c_a/ϵ and c_b/ϵ of section 7.4, c_o/ϵ and c_k/ϵ of section 7.5 can be found out from the corresponding capacitance matrices. The capacitances which are to be found out from the graphs of Fig.7.2 and 7.4 are the fringing capacitances c'_{fo} and c'_f.

In order to find out these capacitances we must first of all choose a value of t/b for the parallel coupled transmission lines between ground plates. Here t is the thickness of the lines and b is the ground plane spacing. If we assume a particular value of t/b we can get a particular curve in Fig.7.2. In order to determine the capacitance c'_{fo}/ϵ we shall have to find out the mutual capacitance between the lines (i.e. $\frac{\Delta c}{\epsilon}$) from the capacitance matrix. For this particular value of t/b and $\frac{\Delta c}{\epsilon}$ we get a value of s/b from the curves. Where s/b is the ratio of the spacing between the lines and the ground plane spacing. From this value of s/b we can get the value of the spacing between the lines S if we assume a value of b. For this particular value of s/b and for the assumed value of t/b we can read the

value of c'_f/ϵ between those two lines from the graph of Fig.7.2.

However for an end line, in order to determine c'_f/ϵ we use the graph given in Fig.7.4. For a particular value of t/b we can easily get the corresponding value of c'_f/ϵ from the curve of Fig.7.4.

7.7. CONSIDERATION OF ACCURACY FOR LINES OF NARROW WIDTHS:

If the bar width w is allowed to become too small, there is interaction of the fringing fields from the two edges, and the decomposition of total capacitance into parallel plane capacitance and fringing capacitances (which are based on infinite bar widths) is no longer accurate. Cohn[31] showed that for a single bar centered between parallel planes, the error in total capacitance from interaction of the fringing fields is about 1.24 percent for $w/(b-t) = 0.35$, where w is the width of the bar, t is its thickness, and b is the ground plane spacing. If a maximum error in total capacitance of approximately this magnitude is allowed, then it is necessary that

$$\left[(w/b) / (1-t/b) \right] > 0.35.$$

Should this inequality be too restricting, it is possible to make approximate connections based on an increase in the parallel plate capacitance, to compensate for the loss of fringing capacitance due to interaction of fringing fields. If an initial value w/b is found to be less than $0.35\ [1-(t/b)]$, a new value, w'/b can be used, where

$$w'/b = \left\{ 0.07\ [1-(t/b)] + w/b \right\} / 1.20 \quad \ldots\ldots(7.16)$$

provided that $0.1 < (w/b) / [1-(t/b)] < 0.35$.

7.8. PARALLEL COUPLED TRANSMISSION LINES BETWEEN GROUND PLANES WITH ONE END CLOSED

Let us again consider the array of parallel coupled lines between ground planes of Fig.7.6. Let us assume that the left side of line 0 of the array is closed by ground walls as shown in Fig.7.7.

For this case the total capacitance to ground of line number 0,

$$= C_0 = 2\left[C_p^0 + (C'_{fe})_{0,1} + C'_{fo}\right]$$

In order to find out the width of line no.0, we need to use the equation

$$\frac{w_0}{b} = \frac{1}{2}\left(1 - \frac{t}{b}\right)\left[\frac{1}{\epsilon}(C_0) - \frac{C'_{fo}}{\epsilon} - \frac{(C'_{fe})_{0,1}}{\epsilon}\right]$$

In order to find the spacing between the end ground wall and line no.0, we shall use the graph given in Fig.7.3. From this graph we shall get s/b and thus get s. The spacing between the end ground wall and line no.0 will be s/2.

7.9. THE EXPANDED PLOT OF FRINGING CAPACITANCES VS. s/b.

Based on conformal mapping analysis even and odd mode fringing capacitance curves have been presented by Getsinger. These curves have been shown at the beginning of this chapter. Although fringing capacitance curves have been provided for wide ranges of bar thickness and coupling, there is insufficient data for very light coupling. Furthermore, the accuracy with which capacitance data can be read from these curves for tightly coupled bars is inadequate. R.R. Gupta [15] published even and odd mode fringing capacitance curves, on an expanded scale, for tightly coupled coplanar rectangular bars between parallel ground planes. Accurate values of mode capacitances have been calculated

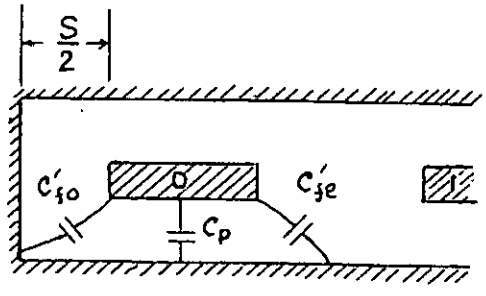

Fig. 7.7. Parallel coupled transmission lines between ground planes with one side closed.

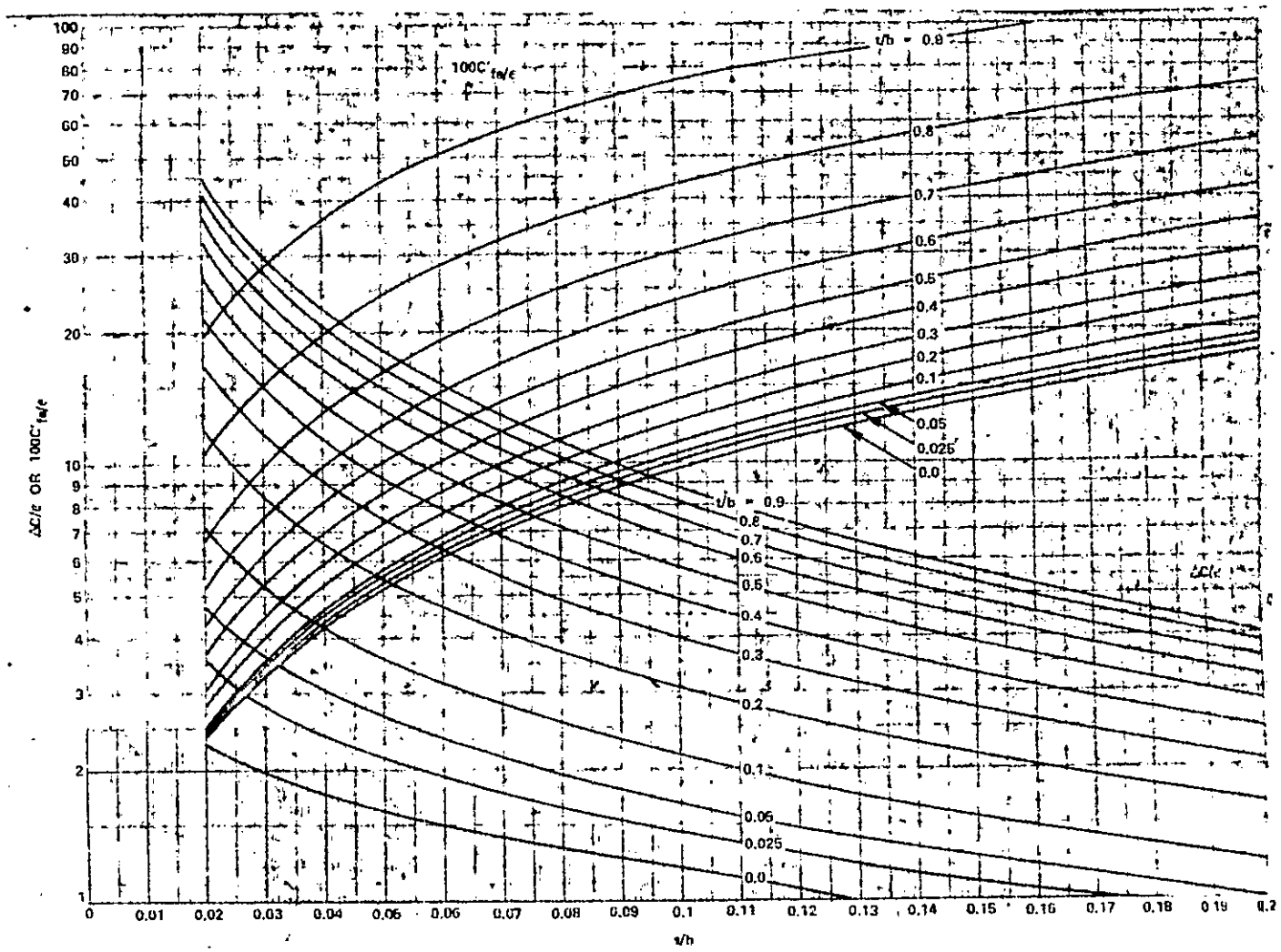

Fig 7.8. Expanded plot of normalized even mode capacitance c'_{fe}/ϵ and interbar capacitance $\Delta c/\epsilon$ for coupled rectangular bars.

by him by numerically solving the laplace equation for the lower and upper bounds on the mode capacitance. According to him the computed capacitance data presented is the average of the two bounds and is correct to within $\pm 1/4$ percent of the exact data (before plotting) A plot of these curves is presented in fig. 7.8.

7.10 CALCULATION OF LENGTH OF EACH NETWORK OF THE ELLIPTIC FUNCTION DIGITAL BANDPASS FILTER:

In the previous sections the procedures of obtaining widths of each line and the spacing between the lines of the digital line filter was presented. In this section the procedures of obtaining the length of the lines of each network of the elliptic function digital bandpass filter will be presented. In chapter 6 it has been shown that the filter consists of two networks, lengths of each network should be one eighth wavelength long at the centre frequency.

Length of network 1:

Let us assume that the centre frequency is f_o'. We can then find the wavelength from the relation $\lambda_0 = v/f_o$ where v = velocity of light = 3×10^{10} cm/sec. The length of network will then be simply equal to $\frac{\lambda_o}{8}$ cm. $\ell_1 = \frac{\lambda_o}{8}$

Length of network 2

Theoretically the length of network 2 should also be equal to $\lambda_o/8$. But due to the presence of the fringing end effect capacitances at the free end of the lines of network 2 it is necessary to shorten the length of the lines of network 2. As illustrated in Fig.7.9 these fringing end effect capacitances are distributed along the width of the lines.

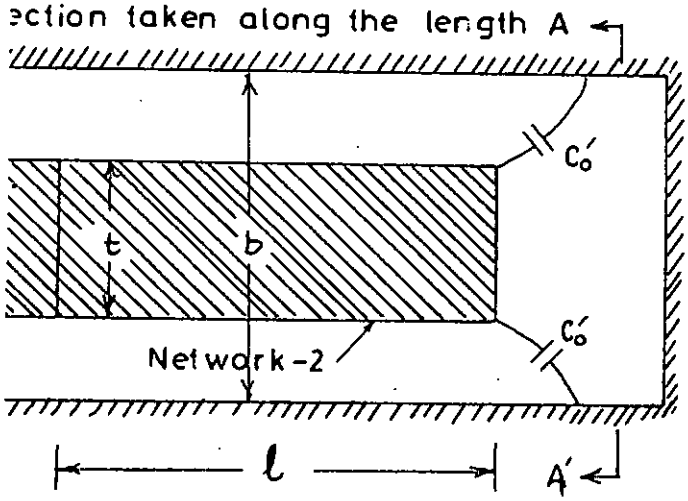

Length of network 2

(a)

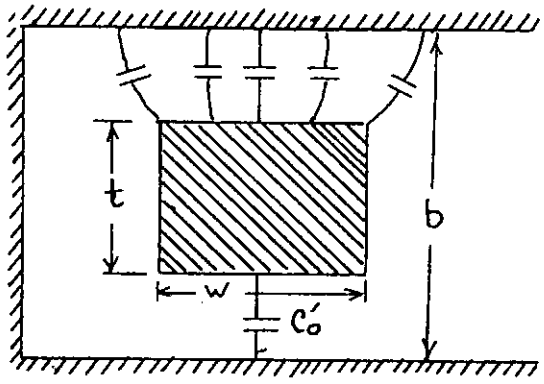

View towards AA' (Only 1 line shown)

(b)

g. 7·9. Parasitic end effect capacitance of network-2.

If we now intend to calculate the line dimensions from the existing matrix for network 2 the capacitance of each line of network 2 to ground that we shall get will be greater than that which was estimated. This will definitely introduce error in the calculation of widths. In order to get the exact dimensions, that is in order to get the actual capacitance of the matrix from the digital lines we need to shorten the lines and also we need to augment the mutual distances between the lines. So formulas must be developed, which are applicable to such cases, in order to overcome this difficulty and in order to get the accurate results.

Derivation of the formula for length correction of network-2

Let us consider that the corrected length of network-2 is l' and the length before correction is l corresponding to one eighth of wave-length.

Therefore from Fig.7.9b it is evident that

$$\frac{\text{Capacitance}}{\epsilon} = \frac{\text{Area}}{\text{distance}} = \frac{w(l-l')}{\frac{1}{2}(b-t)} = c_o w$$

$$\therefore l' = l - \tfrac{1}{2} b c_o (1 - t/b) \qquad \ldots\ldots(7.17)$$

If we assume $t/b = 0.6$

We get $$l' = l - .2 b c_o \qquad \ldots\ldots(7.18)$$

The value of c_o may be obtained from Getsinger's [9] graph given in Fig.7.14. From the value of c_o thus obtained and by using the formula (7.17) we can get exactly the corrected length of network-2.

G.L. Matthaei and R.J. Wenzel while working on interdigital filters with such rectangular bar configuration, had to arbitrarily shorten the lengths to get the accurate result. But here a formula is presented whereby we can know how much we need to shorten to take into account of the effect of parasitic lumped end effect capacitances. However the equation has been obtained from the assumption that the distribution of lumped capacitance along the end of any bar in network-2 is proportional to the distribution of capacitance to the ground plates across the width of the corresponding bar, and that the distance $\ell-\ell'$ is considerably shorter than a quarter wavelength. This compensation procedure also neglects the interbar fringing capacitances.

Augmentation of the coupling admittances:

Due to the shortening of length of each line of network-2, the poles of infinite attenuation will be shifted i.e. the poles of infite attenuation $\lambda_{r\pm} = \tan\beta_\pm \ell$ will become $\tan\beta_\pm \ell'$. This means that the value of admittance $Y_{r\pm} \tan\beta_\pm \ell$ will change to a new value. Here $Y_{r\pm}$ is the theoretically derived coupling admittance forming part of the resonant circuit which produces the pole of infinite attenuation at the normalized frequency $\tan^{-1}\lambda_{r\pm}$.

In order to maintain the product $Y_{r\pm}\tan\beta_\pm \ell$ unchanged (since this would give us the same resonant frequency) we need to change $Y_{r\pm}$ to a new value $Y'_{r\pm}$. This means we should make

$$Y_{r\pm}\tan\beta_\pm \ell = Y'_{r\pm}\tan\beta_\pm \ell'$$

$$\text{or,}\quad Y_{r\pm}\lambda_{r\pm} = Y'_{r\pm}\tan\left(\frac{\ell'}{\ell}\tan^{-1}\lambda_{r\pm}\right)$$

$$\text{or,}\quad Y'_{r\pm} = \frac{Y_{r\pm}\lambda_{r\pm}}{\tan\left(\frac{\ell'}{\ell}\tan^{-1}\lambda_{r\pm}\right)} \qquad (7.19)$$

So we find that in order to maintain the correct location of the poles of infinite attenuation due to the reduction in length of network-2, the coupling admittance in network-2 must be augmented according to the Equation (7.19). This correction must also be applied at the center frequency to the admittances between the end lines and the ground end walls.

C H A P T E R -8

DESIGN OF BANDPASS FILTERS AND THEIR PHYSICAL REALIZATION:

8.1. INTRODUCTION:

Two examples of the realization procedure of elliptic function bandpass filter which has been developed is presented in this chapter. While designing and calculating the physical dimensions tables of Everev[14], Saal[16] and Nomographs[14] were used. The graphs of Getzinger[7] were used in calculating the physical dimensions from static capacitance values.

8.2. DESIGN OF EXPERIMENTAL FILTER NO.1:

The requirements for this filter are that the stopband attenuation level (A_{min}) should be 60.1 dB, passband VSWR should be less than 1.222; bandwidth should be 11%. The center frequency of this bandpass elliptic function filter should be 2150 mc/s. It is also specified that in the transition region; 60.1 dB attenuation should occur at 2420 mc/s and at 1880 mc/s respectively.

Determination of Ω_s and n :

Depending on the information given, the bandpass characteristic of Fig.8.1a can be drawn, where the edges of the passband are shown to be 2031.75 mc/s. and 2268.25 mc/s respectively for 11% bandwidth. From the given passband VSWR we can find reflection coefficient ρ and thus using Eq.(5.12) we can find A_{max} - the maximum attenuation in the passband. In this case we find A_{max} = 0.044 dB for a VSWR = 1.222 i.e. for a ρ = 10%. In order to find Ω_s we need to convert the given frequencies in the bandpass to the lowpass frequencies. In order to find the complexity of the filter - n, we need to find Ω_s from the lowpass

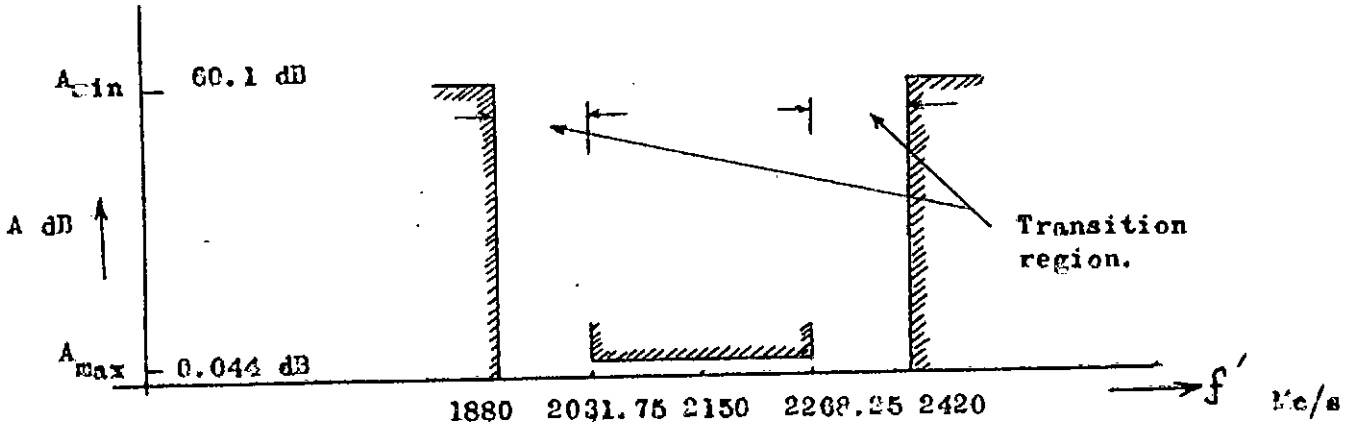

a) BAND PASS (DISTRIBUTED)

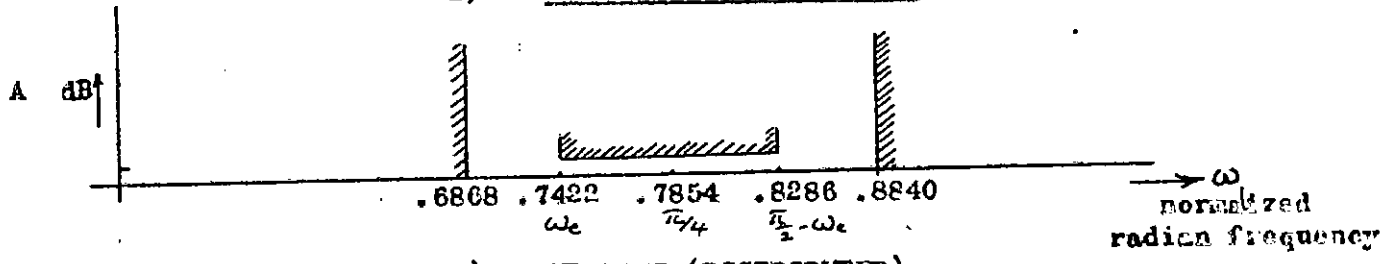

b) BAND PASS (DISTRIBUTED)

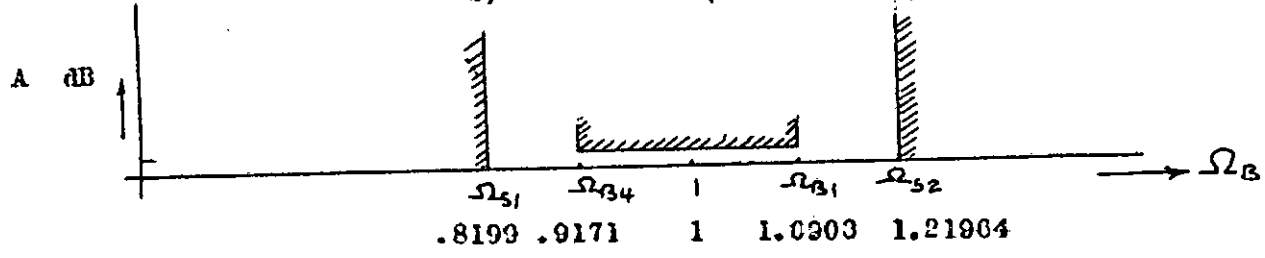

c) BAND PASS (LUMPED)

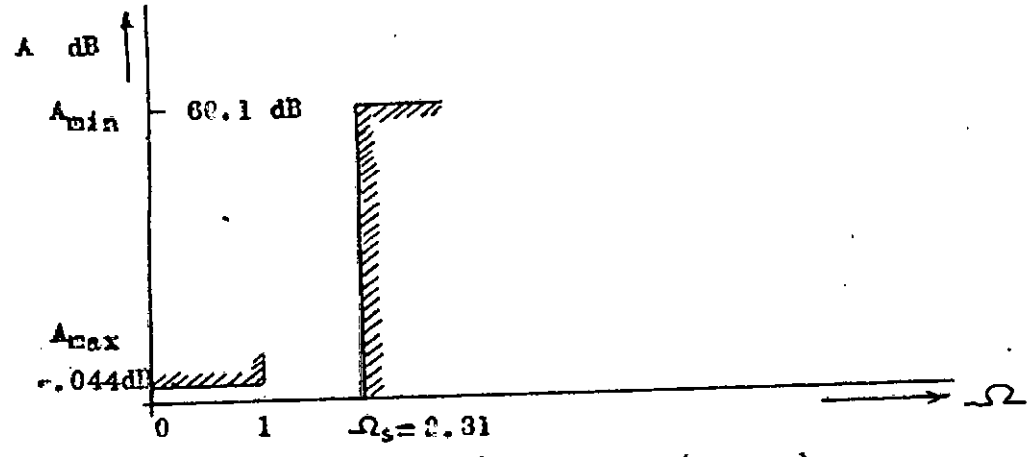

d) LOW PASS (LUMPED)

Fig. 8.1. Prescribed filter specifications for Experimental Filter no.1.

frequency response. From Fig.8.1a we can easily find out the corresponding normalized radian frequencies ω of Fig.8.1b. Since we know that $\Omega_B = \tan\omega$ we can also get the corresponding frequencies in Ω_B scale by using this relation. To recall that the low-pass to band-pass transformation was $\Omega = a\left(\Omega_B - \frac{1}{\Omega_B}\right)$. So referring to Fig.8.1c and Fig.8.1d corresponding to the value of Ω_S in the low-pass we get $\Omega_S = a\left(\Omega_{S_2} - \frac{1}{\Omega_{S_2}}\right) = a\left(\Omega_{S_2} - \Omega_{S_1}\right)$ and corresponding to the passband edge frequencies in the low-pass - Ω_c, we get $\Omega_c = a\left(\Omega_{B_1} - \frac{1}{\Omega_{B_1}}\right) = a\left(\Omega_{B_1} - \Omega_{B_4}\right)$. From these two relations we get $\frac{\Omega_S}{\Omega_c} = \frac{\Omega_{S_2} - \Omega_{S_1}}{\Omega_{B_1} - \Omega_{B_4}}$ (8.1)

For our case $\Omega_c = 1$, hence using this relation we can thus find the value of Ω_S . For this case Ω_S is found to be 2.31. This means that the transition region steepness in the lowpass response should be $\Omega = \frac{\Omega_S}{\Omega_c} = 2.31$

Now in order to determine n we shall use the Nomographs given in chapter 5. For $A_{min} = 60.1$ dB, $A_{max} = 0.044$ dB and for $\frac{\Omega_S}{\Omega_c} = 2.31$ we get n = 5 from the nomograph.

Lowpass Prototype:

From the data now available we can now find out the low-pass prototype element values from Zverev[14] (from the tables for elliptic function lowpass filter) or from R.Saal's[16] 'Filter Katalog'. The following low-pass prototype element values are thus obtained for n=5, $\rho = 10\%$ and $A_{min} = 60.1$ dB: and for the termination of $K^2 = 1.0$.

$C_1 = 0.9265$; $C_3 = 1.666$ $L_2 = 1.3067$

$C_2 = 0.05866$; $C_4 = 0.1607$ $L_4 = 1.17253$. (8.2)

$C_5 = 0.8363$

and $\Omega_2 = 3.6119$; $\Omega_4 = 2.3038$

The diagram of the low-pass prototype is shown in Fig.8.2.

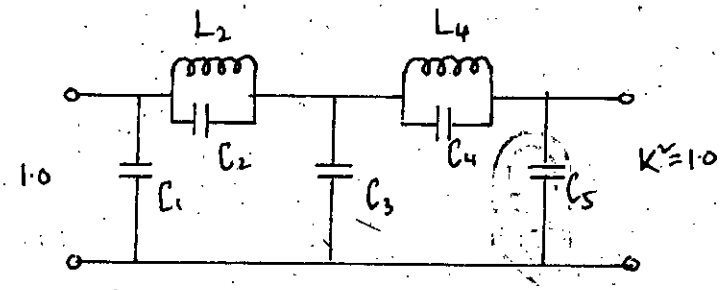

Fig.8.2. Low-pass prototype for n=5, and $K^2 = 1.0$.

Calculation of m'a' and poles of infinite attenuation

From Fig.8.1b it is seen that the center frequency is normalized to $\frac{\pi}{4} = 0.7854$ radian so that the band edge frequency ω_c will be .7422 for the 11% bandwidth filter.

Thus we get $a = \frac{\tan 2\omega_c}{2} = \frac{11.54}{2} = 5.77$ .....(8.3)

Since the center frequency is 2150 MHz, therefore the length of the elements of network-1 $= \frac{\lambda_0}{8} = .686$ inch.

By using the given formulas (6.9a), (6.9b) we got

$\lambda_{2+} = 1.361$ $\lambda_{4+} = 1.219$

$\lambda_{2-} = .735$ $\lambda_{4-} = 0.820$ .....(8.3a)

The corresponding actual frequencies are

$$f' = \left(\tan^{-1}(\lambda_{xi}) \times \frac{\pi}{180} \div \frac{\pi}{4}\right) 2150 \text{ MHz}$$

$f_1' = 1735$ MHz. $f'_3 = 2419.3$ MHz.

$f'_2 = 1880.14$ MHz. $f'_4 = 2565.35$ MHz.

These are the frequencies at which the poles of infinite attenuations are located in distributed bandpass response.

Characteristic Admittance Matrices:

The values of λ's are now used to calculate the element values of the characteristic admittance matrices (6.25), (6.23) and (6.24). The following matrices then result:

Network-1

(0)	(1)	(2)	(3)	(4)	(5)	(6)
1	-1	0	0	0	0	0
-1	7.3113	-.9654	0	0	0	0
0	-.9654	1.4867	-.5213	0	0	0
0	0	-.5213	10.7792	-2.3051	0	0
0	0	0	-2.3051	3.8558	-1.5507	0
0	0	0	0	-1.5507	7.3761	-1
0	0	0	-0	0	-1	1

(8.4)

Network-2

(1)	(2)	(3)	(4)	(5)
5.8672	-.5213	0	0	0
-.5213	1.4867	-.9654	0	0
0	-.9654	12.1290	-1.5507	0
0	0	-1.5507	3.8558	-2.3051
0	0	0	-2.3051	7.1305

(8.5)

These values of characteristic admittances of these matrices may not give us a physically realizeable bandpass filter. It has been mentioned in chapter 6 that for physical realizeability admittance scalling is necessary . A discussion on this matter was given in section 6.8. There it was mentioned that at the begining every line in the

stepped digital filter, except the lines on which input and output ports are situated, may be scaled by the factor $1/\sqrt{a}$. However in this physical example we shall at the begining scale only lines(1) and (5) of both the network by the factor $1/\sqrt{a} = 1/\sqrt{5.77} = .4163$. This procedure and the following admittance scaling procedure generally result in capacitance matrices which give a physically realizeable network.

After scaling lines(1) and (5) of both network by the factor $1/\sqrt{a}$ the matrices which result are shown in Eq.(2a), and Eq.(2b) of Appendix-A.

The remaining lines were then scaled such that the corresponding main diagonal entries in the capacitance matrix representing network-1 were respectively equal to, and a factor 1.2 times greater than, the main diagonal value of line (1) upto the center line from the input, and line(5) upto and including the center line from the output. This will be clear if we go through the following steps.

Thus we make C_{44} = 1.2 times C_{55} and make necessary changes in other related characteristic admittances as we have shown in the procedure for the change in admittance level in chapter 3 and 4. Accordingly we make C_{33} = new C_{44} and other necessary changes in the admittances level of the matrix (2a) of Appendix-A. Similarly we make C_{22} = 1.2 times C_{11}. This is done in Network-1 in matrix(2a) of Appendix-A. Exactly similar changes in the admittance level of each line were carried out in network-2 also. That means line number(4) of network-1 and line number(4) of network-2 must be multiplied by the same factor. The change in admittance levels must be done as shown in Chapter-3 and 4.

This simple procedure of changing the admittance levels results in or near optimum relationship between the coupling and ground capacitances of both networks-1 and 2.

The matrices for network-1 and 2 which were obtained after the above mentioned changes in admittance level are the matrices (3a) and (3b) of Appendix-A. The elements of matrices (3a) and (3b) of Appendix-A are the characteristic admittance values. In order to get the static capacitance matrices for air as dielectric, we need to multiply these matrices by η_o . The static capacitance values are still normalized with respect to the termination impedance. In order to convert the values to a 50-ohm system we need to divide these values by 50. Therefore in order to convert the characteristic admittance values of matrices(3a) and (3b) (of Appendix-A) to the static capacitance values in a 50 ohm system we need to multiply the matrices by a factor $\frac{\eta_o}{Z_o}$ = $\frac{376.7}{50}$ = 7.534.

After multiplying each element of the matrices for both the network by 7.534 we get the following static capacitance matrices:

Network-1

(0)	(1)	(2)	(3)	(4)	(5)	(6)
7.534	-3.136	0	0	0	0	0
-3.136	9.546	-3.062	0	0	0	0
0	-3.062	11.456	-1.395	0	0	0
0	0	-1.395	11.558	-3.848	0	0
0	0	0	-3.848	11.558	-3.068	0
0	0	0	0	-3.068	9.631	-3.136
0	0	0	0	0	-3.136	7.534

(8.6)

Network-2

(1)	(2)	(3)	(4)	(5)
7.661	-1.653	0	0	0
-1.653	11.456	-2.583	0	0
0	-2.583	11.269	-2.588	0
0	0	-2.588	11.958	-4.561
0	0	0	-4.561	9.312

(8.7)

The values are now ready for calculating the physical dimensions. We shall use a rectangular bar configuration and we shall use the procedure discussed in chapter-7 for this purpose.

If we are to find out the physical dimensions, we need to find the capacitance of each line to ground and the capacitance between lines. The capacitance between lines can be directly read from the above matrices (mutual capacitances), but the capacitance of each line to ground can be found by adding the respective column or row.

Width Calculation for Network-1

The following is the table which presents all the values of self capacitance (between line and ground), mutual capacitance, fringing capacitance from the Getsinger's[7] graphs, the width of the lines and the spacing between lines of network-1.

k	$c_{k/\epsilon}$	$\frac{c_{k,k+1}}{\epsilon}$	$\frac{c'_{fe}}{\epsilon}{}_{k,k+1}$	$w_{k/b}$	w_k inches	$s_{k,k+1}$	$s_{k,k+1}$ inches
0	4.398	3.136	0.43	0.1135	.071	0.195	0.122
1	3.348	3.062	0.42	0.1648	0.103	0.205	0.128
2	6.999	1.395	0.7	0.475	0.297	0.385	0.261
3	6.315	3.848	0.35	0.4215	0.264	0.165	0.103
4	4.642	3.068	0.42	0.311	0.194	0.205	0.128
5	3.427	3.136	0.42	0.175	0.1095	0.2	0.125
6	4.398			0.1155	0.0722		

(9.8)

In this table,

k = line number

c_k = the static capacitance of kth line to ground

$c_{k,k+1}$ = the static capacitance between kth and k+1th line

w_k = width of kth line in inches

$s_{k,\,k+1}$ = spacing between kth and (k+1)th lines in inches.

For this case we have chosen t/b = 0.6 and t = 0.375" that is b= 0.625". The graph of Fig.7.3 was used for t/b = 0.6 to get the necessary values of s/b and c'_{fe} . To find the value of c'_f the graph of Fig.7.5 was used.

The width calculations are shown below

$$w_o/b = \tfrac{1}{2}(1-t/b)\left[\tfrac{1}{2}\left(\frac{c_k}{\epsilon}\right) - \frac{c_f'}{\epsilon} - \frac{(c_{fe})_{o,1}}{\epsilon}\right]$$

$$w_k/b = \tfrac{1}{2}(1-t/b)\left[\tfrac{1}{2}\left(\frac{c_k}{\epsilon}\right) - \frac{(c_{fe}')_{k-1,k}}{\epsilon} - \frac{(c_{fe}')_{k,k+1}}{\epsilon}\right] \qquad (8.9)$$

w_o/b = ½ (1-.6) (½ x 4.398 - c'_f/ϵ - .42) = .1135

$\therefore w_o$ = .071"

w_1/b = ½ (1-.6) (½ x3.348-.43 - .42)= .1648, w_1= .103"

w_2/b = .2 (½ x6.999 -.42-.7) = .475, w_2 = .297"

w_3/b= .2 (½ x6.315 -.7-35) =.4215 w_3=.264"

w_4/b= .2(½x4.642-.35-.42) = .311 w_4= .194"

w_5/b= .2(½x3.427 -.42-.42) =.175 w_5=.1095"

w_6/b= .2 (½x4.398-.42-1.2) =.1155 w_6 = .0722"

Length and Width Calculation for Network-2:

We can now calculate the dimension of Network-2. Using equation (7.18) the length of network-2 becomes

$$l' = l - .2\, c_o\, b$$

$$l' = 0.686 - .2x1.2x0.625 = 0.536 \text{ inches} \qquad (8.10)$$

Now using equation (7.19) the coupling admittances $Y_{r,t}$ of matrix (8.7) becomes $Y'_{r,t}$ of the following table.

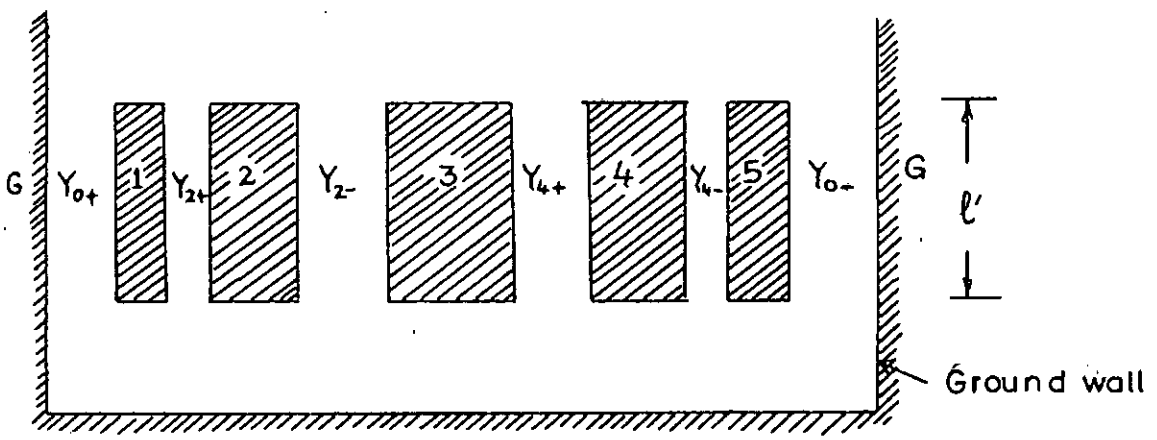

Fig. 8·3 Network 2 showing the coupling admittances.

$r_{\pm}$	$Y_{r_{\pm}}$	$Y'_{r_{\pm}}$
0_{-}^{+}	2.4	3.41
2^{+}	1.653	2.5
2^{-}	2.583	3.51
4^{+}	2.588	3.81
4^{-}	4.561	6.27

(8.11)

Here $Y_{0^{+}}$ and $Y_{0^{-}}$ are assumed to be 3.41 for convenience of construction.

After this we can make the following table by use of Getsinger's Graph and his formula for width calculation.

k	$\frac{C_k}{\epsilon}$	$\frac{C_{k,k+1}}{\epsilon}$	$\frac{(C'_{fe})_{k,k+1}}{\epsilon}$	$\frac{\omega_k}{b}$	ω_k inch.	$\frac{S_{k,k+1}}{b}$	$S_{k,k+1}$ inch.
0		c_{01} =3.41		.159			.162"
1	(2.59	2.5	.5	.159	.0995"	.245	.153"
2	7.22	3.51	.38	.546	3.41"	.18	.1125"
3	6.098	3.81	.37	.4598	.287"	.17	.106"
4	4.409	6.27	.225	.322	.2"	.10	.0625"
5	1.349	3.41		.09	.056"		.162"

(8.12)

The width calculations of the lines are shown below:

$w_2/b = .2\ (\frac{1}{2} \times 7.22 - .5 - .38) = .546 \quad \therefore w_2 = .341"$

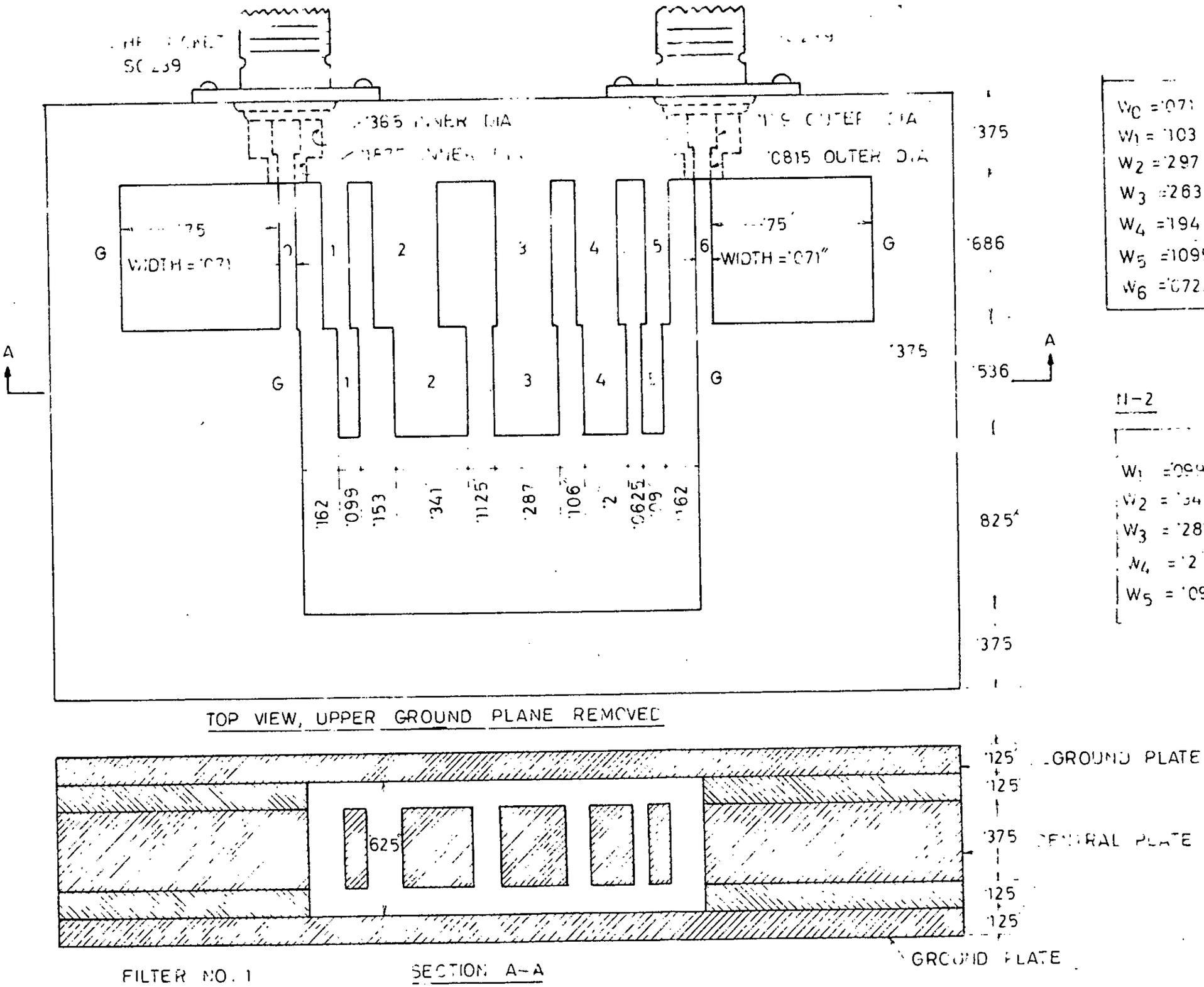

W_0 = .071	S_{01} = .122
W_1 = .103	S_{12} = .128
W_2 = .297	S_{23} = .261
W_3 = .263	S_{34} = .103
W_4 = .194	S_{45} = .128
W_5 = .1095	S_{56} = .125
W_6 = .0722	S_{6G} = .75

TOP VIEW, UPPER GROUND PLANE REMOVED

N=2

	S_{01} = .162
W_1 = .0945	S_{12} = .153
W_2 = .341	S_{23} = .1125
W_3 = .287	S_{34} = .106
W_4 = .2	S_{45} = .0625
W_5 = .09	S_{5G} = .162

FILTER NO. 1

SECTION A–A

FIG NO. 8·4a. DRAWING OF THE EXPERIMENTAL UHF ELLIPTIC FUNCTION BANDPASS FILTER, CENTER FREQ. = 2150 MHz, BANDWIDTH = 11%, Amin = 60·1 dB, P = 10%.

from the central conductors) . The transmission lines except the input and output lines are stepped. Slots were cut in the central plate according to the dimensions and drawing given in the top view of Fig.8.4a. These slots were cut by drilling holes, cutting by jewellary saws and then by filing by means of jewellery files. By this method the transmission lines and the spacings were created from a .375 inch. thick machined brass plate. The top and botton plates have well finished surfaces. Fig.8.4a clearly shows the connection of the input and output connectors to the input and output transformer elements.

The photograph of the filter with its cover plate opened is shown in Fig.8.4b.

In order to improve the performance of the filter it was necessary to add tuning screws. A separate top cover plate was taken for this purpose. Holes and threads were cut on it in order to place the tuning screws. The holes and threads were made such that the tuning screws appear on the transmission lines of both the networks.

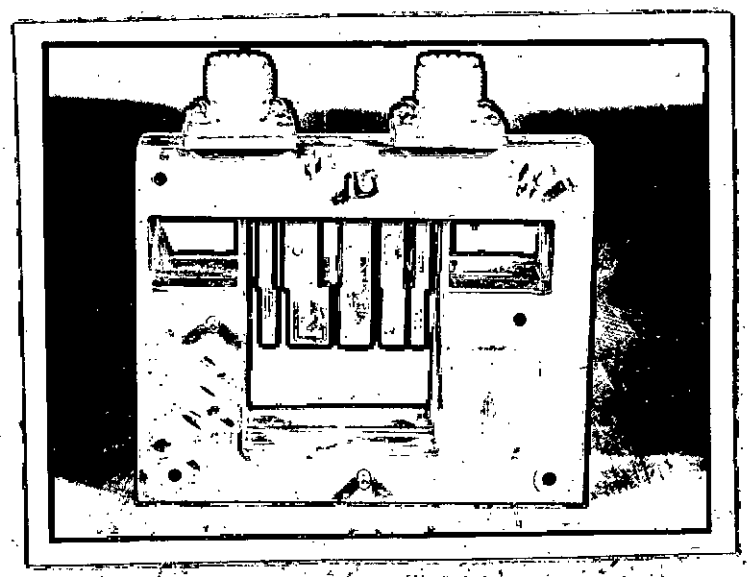

Fig. 8.4b Photograph of Filter no. 1 with top cover removed

8.3. DESIGN OF EXPERIMENTAL FILTER NO.2:

In this section we design another elliptic function bandpass filter with the following requirements:

A_{min} = Stop band attenuation level = 63.52dB; ρ = 10% in the pass band, this corresponds to passband maximum loss A_{max} = .044dB . Bandwidth-required = 10% where the center frequency is desired to be 1.6 k mc/s. It is also mentioned that in the transition regions 63.52 dB attenuation occur at frequencies 1215 mc/s and at 1985 mc/s. respectively. We want to design and construct this filter.

Determination of Ω_s and n.

On the basis of the design requirements, Fig.8.5a can be drawn where it is clearly seen that the edges of passband are at 1520 mc/s and at 1680 mc/s. respectively. As discussed before Fig.8.5b can be drawn from Fig.8.5a. Since we know that $\Omega_B = \tan\omega$ we can thus also draw Fig.8.5c. Using equation (8.1) i.e. $\frac{\Omega_s}{\Omega_c} = \frac{\Omega_{s_2} - \Omega_{s_1}}{\Omega_{B1} - \Omega_{B4}}$ we can find out the value of Ω_s of Fig.8.5a, since in our case Ω_c =1. Thus the value of Ω_s is found to be 2.436. Thus the steepness of the transition region of the lowpass response is known. As before using the Nomographs given in chapter-5.for A_{min} = 63.52 dB, A_{max} = .044dB and for $\frac{\Omega_s}{\Omega_c}$ =2.436 we get n=5.

Now for n=5, ρ = 10%, A_{min} = 63.52 dB from the tables given in the book of 'Saal' or in the book of Zverev we get the low-pass prototype element values. These are as follows:

g_1 = .93328 $\quad$ g_3 = 1.68509

g_2 = .04993 $\quad$ g_4 = .13577, $\quad$ g_5 = .85596

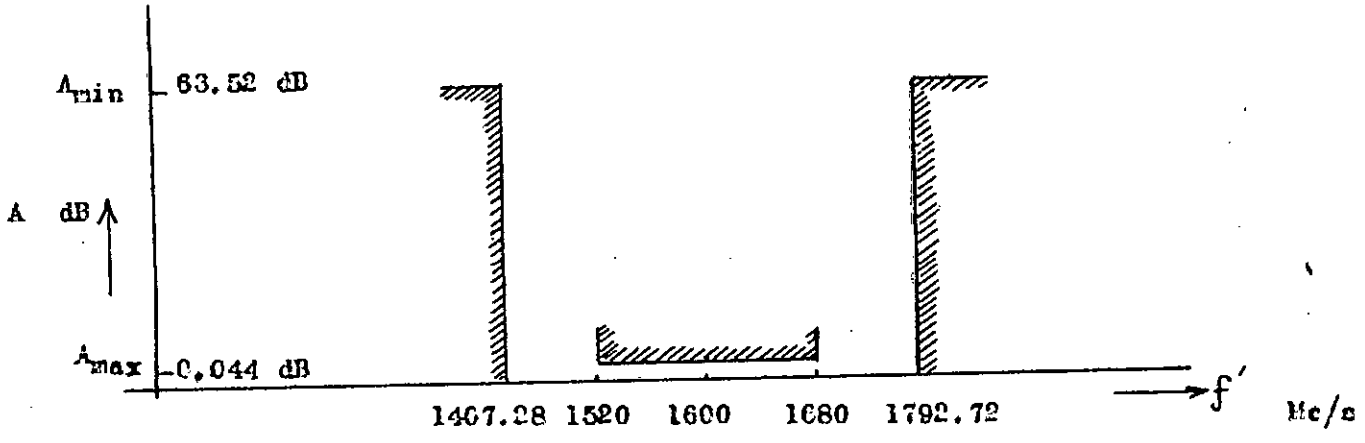

a) BAND PASS(DISTRIBUTED)

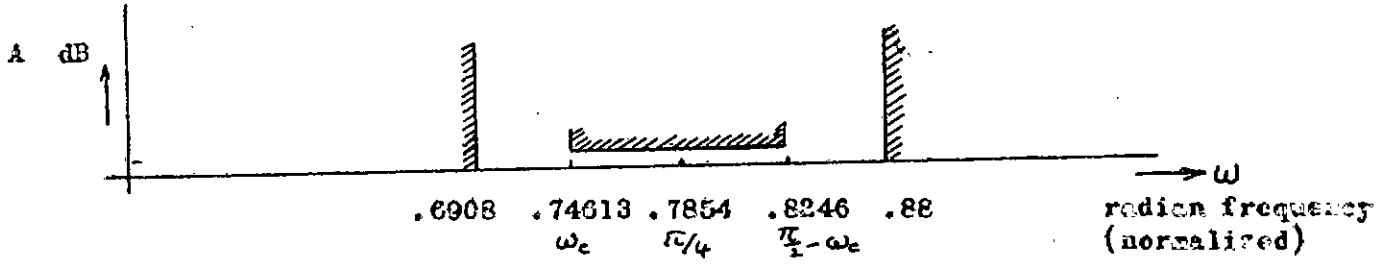

b) BAND PASS (DISTRIBUTED)

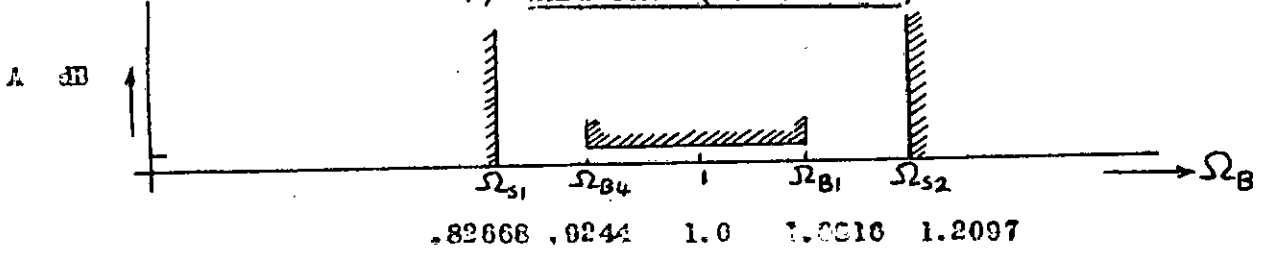

c) BANDPASS (LUMPED)

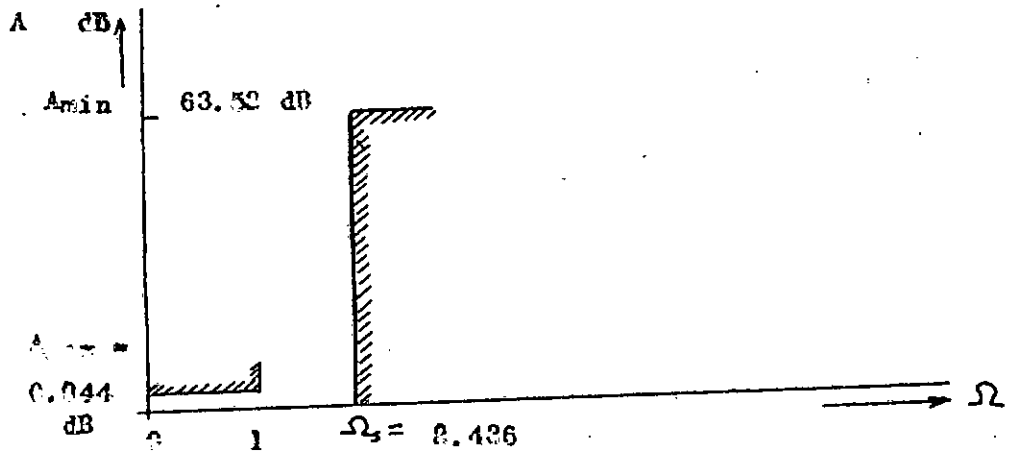

d) LOW PASS (LUMPED)

Fig. 8.5. Prescribed filter specifications in a) and b) distributed cases, c) Lumped bandpass case and d) in Lumped lowpass case for filter no.8.

and $\Omega_2 = 3.9007$, $\Omega_4 = 2.4767$ (8.13).

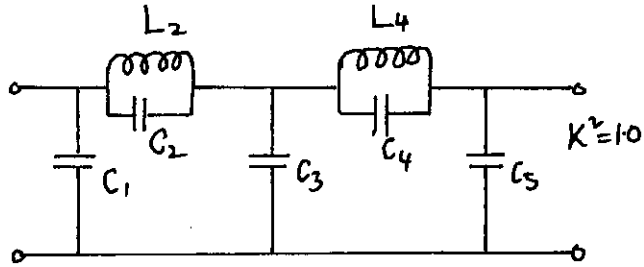

Fig.8.6. Lowpass prototype for n=5, $K^2 = 1.0$

From Fig.8.5b it is seen that the centerfrequency is normalized to $\frac{\pi}{4} = 0.7854$ radian so that the band edge frequency ω_b will be .74613 for 10% bandwidth.

Then we get $a = (\tan 2\omega_b)/2 = 6.3534$

and $1/\sqrt{a} = 0.396731$ (8.14).

The length of network for a center frequency of 1.6 k mc/s is $\lambda_0/8 = 0.923"$

By using the formulas (6.9a) and (6.9b) we get

$$\lambda_{2+} = 1.3530 \quad , \quad \lambda_{4-} = .8239$$
$$\lambda_{2-} = 0.7391 \quad , \quad \lambda_{4+} = 1.2137 \qquad (8.15)$$

The corresponding actual frequencies at which the poles of infinite attenuation are located are

$f' = \left(\tan^{-1}(\lambda_{r\pm}) \times \frac{\pi}{180} \div \pi/4\right) 1600$ MHz

$f_1' = 1296.644$ MHz. $f_3' = 1796$ MHz.

$f_2' = 1403.915$ MHz $f_4' = 1903.358$ MHz.

Characteristic Admittance Matrices:

The values of λ's obtained are now used to calculate the element values of the characteristic admittance matrices (6.25) and (6.24). The following matrices then result:

Network-1

(0)	(1)	(2)	(3)	(4)	(5)	(6)
1	-1	0	0	0	0	0
-1	7.8274	-.8979	0	0	0	0
0	-.8979	1.3885	-.4905	0	0	0
0	0	-.4905	13.32984	-2.1333	0	0
0	0	0	-2.1333	3.5814	-1.4481	0
0	0	0	0	-1.4481	7.8864	-1
0	0	0	0	0	-1	1

(8.16).

Network-2

(1)	(2)	(3)	(4)	(5)
6.42	-.4905	0	0	0
-.4905	1.3885	-.8979	0	0
0	-.8979	13.0521	-1.4481	0
0	0	-1.4481	3.5814	-2.1333
0	0	0	-2.1333	7.5715

(8.17)

Now scaling lines 1 and 5 of both network by $1/\sqrt{a}$ we get the matrices (2a) and (2b) of Appendix-B. After this scaling on the remaining lines were done as follows: In network 1, C_{44} was made 1.2 times C_{55}, C_{22} was made 1.2 times C_{11} and C_{33} was made equal to C_{44}. However operation on a particular line is carried out on both networks. After these operations the resulting characteristic admittance

matrices are shown in Appendix-B as matrices (3a) and (3b).

In order to get the static capacitance values and also in order to convert the values to a 50 ohm system we need to scale the matrices (3a) and (3b) of Appendix B by 7.534. Thus we get the following static capacitance matrices.

Network-1

(0)	(1)	(2)	(3)	(4)	(5)	(6)
7.534	-2.9887	0	0	0	0	0
-2.9887	9.2819	-2.7695	0	0	0	0
0	-2.7695	11.1383	-1.2748	0	0	0
0	0	-1.2748	11.2226	-3.4204	0	0
0	0	0	-3.4204	11.2226	-2.7913	0
0	0	0	0	-2.7913	9.3520	-2.9887
0	0	0	0	0	-2.9887	7.534

(8.18)

Network-2

(1)	(2)	(3)	(4)	(5)
8.2949	-1.5128	0	0	0
-1.5128	11.1383	-2.3340	0	0
0	-2.3340	10.9891	-2.3521	0
0	0	-2.3521	11.2226	-4.1121
0	0	0	-4.1121	8.9783

(8.19)

Calculation of physical dimension of Network-1

We choose $t/b = 0.6$, and $t = 0.6"$, therefore, we get $b = 1"$.

Length of network-1 = $\frac{\lambda_0}{8}$ = 0.9227 inches.

The values of fringing capacitances, spacing between lines, widths of the lines etc. are calculated as mentioned in chapter-7. The following table shows the values of self capacitances, mutual capacitances, fringing capacitances, widths of the lines and the spacing between the lines.

k	c_k/ϵ	$\frac{c_{k,k+1}}{\epsilon}$	$\frac{c'_{fe\ k,k+1}}{\epsilon}$	w_k/b	w_k inches	$\frac{s_{k,k+1}}{b}$	$s_{k,k+1}$ inch.
0	4.5453	2.9887	0.432	0.128130	.13	.209	.209
1	3.5237	2.7695	0.478	0.17	.17	.223	.223
2	7.094	1.2748	0.718	0.47	0.47	0.406	0.406
3	6.5278	3.4204	0.4	0.429	0.429	0.187	0.187
4	5.0109	2.7913	0.46	0.329	0.329	0.22	0.22
5	3.572	2.9887	0.432	0.179	0.179	0.209	0.209
6	4.5453	-	-	0.1283	.13		

(8.20)

Width calculations:

$w_o/b = \frac{1}{2}(1-t/b)\left[\frac{1}{2}\left(\frac{C_p}{\epsilon}\right) - \frac{C_f'}{\epsilon} - \frac{(C_{fe}')_{0,1}}{\epsilon}\right]$

$= 0.2(\frac{1}{2}(4.5453) - 1.2 - .432) = 0.12813.$ $\quad w_o = 0.12813.$

But we know that if w_k/b is $< .35\ (1 - t/b)$ then correction must be applied.

Here $0.35\ (1-t/b) = .14$, this means that w_o/b is $< .14$

Therefore, correction must be applied.

$w'_o/b = \frac{\text{corrected width}}{b} = \frac{(.07\ (1-t/b) + w/b)}{1.2} = .13$

$\therefore\ w'_o = .13$ inches.

Similarly w'_6 = .13 inches.

Now,

$$w_k/b = \frac{1}{2}\left(1-\frac{t}{b}\right)\left[\frac{1}{2}\left(\frac{t_k}{\epsilon}\right) - \frac{(C'_{fe})_{k-1,k}}{\epsilon} - \frac{(C'_{fe})_{k,k+1}}{\epsilon}\right]$$

w_1/b = .2 (½ x 3.5237 - .452 - .478) = .17037. $\therefore$ w_1 = .17 inches

w_2/b = .2 (½ x7.098 -.478 - .718) = .4702. $\therefore$ w_2= .4702 inch.

w_3/b = .2 (½ x 6.5278 - .718 - .4)= .42918 $\therefore$ w_3 = .42918 inch.

w_4/b = .2 (½ x 5.0109 -.4-.46) = .32909 $\therefore$ w_4 = .329 inch.

w_5/b = .2(½ x 3.572- .46 -.432) = .179 $\therefore$ w_5 = .179 inch.

Calculation of physical dimension of Network-2

Applying length correction for the parasitic lumped end effect capacitances the corrected length is

$$l' = l - .2b\,c_o = l - .2\,c_o = .922736 - .2 \times 1.2 = .6827"$$

and l'/l = .6827/ .9227 = .73989.

Augmenting the mutual capacitance values due to shortening of length, we get;

$$Y'_{o\pm} = \frac{2.1016}{\tan(.73989 \times \tan^{-1} 1)} = 3.2$$

For this case we have assumed Y_{81} and Y_{5G} to be equal to 2.1016. It has been assumed that this would give suitable dimensions.

Thus

$Y'_{2\pm}$ = 2.4735 Y'_{2-} = 3.3882

Y'_{4+} = 3.7372 Y'_{4-} = 6.0584.

The following chart may now be prepared as we have done previously by use of formulae of chapter-7 and Getsinger's[9] graph

Thus

k	c_k/ϵ	$\frac{c_{k,k+1}}{\epsilon}$	$\frac{c'_{fe}{}_{k,k+1}}{\epsilon}$	w'_k/b	w_k inch.	$c_{k,k+1}$	$c_{k,k+1}$ inch.
0	6x7821	3.2					
1	3.5821	2.47	.50	.258	.258"	.285	.285"
2	7.2915	3.3882	.41	.54715	.547"	.193	.193"
3	6.303	3.7372	.378	0.4727	.475"	.175	.175"
4	4.7584	6.0584	.255	.3492	.349"	.108	.108"
5	4.8662-3.2 = 1.666	3.2		.1156	.1156"	.285	.285"

(8.21)

Width calculations for network-2:

$w_1/b = .2(\frac{1}{2}x3.5821 - .50) = .258$, $b=1"$

$w_2/b = 2.(\frac{1}{2} \times 7.2915 - .41 - .50) = .54715$

$w_3/b = .2 (\frac{1}{2} \times 6.303 - .378 - .41) = .4727$

$w_4/b = .2 (\frac{1}{2} \times 4.7584 - .378 - .255) = .34924$

$w_5/b = .2 (\frac{1}{2} \times 1.666 - .255) = .1156$

Spacing between the lines are calculated as before. The spacing between ground end wall and line 1 also between end wall and line 5 are found out with the help of figure 7.3 as mentioned before.

Construction of Filter No.2:

The drawing of the section through the central plate of filter no.2 along with other necessary dimensions is presented in Fig.8.7a. In this figure the cross sectional view is not shown. However it will be the same as shown in Fig.8.4a except that the ground plane spacing is now 1 inch and the thickness of the central plate is now 0.6 inch.

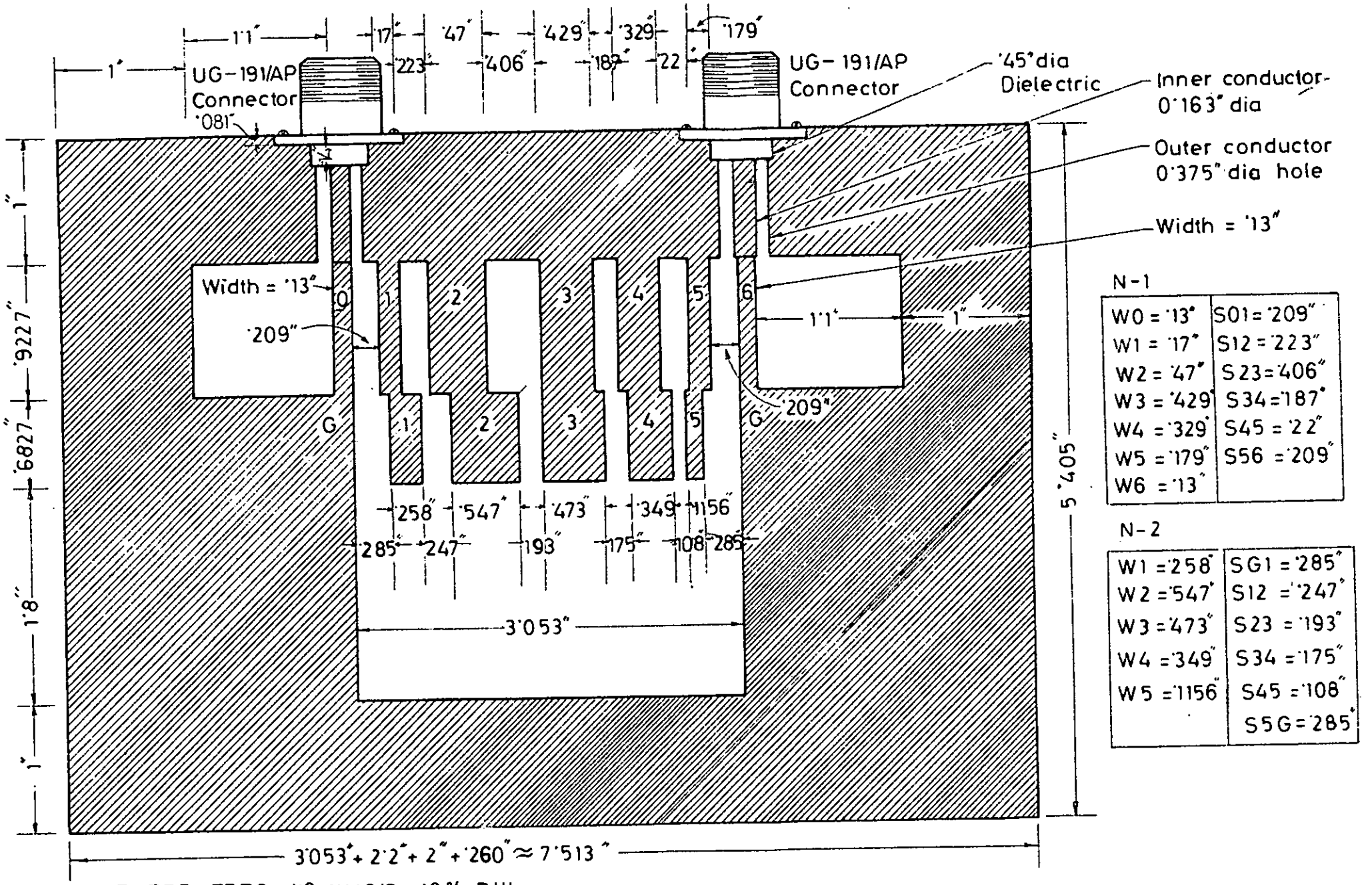

N-1

W0 = ·13"	S01 = ·209"
W1 = ·17"	S12 = ·223"
W2 = ·47"	S23 = ·406"
W3 = ·429"	S34 = ·187"
W4 = ·329"	S45 = ·22"
W5 = ·179"	S56 = ·209"
W6 = ·13"	

N-2

W1 = ·258"	SG1 = ·285"
W2 = ·547"	S12 = ·247"
W3 = ·473"	S23 = ·193"
W4 = ·349"	S34 = ·175"
W5 = ·1156"	S45 = ·108"
	S5G = ·285"

CENTER FREQ. 1·6 KMC/S, 10% BW

FILTER NO. 2

FIG 8.7a DRAWING OF EXPERIMENTAL UHF ELLIPTIC FUNCTION BANDPASS FILTER USING STEPPED DIGITAL LINES (Section through central plate)

The top, bottom and the other two plates (necessary for maintaining gap between the transmission lines and the ground plates) were constructed as before by simply machining and cutting brassplates. However the slots in the central plate were cut for this filter by means of Endmill cutter machine. This machine was chosen in order to maintain better accuracy in dimension.

A photograph of the filter with its cover plate opened is shown in Fig. 8.7b.

As before, tuning screws were necessary in order to improve the performance of the filter. These were placed on the top plate such that the screws appear in between lines of each network.

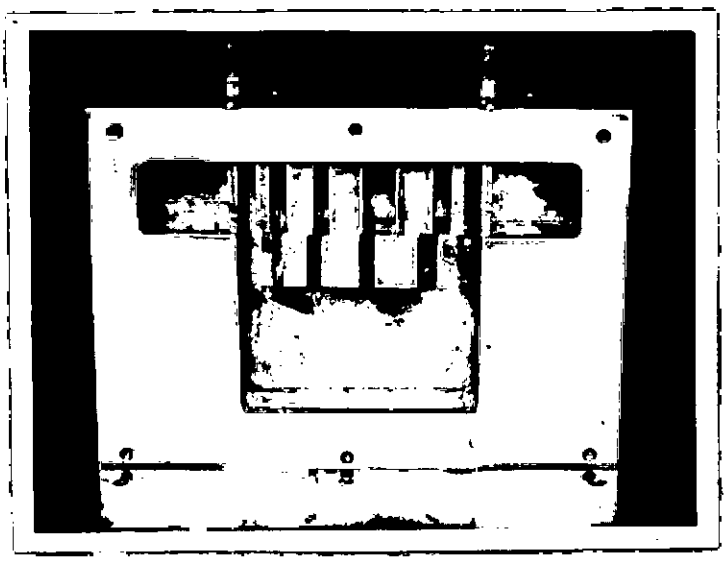

Fig.8.7b. Photograph of Filter no. 2. with cover plate removed.

C H A P T E R - 9

MEASUREMENT OF INSERTION LOSS CHARACTERISTICS OF THE FILTERS:

9.1. INTRODUCTION:

In chapter 8 two UHF elliptic function bandpass digital filters were designed and it has been mentioned there that both of these filters were ultimately constructed by machining brass plates. In this chapter two measurement set-ups are presented with the help of which the attenuation or the insertion loss characteristics of the filters were measured. These are (i) heterodyning method (using I-F amplifier and Mixer rectifier) and (ii) the method using thermistor mount and power meter. Plots of the insertion loss versus frequency are also presented for these measured data.

9.2. MEASUREMENT OF INSERTION LOSS CHARACTERISTIC OF THE FILTERS BY HETERODYNING METHOD USING TYPE DNT DETECTOR:

A set up for measuring the insertion loss characteristics of the filters using type 1216-A Unit I-F Amplifier and a type 874-MR Mixer Rectifier is shown in Fig.9.1. The type 1216-A Unit I-F Amplifier is a four stage high gain, intermediate-frequency amplifier operating at a frequency of 30 mc/s with a bandwidth of 0.7 mc/s. The relative signal level is indicated on a meter. The meter is calibrated in a decibel scale. A precision resistance type step ATTENUATOR is provided for determining relative signal levels beyond the range of the meter.

The amplifier is used in conjunction with a Type 874-MR Mixer Rectifier and a Unit oscillator to form a sensitive, wide frequency range, well shielded VHF and UHF detector which is referred to as a Type DNT

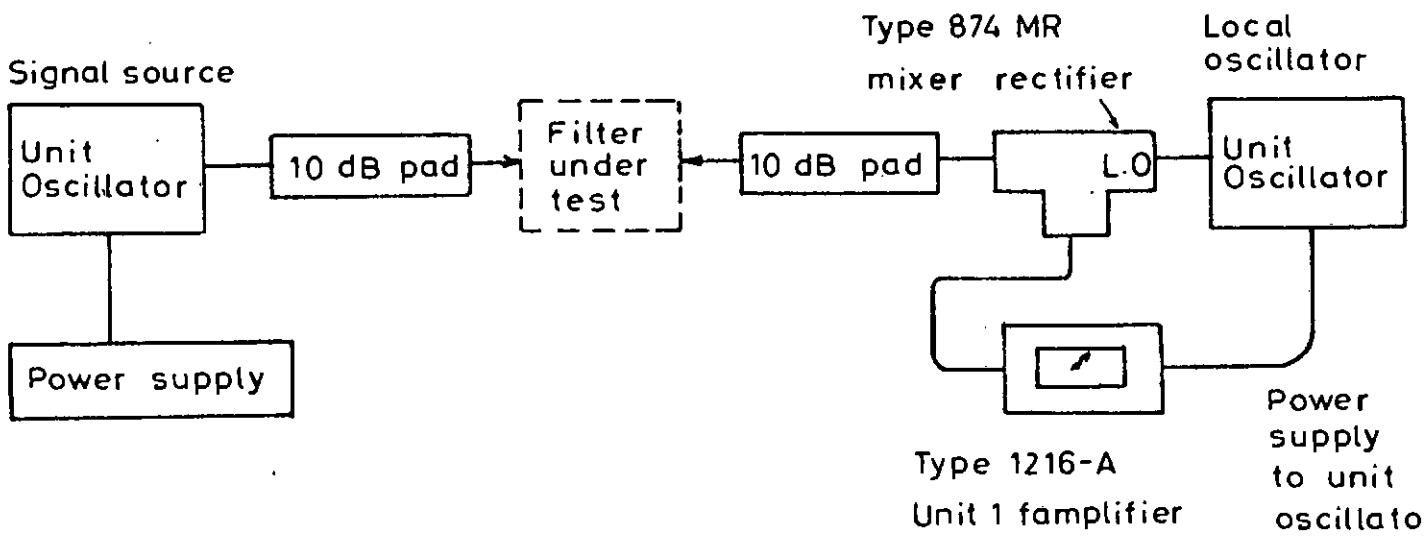

Fig 9·1. Block diagram of the set up for measuring the insertion loss of the filters by heterodyning method.

Detector. An incoming signal and the signal from the local Unit Oscillator, which is set to a frequency 30 mc/s above or below the frequency of the signal to be detected, are mixed in the Mixer Rectifier, and the 30 mc/s difference frequency produced is amplified and detected by the instrument. Satisfactory performance is also obtained when the signal is heterodyned with harmonics of the local Unit-Oscillator frequency, hence, a very wide frequency range can be covered.

In order to get the insertion loss of the filters we must use a source of rf power to drive the filter as shown in Fig.9.1. The filter under test is connected between the generator and detector as shown in Fig.9.1. For a particular signal frequency the local oscillator frequency should be set 30 mc/s above or below the signal frequency. The step ATTENUATOR of the I-F Amplifier is then adjusted to produce a meter reading within the calibrated Decibels portion of the meter scale, the local oscillator frequency is slightly readjusted for peak response. The sum of the step ATTENUATOR and decibel meter scale reading is obtained. The filter under test is then removed and the generator and detector are connected directly together. The I-F amplifier step ATTENUATOR is then readjusted if necessary, to produce a meter reading within the calibrated decibels portion of the scale, and the sum of the step ATTENUATOR and meter decibels readings are obtained. The insertion loss of the filter under test in decibels is equal to the difference in the sums obtained in the two measurements. For maximum accuracy, the local oscillator tuning should be checked for frequency drift and the I-F amplifier step ATTENUATOR and meter reading should be rechecked. The readings for the insertion loss of both the filters over the frequency ranges of interest were taken by this method. The complete set of readings for both Filter

no.1 and Filter no.2 are given in Table nos.1,2,3 and 4. The plot of the measured attenuation characteristic for filter no.1 (without any tuning) is given in Fig.9.2, for filter no.1 (after tuning) is given in Fig.9.3. Also the measured attenuation characteristic for filter no.2(without tuning) is presented in Fig.9.4 and for filter no.2 (after tuning) is presented in Fig.9.5.

TABLE No.1

MEASURED ATTENUATION CHARACTERISTIC OF FILTER NO.1(BEFORE TUNING)

Frequency MHz	Attenuation db	Frequency MHz	Attenuation dB
1750	58	2200	3.1
1980	61	2220	7.1
1800	64.2	2240	5.8
1820	69.1	2260	7.1
1840	64.5	2280	13
1860	56.2	2300	22
1880	51	2320	32.3
1900	48	2340	42.3
1920	49.3	2360	54.4
1940	41.1	2380	65.2
1960	20	2390	70.3
1980	20.5	2400	64.4
2000	16	2420	61.5
2020	10.1	2450	59.5
2040	3	2480	61
2060	1	2500	63
2080	1	2520	67
2090	2	2560	70
2100	4.1	2580	73.5
2120	1	2600	62
2140	2	2620	62
2160	5.2	2640	67.5
2180	2	2660	61

TABLE No.2

MEASURED ATTENUATION CHARACTERISTIC OF FILTER NO.1(AFTER TUNING)

Frequency Mc/s.	Attenuation dB	Frequency Mc/s.	Attenuation dB
1750	51.1	2140	1.5
1780	47.6	2150	6.4
1800	50.0	2180	4.8
1820	57.1	2200	1.3
1840	44	2210	0.1
1880	38	2220	1
1900	33.1	2240	5
1920	20.4	2260	10
1950	17.2	2280	20
1980	12	2300	30
2000	8	2320	40.1
2010	4	2340	48.1
2020	3.2	2350	60
2040	3.2	2380	65.2
2050	4.2	2400	50.3
2060	1.5	2420	47
2080	1.6	2460	46.5
2100	2.5	2480	48.2
2110	4.5	2490	52
2120	0.08	2500	48

TABLE NO.3

MEASUREMENT OF ATTENUATION CHARACTERISTIC OF TILTER NO.2(BEFORE TUNING)

Frequency MHz	Attenuation dB	Frequency MHz.	Attenuation dB
1330	51	1535	6
1340	46	1540	4.2
1350	42	1550	2.1
1370	41	1560	4
1390	43.1	1570	5.5
1400	47	1580	0
1410	43	1590	2.5
1420	43	1600	3
1430	32	1610	25
1440	24.2	1620	65.5
1460	12.1	1640	55
1470	9	1650	50
1480	7	1670	50.4
1490	5.1	1680	54.1
1500	4.1	1690	58
1510	0	1710	53.3
1530	3	1740	57

TABLE NO.4

MEASURED ATTENUATION CHARACTERISTIC OF FILTER NO.2(AFTER TUNING)

Frequency mc/s	Attenuation dB	Frequency mc/s	Attenuation dB
1320	50	1530	0
1320	48	1540	0
1350	58.5	1545	0.3
1360	50	1550	0
1370	53	1555	-1.2
1380	46.5	1560	0
1390	40	1570	2.1
1400	35.3	1580	2.1
1420	24	1600	5
1430	17	1610	20.1
1440	14.3	1620	40.3
1450	12.1	1630	63.1
1460	7	1632	66
1470	0	1640	63.4
1475	-1.3	1650	64.2
1482	0	1670	55.3
1490	1.5	1700	53
1500	0	1720	55
1510	0.5	1730	57
1515	1	1750	53
1520	1		

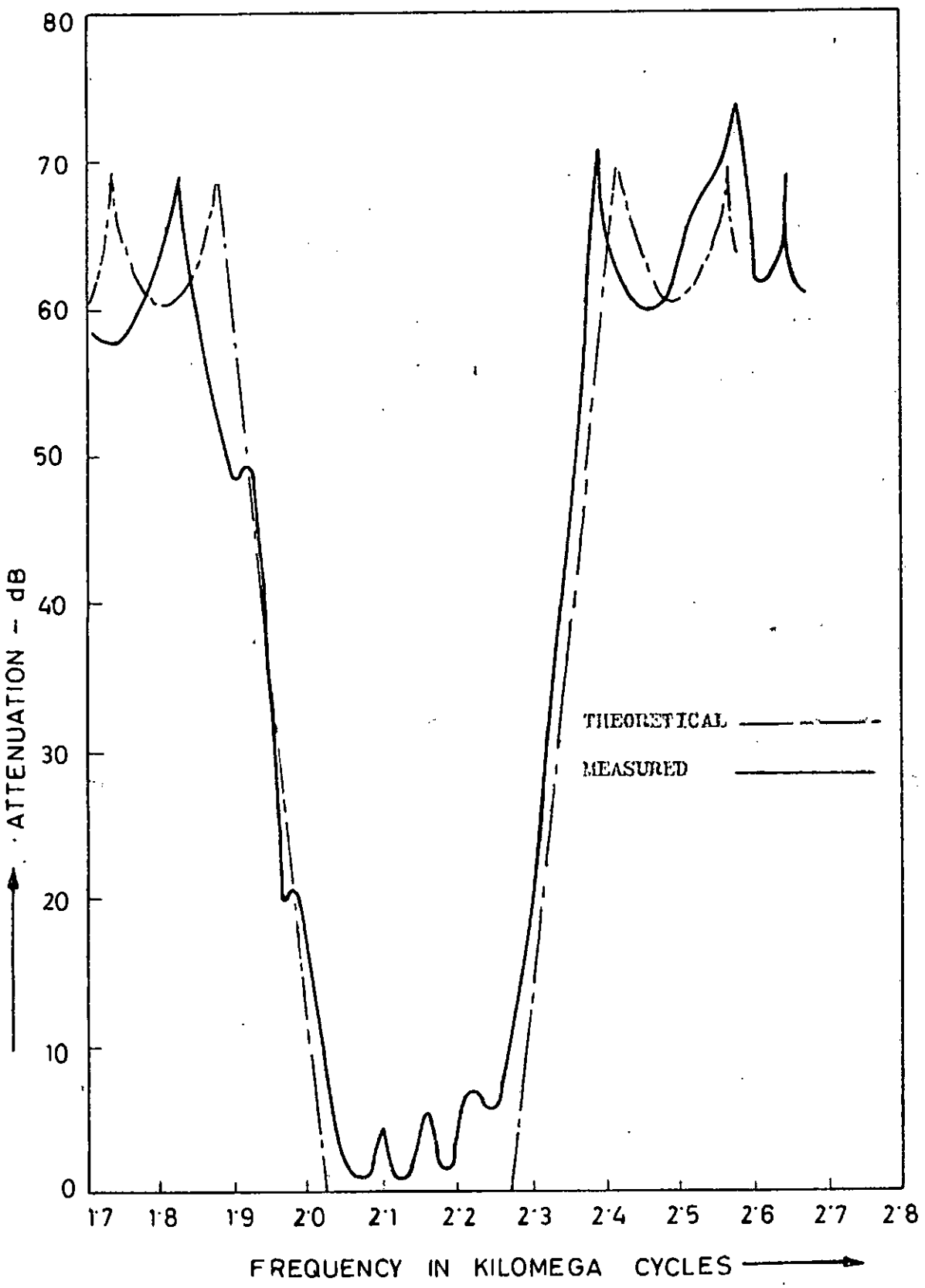

FIG. 9·2 THEORETICAL & MEASURED ATTENUATION CHARACTERISTIC OF EXPERIMENTAL FILTER NO. 1 (WITHOUT TUNING)

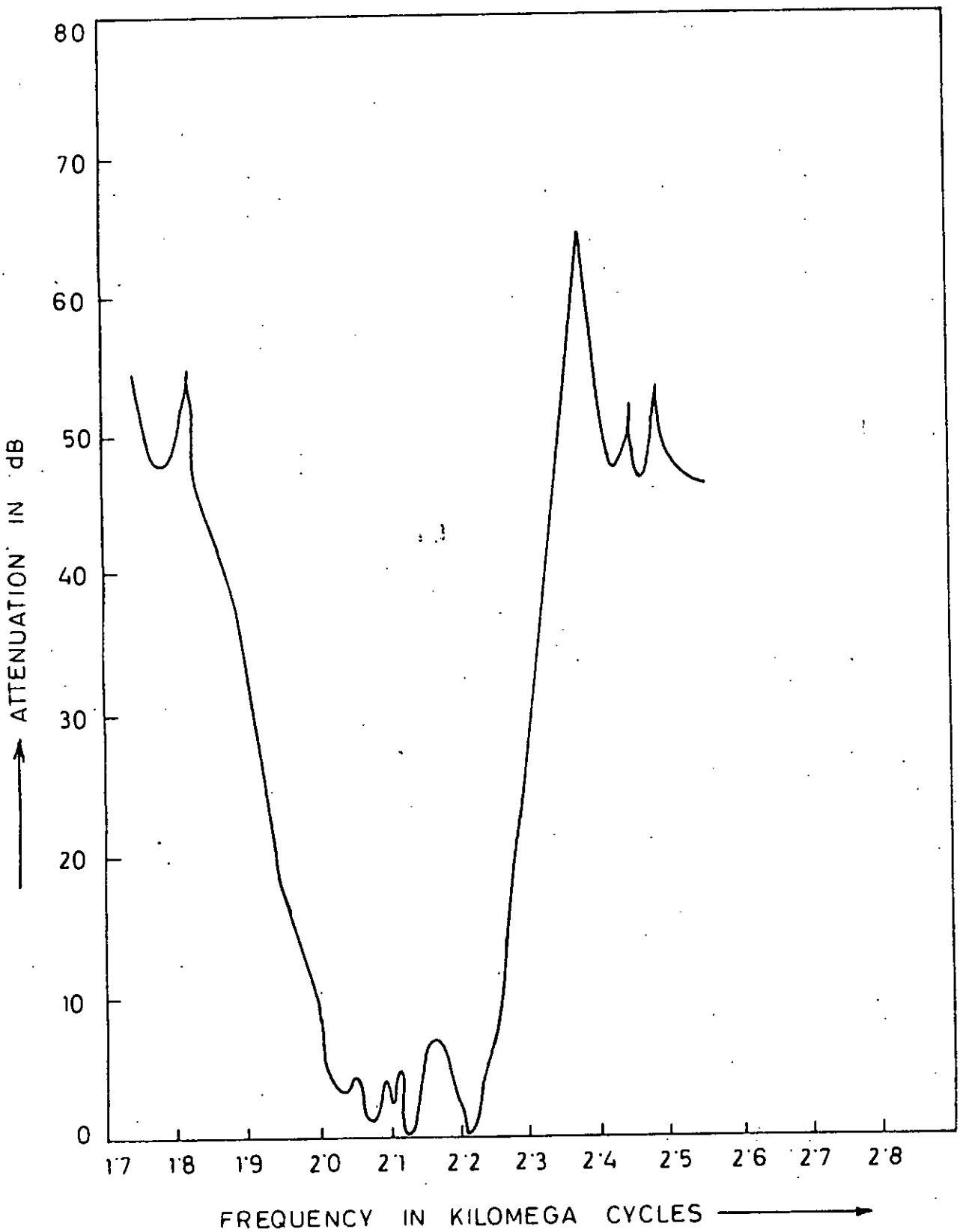

FIG. NO. 9·3. MEASURED ATTENUATION CHARACTERISTIC OF EXPERIMENTAL FILTER NO. 1 AFTER TUNING BY MEANS OF TUNING SCREWS.

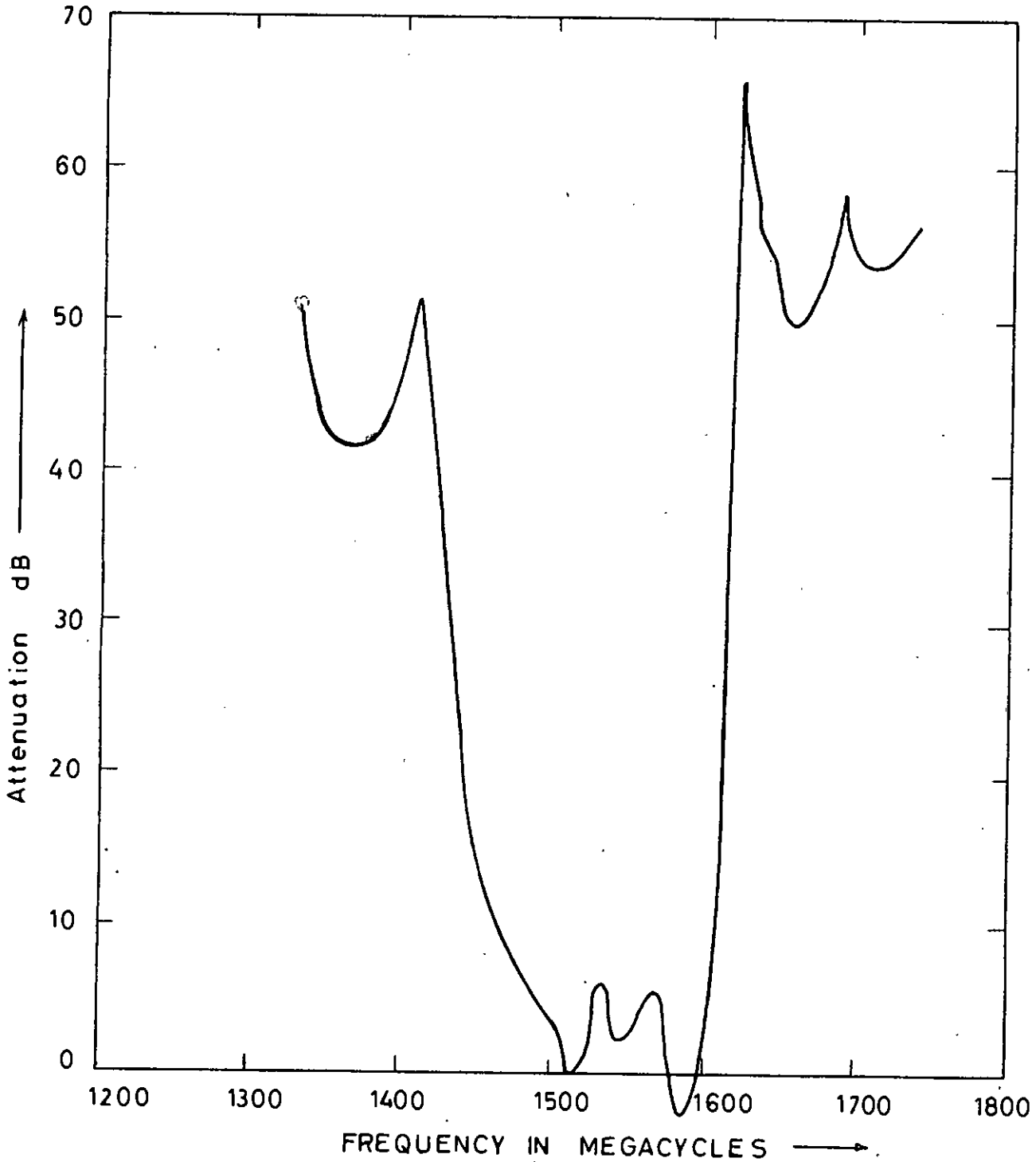

Fig. 9-4 Measured attenuation characteristic of experimental filter no. 2. (Before tuning).

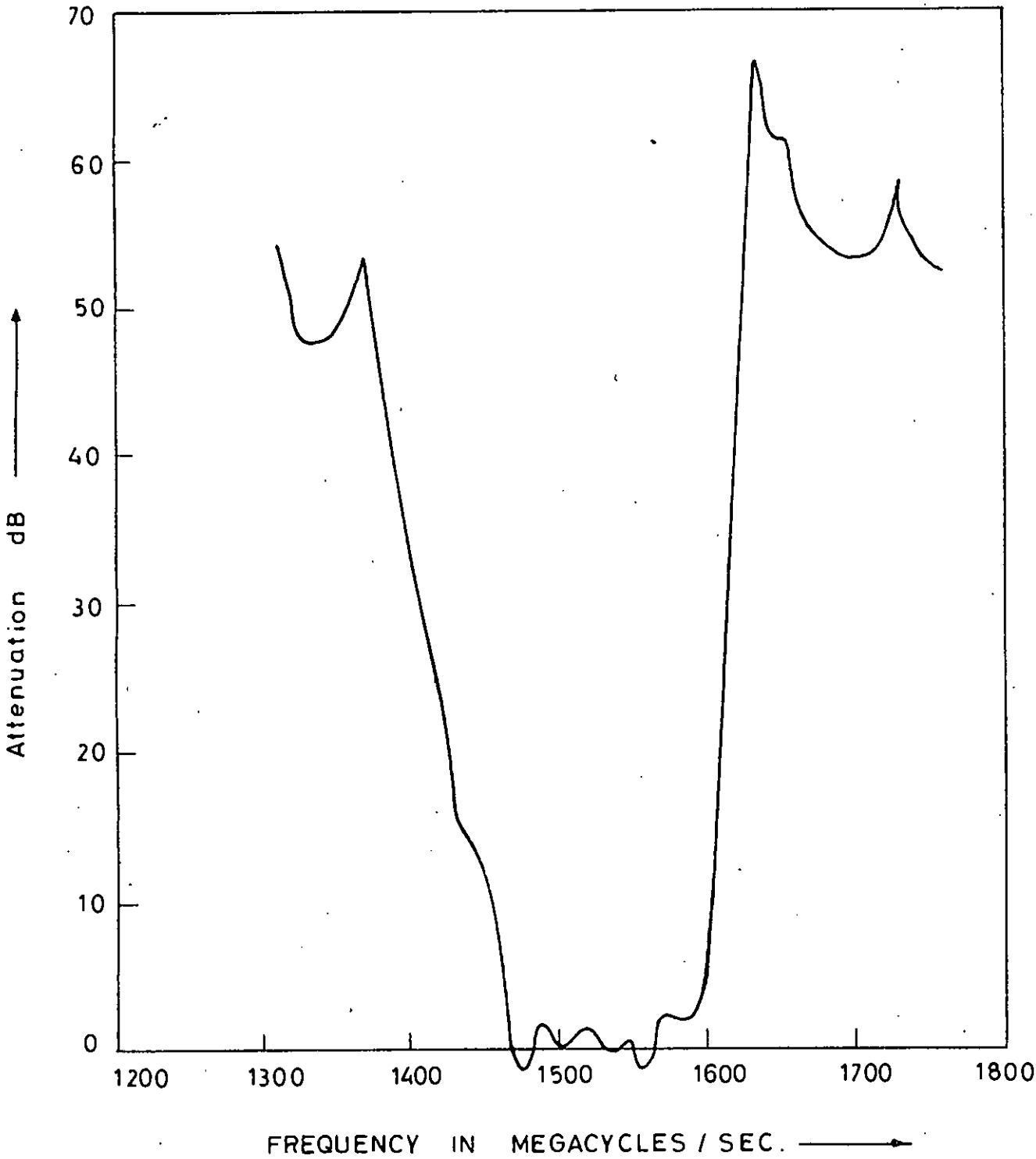

Fig. 9·5. Measured attenuation characteristic of experimental filter no. 2 (After tuning).

9.3. MEASUREMENT OF INSERTION LOSS CHARACTERISTIC OF FILTERS BY MEANS OF POWER METER:

Let us first of all discuss something about the thermistor mount and the power meter and the arrangement for measuring the power. The arrangement for measuring Average Power with the help of a hp-430-C Microwave power meter and a 477B coaxial thermistor mount is shown in Fig.9.6. With the help of this arrangement average power upto 10mw may be measured if the frequency range is within 10 mc/s to 10 Gc/s.

Thermistors are resistive devices which are capable of dissipating r.f. power and using the thermal energy absorbed to change resistance. The thermistor has a negative coefficient of temperature and is constructed generally of a small amount of semiconducting materials suspended by two fine wires. The hp 477B coaxial thermistor mount is designed to operate at 200 ohm. resistance with negative temperature coefficient.

The thermistor mount forms one leg of a self balancing bridge of the power meter balanced for the operating resistance of the thermistor mount. The power meter contains such a bridge, a 10.8 kc oscillator, a d.c. bias circuit, and a meter circuit. Initially, the thermistor element is connected to the instrument bridge circuit but is not connected to an r.f. power source. The thermistor mount bridge is balanced when the element changes from its cold resistance to its operating resistance. The change takes place as the element absorbs power from the oscillator and d.c. power from the bias circuit of the power meter.

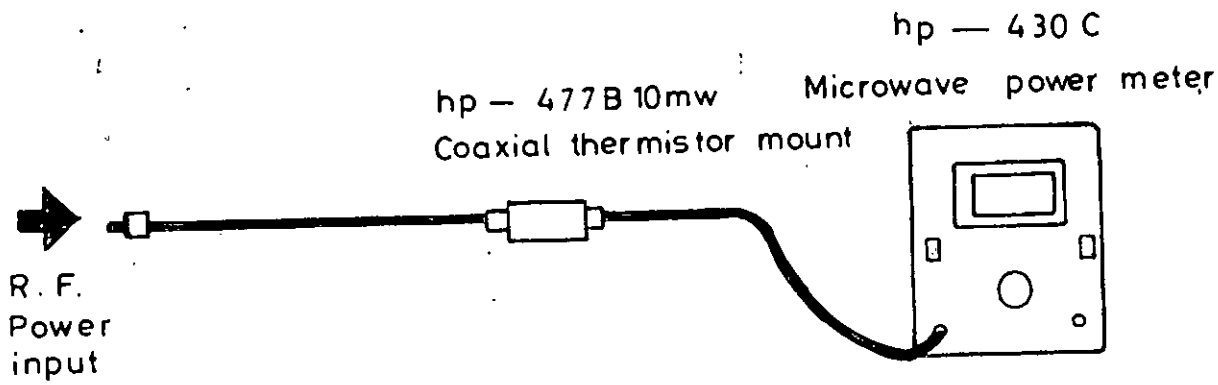

Fig. 9·6. Arrangement for measuring average power.

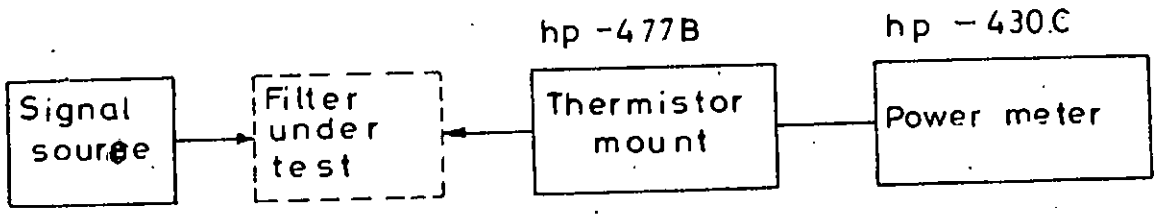

Fig. 9·7. Block diagram of the set-up for the measurment of insertion loss of filters by using power meter and thermistor mount.

The power meter indicator is set zero by means of zero set nobs. The r.f. power source is now connected to the thermistor mount. The thermistor element absorbs the external r.f. power, heats, and changes its resistance which unbalances the bridge . This action causes the output from the oscillator inside the power meter to decrease to accomodate the external r.f. power through the thermistor element. The voltmeter circuit inside the power meter measures the amount of this power decrease from the oscillator of the power meter and displays the measurement calibrated as a power increase added by the external r.f. source.

Our aim is to measure the insertion loss characteristic of the digital elliptic function filter. The block diagram for measuring the insertion loss of a filter by using the power meter and the thermistor mount is shown in Fig.9.7. In this case the power meter with only the thermistor mount connected to it (without giving any signal) is balanced with the range switch in 10mw i.e. 10 DB1 position and with proper biasing. The thermistor mount is then connected to the signal source. The attenuator in the signal source is properly adjusted so that the pointer is in the 0 DB1 position or near 0 DB1 position. The signal source is then disconnected and the filter is then inserted in between the signal source and the thermistor mount as shown in Fig.9.7. The reading at this moment is noted. The difference between the reading without the filter and that with the filter in dB will give the insertion loss of the filter at that particular frequency. The procedure is repeated over the whole range of frequency of interest.

However for our case the readings were taken for the passband only because outside the passband the loss is too high to be determined with this method. The readings were taken in the passband only for Filter no.2. The readings are given in Table no.5 and a plot of the attenuation Vs. frequency, based upon these readings is also given in Fig.9.8.

TABLE NO. 5

MEASURED ATTENUATION CHARACTERISTIC OF FILTER NO.2 (AFTER TUNING) IN THE PASSBAND ONLY.

Frequency mc/s	Attenuation dB
1460	8
1468	0
1475	-1.9
1485	2.4
1500	0
1510	1.18
1540	0
1545	0
1560	-1.9
1570	2.2
1580	2.2
1590	2.4
1600	8

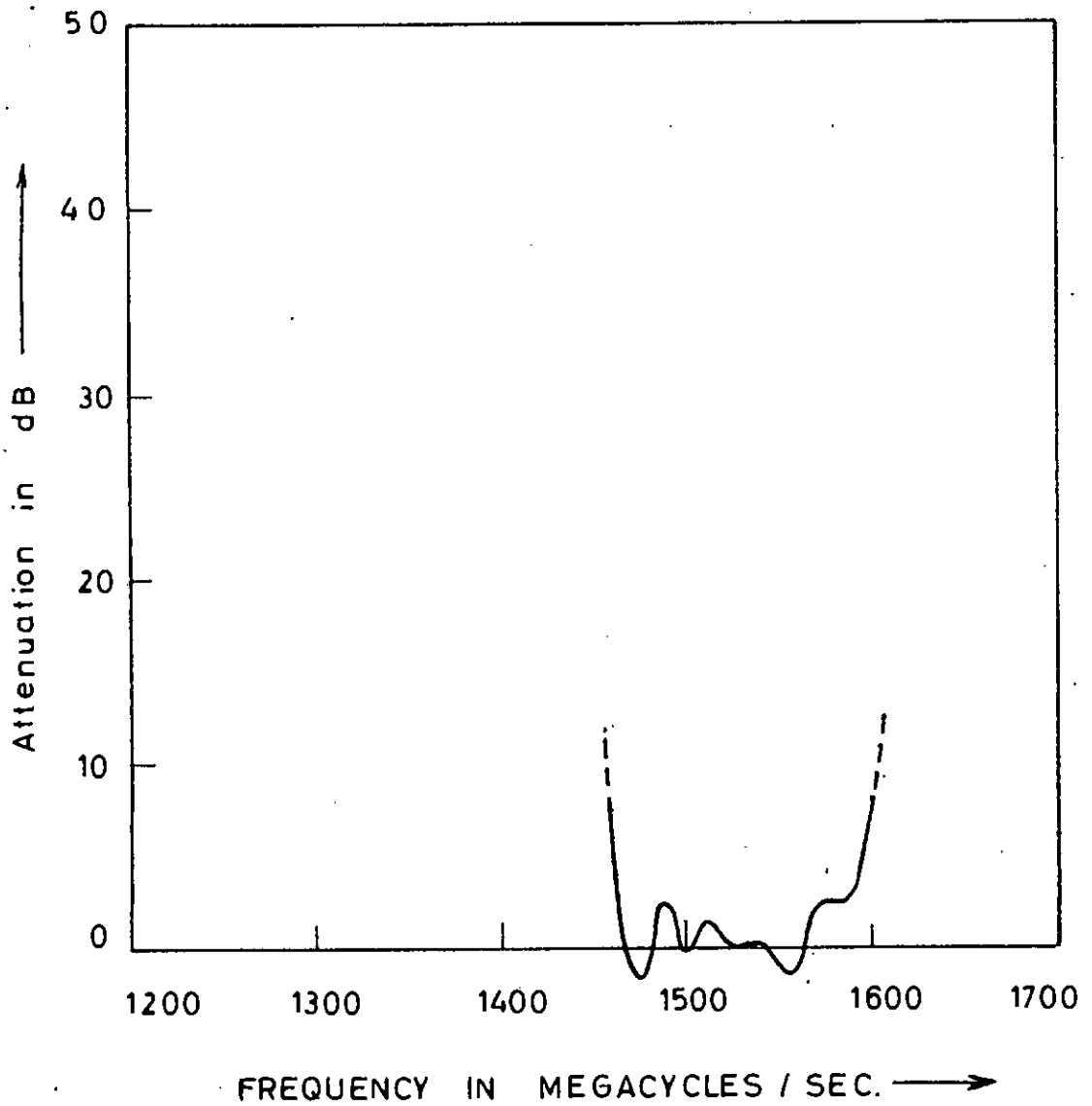

Fig. 9.8 Attenuation characteristic of experimental filter no. 2 (After tuning).

Readings taken in the passband only by power meter.

CHAPTER-10

DISCUSSION AND CONCLUSION

Two elliptic function bandpass filters were designed and constructed using the realization procedure developed in this study. Filter no.1 with center frequency of 2150 MHz was designed to have a maximum passband attenuation of 0.044 dB, (corresponding to a maximum passband VSWR of 1.222), minimum stopband attenuation of 60.1 dB and a bandwidth of 236.50 MHz. The measured attenuation characteristics of Filter no.-1 were presented in Fig.nos. 9.2 and 9.3. The curve of Fig.9.3 which was obtained after tuning, shows that the maximum passband attenuation is 7 dB, the minimum stop band attenuation is 47 dB, the center frequency is 2125 MHz and the bandwidth is approximately 237 MHz. It is observed that the passband attenuation is more than the theoretically predicted value and the minimum stop band attenuation is 13.1 dB less than the theoretically predicted value. The center frequency and band width were almost same for this Filter no.-1.

Filter no.-2 was designed for a center frequency of 1600 MHz to have a maximum passband attenuation of 0.044 dB, a minimum stopband attenuation of 63.52 dB and a band width of 160 MHz. The measured attenuation characteristics of Filter no.-2 were presented in Fig nos.9.4 and 9.5. The curve of Fig.9.5 which was obtained after tuning, shows that the maximum passband attenuation is 2 dB, the minimum stopband attenuation is 48 dB, the center frequency is 1532 MHz and the bandwidth is 125 MHz. It is observed that the maximum passband attenuation is 1.956 dB more than the theoretically predicted value and the minimum stopband attenuation is 15.52 dB less than the theoretically predicted

value. The value of the center frequency has decreased by 4.25%. The band width has shrinked by 35 MHz. It is also observed that for both of these filters tuning improved the results to some extent.

Although it is seen that for both the filters the measured attenuation characteristics deviated to some extent from the theoretically predicted characteristics, the overall performances of both these filters were not unsatisfactory.

Both Filter no.-1 and Filter no.-2 were constructed by machining brass plates. In the construction of these filters, accuracy in physical dimension is very much necessary. For example while constructing the filters if some inaccuracy introduces in the lengths of the lines then this changes the center frequency. If there is an increase in length then there will be a decrease in the value of the center frequency and vice versa. For example, the total length of the lines of Filter no.-2 (before length correction) was equal to 1.8454 inch. (total length = $\lambda_0/4 = v/4f_0'$). This corresponds to a center frequency of 1600 MHz. Now if during machining, due to some inaccuracy introduced, the length remains 1.86 inch. then the corresponding center frequency become 1587 MHz. This shows that a small change in length of .0146 inch. causes a significant change in the center frequency. So this may be one of the reasons due to which a shift in center frequency was observed in the case of Filter no.-2. Again referring to the length correction formula for network-2 given in section 7.10 it may be recalled here that the assumptions on which that formula was developed were not exactly accurate. So there is some inaccuracy in that formula. But no other formula is available which can give us a better and more accurate result.

This may be another reason for the shift of the center frequency.

Curves of $\Delta c/\epsilon$ vs. s/b in Fig.7.2 shows that a slight change in s (the spacing between the lines) in the initial portion of the curve causes considerable change in Δc (mutual capacitance between lines). For example for a t/b = 0.6 and b=1" if s changes from .1" to .11" then the value of c decreases from 6 to a value of 5. So it is seen that Δc is a very sensitive function of s for our case. It is very likely that due to the inaccuracy of machining some error may be introduced in the interbar spacing(s). This causes a change in the capacitance matrix which in turn causes a change in the response of the filter. Therefore, the accuracy in the response is very much dependent on the accuracy of machining.

Again much difficulty was faced in connecting the input and output connectors to the input and output transformer elements. Due to the difficulty in machining it was almost impossible to maintain a high degree of accuracy at those connections. For example, for the connection between the transformer element and the connector it was necessary to construct a conxial transmission line of 50 ohms. characteristic impedance as shown in Fig. 10.1. But due to the lack of accuracy in physical dimension and due to the fact that the central conductor may become eccentric with the outer conductor of the transmission line, the characteristic impedance may not remain 50 ohm. So at these input and output ports impedance mismatch may be present. This mismatch is very much undesireable. Because such a mismatch causes an increase in loss in the passband.

Considering the tolerance within which the different elements of the filter could be machined with our facilities, the

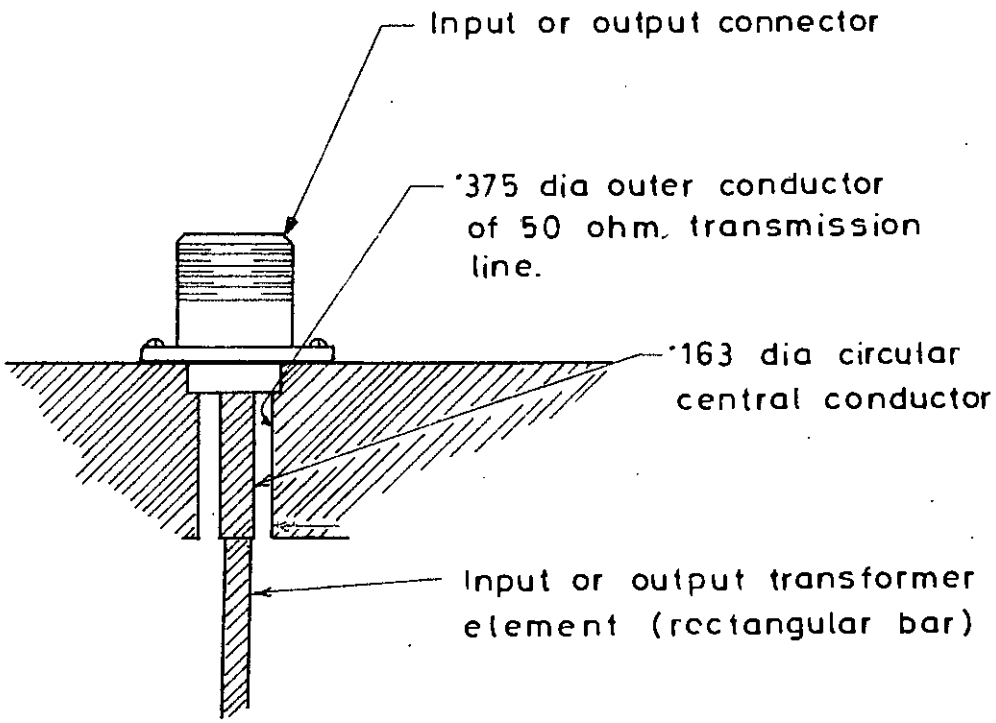

Fig. 10·1. Details of connecting input or output connector to the input or output transformer element.

performances of the filters can be deemed quite satisfactory.

Theoretically this type of filter should be constructed with materials having infinite conductivity . The brass plates that were used for the construction of our filters were purchased from local market and were not meant for this kind of work. This may cause some loss in the passband.

Considering the availability of materials and considering the machining facilities that we have, we can say that the difference that appeared between the theoretical and measured characteristics was tolerable. Even with the existing facilities filters in the UHF range can be designed and constructed with acceptable measured performance.

APPENDIX-A

SCALING OF CHARACTERISTIC ADMITTANCE MATRICES OF EXPERIMENTAL FILTER NO.1

The characteristic admittance matrices (8.4) and (8.5) for filter no.1 are as shown below:

Network-1

(0)	(1)	(2)	(3)	(4)	(5)	(6)	
1	-1	0	0	0	0	0	
-1	7.3113	-.0654	0	0	0	0	
0	-.9654	1.4867	-.5213	0	0	0	
0	0	-.5213	10.7792	-2.3051	0	0	
0	0	0	-2.305	3.8558	-1.5507	0	(1a)
0	0	0	0	-1.5507	7.3761	-1	
0	0	0	0	0	-1	1	

Network-2

(1)	(2)	(3)	(4)	(5)	
5.8672	-.5213	0	0	0	
-.5213	1.4867	-.9654	0	0	(1b)
0	-.9654	12.1290	-1.5507	0	
0	0	-1.5507	3.8558	-2.3051	
0	0	0	-2.3051	7.1305	

Lines(1) and (5) of both the network are then scaled by the factor = .4163. The resulting matrices are as follows:

Network-1

(0)	(1)	(2)	(3)	(4)	(5)	(6)
1	.4163	0	0	0	0	0
-.4163	1.2671	.4019	0	0	0	0
0	0.4019	1.4867	-.5213	0	0	0
0	0	-.5213	10.7792	-2.3051	0	0
0	0	0	-2.3051	3.8558	-.6456	0
0	0	0	0	-.6456	1.2784	-.4163
0	0	0	0	0	-.4163	1

(2a)

Network-2

(1)	(2)	(3)	(4)	(5)
1.0168	-.217	0	0	0
-.217	1.4867	-.9654	0	0
0	-.9654	12.1290	-1.5507	0
0	0	-1.5507	3.8558	-.9596
0	0	0	-9596	1.2358

(2b)

After further scaling the remaining lines of both networks as described in chapter 8 the following matrices result.

Network-1

(0)	(1)	(2)	(3)	(4)	(5)	(6)
1	-0.4163	0	0	0	0	0
-0.4163	1.2671	-.4064	0	0	0	0
0	-.4064	1.5206	-.1852	0	0	0
0	0	-.1852	1.5341	-.5106	0	0
0	0	0	-.506	1.5341	-.4072	0
0	0	0	0	-.4072	1.2784	-.4163
0	0	0	0	0	-.4163	1

(3a)

Network-2

(1)	(2)	(3)	(4)	(5)
1.0169	-.2194	0	0	0
-.2194	1.521	-.3429	0	0
0	-3429	1.4958	-.3435	0
0	0	-.3435	1.5341	-.6054
0	0	0	-.6054	1.236

(3b)

To get the static capacitance matrix from the matrices we need to multiply each element by $\eta_0 = 377.7$ since air will be used as dielectric . Moreover to convert the capacitance values in a 50 ohm. system, we need to multiply bolt the matrice by 1/50. This means to get the static capacitance matrices for a 50 ohm system we need to multiply both the matrices by ($\frac{\eta_0}{Z_0} = \frac{376.7}{50} = 7.534$) 7.534. The above matrices after this multiplication becomes.

Network-1

(0)	(1)	(2)	(3)	(4)	(5)	(6)	
7.534	-3.136	0	0	0	0	0	
-3.136	9.546	-3.062	0	0	0	0	
0	-3.062	11.456	-1.395	0	0	0	(4a)
0	0	-1.395	11.558	-3.848	0	0	
0	0	0	-3.848	11.558	-3.068	0	
0	0	0	0	-3.068	9.631	-3.136	
					-3.136	7.534	

Network-2

7.661	-1.653	0	0	0	
-1.653	11.456	-2.583	0	0	(4b)
0	-2.583	11.269	-2.588	0	
0	0	-2.588	11.558	-4.561	
0	0	0	-4.561	9.312	

i=6.

APPENDIX-B

SCALING OF CHARACTERISTIC ADMITTANCE MATRICES OF EXPERIMENTAL FILTER NO.2

The characteristic admittance matrices (8.16) and (8.17) for filter no.2 are as shown below:

Network 1

(0)	(1)	(2)	(3)	(4)	(5)	(6)	
1	-1	0	0	0	0	0	
-1	7.8274	-.8979	0	0	0	0	
0	-.8979	1.3885	-.4905	0	0	0	
0	0	-.4905	13.32984	-2.1333	0	0	(1a)
0	0	0	-2.1333	3.5814	-1.4481	0	
0	0	0	0	-1.4481	7.8864	-1	
0	0	0	0	0	-1	1	

Network-2

(1)	(2)	(3)	(4)	(5)	
6.42	-.4905	0	0	0	
-.4905	1.3885	-.8979	0	0	
0	-.8979	13.0521	-1.4481	0	(1b)
0	0	-1.4481	3.5814	-2.1333	
0	0	0	-2.1333	7.5715	

Lines(1) and (5) of both the network are then scaled by the factor $1/\sqrt{a} = .3967$. The resulting matrices are as follows:

Network-1

(0)	(1)	(2)	(3)	(4)	(5)	(6)
1	-.3967	0	0	0	0	0
-3.967	1.232	-.3562	0	0	0	0
0	-.3562	1.3885	-.4905	0	0	0
0	0	-.4905	15.32984	-2.1333	0	0
0	0	0	-2.1333	3.5814	-.5745	0
0	0	0	0	-.5745	1.2413	-.3967
0	0	0	0	0	-.3967	1

(2a)

Network-2

1.1010	-.1946	0	0	0
-.1946	1.3885	-.8979	0	0
0	-.8979	13.0521	-1.4481	0
0	0	-1.4481	3.5814	-.8463
0	0	0	-.8463	1.1917

(2b)

After further scaling the remaining lines of both networks as described in chapter-8 the following matrices, result.

Network-1

(0)	(1)	(2)	(3)	(4)	(5)	(6)
1	-.3967	0	0	0	0	0
-.3967	1.232	-.3676	0	0	0	0
0	-.3676	1.4784	-.1692	0	0	0
0	0	-.1692	1.4896	-.4540	0	0
0	0	0	-.4540	1.4896	-.3705	0
0	0	0	0	-.3705	1.2413	-.3967
0	0	0	0	0	-.3967	1

(3a)

Network-2

(1)	(2)	(3)	(4)	(5)
1.101	-.2008	0	0	0
-.2008	1.4784	-.3098	0	0
0	-.3098	1.4586	-.3122	0
0	0	-.3122	1.4895	-.5458
0	0	0	-.5458	1.1917

(3b)

To get the static capacitance matrices for a 50 ohm system we need to multiply both the matrices by ($\frac{\eta_0}{Z_0}$ = 7.534) 7.534. The above matrices after this multiplication becomes:

Network-1

(0)	1)	(2)	(3)	(4)	(5)	(6)
7.534	-2.9887	0	0	0	0	0
-2.9887	9.2819	-2.7695	0	0	0	0
0	-2.7695	11.1383	-1.2748	0	0	0
0	0	-1.2748	11.2226	-3.4204	0	0
0	0	0	-3.4204	11.2226	-2.7913	0
0	0	0	0	-2.7913	9.3520	-2.9887
0	0	0	0	0	-2.9887	7-534

(4a)

Network-2

(1)	(2)	(3)	(4)	(5)
8.2949	-1.5128	0	0	0
-1.5128	11.138	-2.3340	0	0
0	-2.3340	10.9891	-2.3521	0
0	0	-2.3521	11.2226	-4.1121
0	0	0	-4.1121	8.9783

(4b)

REFERENCES

1. S.B.Cohn, "Parallel- Coupled Transmission Line Resonator Filters", IRE Trans. PGMTT, Vol. MTT-6, pp 223-231 (April 1958).

2. G.L.Matthaei, "Final Report on Microwave Filter and Ferrite Device Research", Report ERL- 123, Electronics Research Laboratory, Ramo-Wooldridge Division of T-R-W Corp, Canoga Park, California (20 Aug.'58).

3. George L. Matthaei, "Interdigital Bandpass Filters", IRE Trans, MTT, November, 1962, pp 479-491.

4. R.J. Wenzel, "Exact Theory of Interdigital Bandpass Filters and related Coupled Structures", IEEE Trans. on Microwave Theory and Technique, Vol.MTT-13, September 1965, pp.559-575.

5. J.D. Rhodes "The Stepped Digital Elliptic Filter", IEEE Trans. on Microwave Theory & Technique, Vol. MTT-17, No.4, April 1969, pp. 178-184.

6. J.T.Bolljahn and G.L. Matthaei "A study of the phase and filter properties of arrays of parallel conductors between ground planes", Proc.IRE, Vol.50, pp.299-311, March 1962.

7. W.J. Getsinger, "Coupled rectangular bars between parallel plates", IRE Trans. on Microwave Theory and Technique, Vol. MTT-10, January, 1962, pp.65-72.

8. George L. Matthaei, "Comb-line Filters of Narrow or Moderate Bandwidth", The Microwave Journal, August 1963, pp 82-91.

9. M.C.Horton R.J. Wenzel "The Digital Elliptic Filter- A Compact Sharp Cutoff Design for Wide Bandstop or Bandpass Requirements", IEEE Trans. on MTT, Vol. MTT-15 No.5, May 1967.

10. H.Ozaki and J.Ishii, "Synthesis of a class of Strip line Filters", IRE Trans. on Circuit Theory June, 1958.

11. E.G.Cristal, "Coupled Circular Cylindrical Rods Between Parallel Ground Planes" IEEE Trans.on MTT, Vol. MTT-12, pp 428-439, July, 1964.

12. E.A. Guillemin, "Synthesis of Passive Network", New-york, Wiley 1957.

13. Paul I, Richards, "Resistor- Transmission Line Circuits", Proceedings of the IRE, February 1948, pp 217-220.

14. Anatol I. Zverev, "Hand Book of Filter Synthesis", Wiley, N.Y., 1967.

15. R.R.Gupta, "Fringing Capacitance Curves for Coplanar Rectangular Coupled Bars", IEEE Trans. on MTT., Vol.MTT-17, August 1969, pp 637-638, Correspondence.

16. R.Saal, Der Entwarf Von Filtern Mit Hilfe Des Katalogen Normierter Tiefpasse, Germany, Telefunken, Backnay/Curtemberg, T., GmbH,1964.

17. R.J.Wenzel, "Exact Design of TEM Microwave Networks using quarter wave lines", IEEE Trans. on MTT., Vol.MTT-12, pp. 94-111 Jan.1954.

18. R.J. Wenzel, "Theoretical & Practical Applications of Capacitance Matrix Transformation to TEM Network Design, "IEEE Trans. Microwave Theory and Technique Vol. MTT-14, December 1966, pp.633-647.

19. J.D. Rhodes, "The Half wave Stepped Digital Elliptic Filters", IEEE Trans, on Microwave Theory and Technique, Vol.MTT 17, No. 12, December 1969, pp1102-1107.

20. G.L.Matthaei, L. Young, E.M.T. Jones, "Microwave Filters, Impedance Matching Networks and Coupled Structures", New-York McGraw Hill, 1964.

21. The Microwave Engineers' 'Hand-Book and Buyers' Guide, Brookline : Manet Horizon House, Microwave Inc. 1963.

22. W.H.Chen, "Linear Network Design and Synthesis", McGraw-Hill, N.Y.'64.

23. S.B.Cohn, "Shielded Coupled- Strip Transmission Line", IRE Trans. on MTT, Vol.MTT-8, pp. 29-38, October 1955.

T.59